DISSERTATION

OUTCOMES OF PELVIC IRRADIATION IN NORMAL AND TUMOR-BEARING DOGS

Submitted by

Michael W. Nolan

Department of Environmental and Radiological Health Sciences

In partial fulfillment of the requirements

For the Degree of Doctor of Philosophy

Colorado State University

Fort Collins, Colorado

Summer 2013

Doctoral Committee:

Advisor: Susan M. LaRue

Barbara J. Biller
James T. Custis
E.J. Ehrhart
Susan L. Kraft
Angela J. Marolf

ABSTRACT

OUTCOMES OF PELVIC IRRADIATION IN NORMAL AND TUMOR-BEARING DOGS

The purpose of this research was to better understand the effects of abdominopelvic irradiation in dogs. Three studies were performed to that end. The first was a clinical investigation, performed by retrospective data analysis, of safety and activity of intensity-modulated and image-guided radiation therapy (IM-IGRT) for treatment of genitourinary (GU) carcinomas in dogs. The second was a prospective study which developed dogs as a novel animal model for studying radiation-induced erectile dysfunction (RI-ED). The third study reviewed pathological changes associated with unexpected colorectal toxicities encountered in the development of the RI-ED model.

As mentioned, the objective of the first study was to assess local tumor control, overall survival and toxicosis following IM/IGRT for treatment of genitourinary carcinomas (CGUC) in dogs. Medical records of patients for which there was intent to treat with a course of definitive-intent IM/IGRT for CGUC were reviewed. Primary tumors were located in the prostate, urinary bladder or urethra of 21 dogs. The total radiation dose ranged from 54-58 Gy, delivered in 20 daily fractions. Grade 1 and 2 acute gastrointestinal toxicoses developed in 33% and 5% of dogs, respectively. Grade 1 and 2 acute genitourinary, and grade 1 acute integumentary toxicoses were documented in 5%, 5% and 20% of dogs, respectively. Four dogs experienced late grade 3 gastrointestinal or genitourinary toxicosis. The subjective response rate was 60%. The median event-free survival was 317 days; the overall median survival time was 654 days. Neither local tumor control nor overall survival were statistically dependent upon location of the

primary tumor. In conclusion, IM/IGRT is generally well-tolerated and provides an effective option for locoregional control of CGUC. And, as compared with previous reports in the veterinary literature, inclusion of IM/IGRT in multimodal treatment protocols for CGUC can result in superior survival times.

The etiopathology of RI-ED is poorly understood, though this is a common complication of men treated for prostate cancer. Purported mechanisms include cavernosal, arteriogenic and neurogenic injuries. Radiation dose to the posterolateral prostatic neurovascular bundles (NVB) and penile bulb (PB) have been associated with RI-ED. Herein, a canine model is described that has been developed to study the pathogenesis of RI-ED. Stereotactic body radiotherapy (SBRT) was used to irradiate the prostate gland, NVB and/or PB of purpose-bred, intact male dogs. Manual evaluation was used to characterize erectile function and quality. Ultrasound of the internal pudendal arteries, prostate and penis, dynamic contrast-enhanced MRI of the NVB and prostate, and electrophysiology of sensory and motor nerves as well as muscle were performed before and after irradiation. Gross necropsy and histopathology was also performed. Erectile dysfunction was a repeatable finding in subjects for whom the prostate, neurovascular bundles and penile bulb were irradiated with 50 Gy, as documented via subjective and objective manual evaluations following SBRT. Irradiated dogs were found to have a decreased extravascular, extracellular volume in the glans penis, longer systolic rise times in the pudendal artery following papaverine injection, abnormal spontaneous EMG activity in the bulbocavernosus muscle, and slower pudendal nerve motor conduction velocities. Radiation dose-dependent changes in internal pudendal arterial function and dysfunction of the pudendal nerve due to axonal loss may contribute to RI-ED. Measurable endpoints have been developed for evaluation

of RI-ED in dogs, that should be used in future studies to refine this novel animal model and perform additional studies aimed at further elucidating the etiopathologic processes underlying RI-ED.

The objective of the final study was to describe the dose-response relationship and time-dependency of late radiation-induced colorectal complications endured by dogs in the RI-ED study. The prostates of nineteen intact male mixed breed hounds were irradiated with one of four different dose/fractionation schemes. Subjects were monitored for signs of colorectal toxicosis for up to one year following irradiation. Gross necropsy and histopathology were performed upon euthanasia. All toxicoses were graded according to the RTOG criteria for gastrointestinal toxicity. The frequency and severity of colorectal ulceration were higher in dogs treated 5 fractions of 10 Gy delivered on consecutive days, as compared with those treated on an every other day schedule. The mechanism for this time-dependency is unclear, but likely related to completeness of epithelial regeneration. Vascular sclerosis and serosal thickening occurred in all treatment groups, in a dose-responsive fashion.

ACKNOWLEDGEMENTS

This dissertation could not have been completed without the help of many people. Special thanks go to my family and friends. I thank my mother, Sharon L. Nolan, for her unwavering love and encouragement, and for reminding me that there are worse things in life than having to work hard. I thank Dr. Jennifer A. Myers; without her support, hours of complaining would have been directed instead at a houseplant. I would also like to thank Dr. Susan M. LaRue who made it her personal mission to see that I completed this program, and left Colorado State University not only a well-trained radiation oncologist, but more importantly, a well-equipped scientist. Dr. LaRue has expanded the outstanding program developed by Dr. Edward L. Gillette, and ensured that CSU will remain at the forefront of clinical and translation radiobiology for years to come. I thank Ms. Anne Golden for her endless patience; this research would never have been completed without her incredible efforts. I also would like to thank the many scientists and clinicians who supported this work. The man who made all of this possible is the late Dr. Todd H. Wasserman. Directly involved in data acquisition and study design were Drs. Susan L. Kraft, Angela J. Marolf, EJ Ehrhart, Sangeeta Rao, Hiroto Yoshikawa, Stephanie Engel, and L. Ray Whalen. Other members of my graduate advisory committee, who provided valuable guidance on these projects, were Drs. James T. Custis and Barbara J. Biller. I couldn't have stayed sane without the support of my residentmate, Dr. Lynn R. Griffin. And none of this would have been possible without the help of a long list of people from the CSU Radiation Oncology and Diagnostic Imaging and Clinical Oncology teams; thanks to all of you! Finally, I would like to thank Varian Medical Systems for their generous financial and intellectual support.

TABLE OF CONTENTS

CHAPTER 1: INTRODUCTION

The role of external beam radiation therapy in management of pelvic malignancies

External beam radiation therapy (EBRT) is a common component of multimodal care for pelvic malignancies in people. EBRT is associated with improved local tumor control in colorectal, cervical and prostate cancer.

Colorectal Cancer. Colorectal cancer is a common pelvic malignancy in men and women. Though rectal cancer has a slightly higher rate of local recurrence as well as slightly higher distant metastatic rate than colon cancer, the two diseases are considered together in this discussion due to similar biologic behavior. Both diseases are characterized by locally invasive lesions with high propensity for dissemination to regional lymph nodes and the liver; post-mortem reports have documented hepatic micrometastases in up to 80% of patients with colorectal cancer.[1] Surgery is the primary treatment for colorectal tumors, with 75% of patients eligible for curative-intent resection, and excellent cure rates for patients with disease limited to the bowel wall.[2,3] Post-operative recurrences are locally extensive in 25-40% of patients, involve peritoneal seeding in 12-28% of cases, and spread to the liver in approximately 40% of patients.[1] Adjuvant chemotherapy improves disease free survival rates in high risk patients (defined as those with American Joint Committee on Cancer stage III disease: any T, N1 or 2, M0).[4] Although a combination of 5-fluorouracil (5-FU) and leucovorin was historically used as the adjuvant chemotherapeutic protocol of choice, recent data has established the combination of 5-FU, leucovorin and oxaliplatin as standard of care for high risk colon cancer, with a 5.3% improvement in the 3 year disease-free survival rate (78.2% vs. 72.9%).[5] Despite the successes of adjuvant chemotherapy, local recurrences after curative-intent surgery are still problematic.

EBRT, particularly in the setting of rectal cancer, has therefore been investigated, though an optimal protocol (pre- vs. post-operative, timing of chemotherapy, fractionation scheme and schedule) has not been established. Conventionally fractionated preoperative radiotherapy (RT) results in a complete response in 10-15% of patients, and short-course preoperative RT reduces local recurrence rates by approximately 50%.[6-8] A combined approach utilizing both pre- and post-operative radiation has also been successful at improving local control rates. Five-year survival rates for patients receiving 5 Gray (Gy) pre-operatively and 45 Gy post-operatively (91%) compared favorably with those receiving only surgery (34%) or only low-dose pre-operative radiation (52%).[9] Finally, post-operative radiation has been investigated for high-risk colorectal cancer, and is associated with improvements in local control (5-year control following 45 Gy post-operative RT was 93% and 72%, respectively, for T4N0 and T4N+ cases, compared with 69% and 47% for people undergoing surgery alone).[10]

Cervical Cancer. Cervical cancer is most common in the developing world. A large proportion of cervical cancers develop subsequent to herpetic genital infections; the role of human papilloma virus (HPV) is well established as a causative agent. Despite screening through annual Pap smears, preventative measures (including education about risk factors for cervical cancer, such as having multiple sexual partners, smoking and unprotected sex) and recent introduction of HPV vaccines (which include recombinant virus-like particles assembled from L1 proteins of HPV types 6, 11, 16 and 18),[1,2] invasive carcinoma of the uterine cervix is estimated to cause 233,000 annual deaths, worldwide.[11,12] This disease is typically locally aggressive, and 40-75% of patients experience regional lymph node metastasis; common distant

[1] Gardasil, Merck and Co., Inc, New Jersey, USA
[2] Cervarix, GlaxoSmithKline, Middlesex, UK

sites of metastasis (in decreasing order of prevalence) include lung, bone and abdominal cavity.[13,14] Primary therapy for localized cervical cancer consists of hysterectomy and/or RT (EBRT or brachytherapy). Chemotherapy has also been investigated for use in cases of bulky and advanced cervical cancer, though it is seldom used alone. Cisplatin is among the most commonly employed anti-neoplastic chemotherapeutic agents used for cervical cancer because of its high activity against squamous cell carcinoma of the uterine cervix. It is also thought to synergize with RT, by increasing the number of free-radical complexes present after irradiation, and inhibiting repair of sublethal damage.[15] The use of concurrent chemoirradiation protocols has resulted in improved local tumor control rates. A meta-analysis was performed, and demonstrated a 12% improvement in overall survival in patients receiving concomitant chemotherapy and RT.[16]

Prostate Cancer. Prostate cancer (PC) is the most commonly diagnosed visceral neoplasm, and is the second most common cause of cancer-related death in men. Prostatic anatomy is most commonly subdivided into four zones: the peripheral zone, transition zone, central zone and anterior fibromuscular stromal zone.[17] More than 70% of prostatic carcinomas arise from the peripheral zone, whereas benign prostatic hyperplasia (BPH) more commonly arises from the transition zone (accounting for >90% of cases).[18] The normal prostate's primary function is synthesis of seminal fluids; this includes production of prostate-specific antigen (PSA), which is a serine protease involved in liquefaction of the seminal coagulum. PSA is produced by normal, hyperplastic and malignant prostatic tissue, and can be used as a screening tool for both BPH and PC. Pre-treatment serum PSA concentrations correlate with tumor stage; for example, 53-67% of men with a serum PSA level of 4-10 ng/mL have prostate-confined disease, whereas PC was

confined to the prostate in 31-56% of cases with a PSA of 10-20 ng/mL. Likewise, pre-treatment PSA levels are predictive of seminal vesicle involvement.[19,20] Synthetic activity and growth of the prostate gland are regulated by androgens; androgen deprivation therapy is therefore an important component of therapy for many androgen receptor positive tumors.[21] Localized PC is generally classified as either low-risk or intermediate-to-high risk; such classification enables stratification of prognosis, and treatment options and outcomes. Risk grouping varies depending on institution, but low risk tumors are generally defined as having a pre-treatment PSA level <10 ng/mL, a Gleason score of 2-6 (Gleason scores are a composite score representing the sum of the histologic grades for the two most common tumor patterns within the PC; each individual grade is based on a scale of 1-5 with one representing small, uniform glands and 5 corresponding to solid tumor without glandular differentiation), and T stage less than 2b (tumor involving more than half of a lobe, but not both lobes).[22] Intermediate risk tumors generally have a PSA of 10-20 ng/mL, or a Gleason score of at least 7, or T stage 2b or higher; high risk tumors have at least two of the intermediate risk factors.[23] But even careful staging and risk stratification doesn't perfectly predict biologic behavior. Many men diagnosed with low-risk PC prior to development of symptoms will have slow growing lesions which may be amenable to watchful waiting or active surveillance.[24] In these cases, decisions for or against treatment are often guided by current quality of life, and overall life expectancy. Other patients with low-risk PC will clearly benefit from therapy for their localized disease. In this scenario, treatment options include radical prostatectomy, prostate-only EBRT and prostatic brachytherapy. Outcomes between these modalities appear similar, and in the absence of comparative phase 3 clinical trials, the choice is often made based upon clinician preference.[25,26] Overall, 10 year progression-free survival rates for patients treated as such are approximately 75%. Although first-line treatment

may involve radical prostatectomy, many cases of intermediate- and high-risk PC are better suited to whole-pelvis RT, in combination with both neoadjuvant and concurrent hormonal therapy (androgen suppression via luteinizing hormone-releasing hormone agonists and anti-androgens).[27] Nodal extirpation and/or irradiation are frequently employed. Such combination therapy is associated with 5-year biochemical control rates of 40-70%.[28,29] To improve these outcomes, addition of cytotoxic chemotherapy is often considered in hormone-refractory, and locally advanced PC; taxols (particularly docetaxel) are the cornerstone of anti-neoplastic chemotherapy for PC.[30]

Complications following pelvic irradiation

Compared to other anatomic sites, radiation-induced normal tissue complications are relatively common in the pelvis. Acute gastrointestinal (GI) and urinary tract toxicities requiring medical management occur in approximately 60% of patients. Symptoms associated with these toxicities arise within the first few weeks of RT, and include rectal discomfort, tenesmus, diarrhea, increased urinary frequency, urgency and dysuria. Acute toxicities are generally self-limiting and fully-resolved a few weeks after completing RT. Late radiation-associated toxicity generally occurs at least six months after completion of RT, and is far less common than acute morbidity. Overall, late radiation-associated toxicity occurs in less than 10% of patients having been treated for pelvic malignancies, but may include injury to either the GI, or genitourinary (GU) tract. It is the minority of late toxic events in the pelvis which require major surgical intervention, or result in death.[31]

Quantifying Adverse Events. There is no single accepted system for classifying and quantifying complications of radiotherapy. The original system for quantification of radiation effects was the Radiation Therapy Oncology Group (RTOG)/European Organization for Research and Treatment of Cancer (EORTC) system. Effects were classified according to organ system and chronicity (early or late), and scored on a 6 point scale, with 0 corresponding to no change from baseline, 1 was mild, 2 was moderate, 3 was severe, 4 was life-threatening and 5 was death. Events were classified as acute if occurring less than 3 months from the start of RT, and late if more than 3 months. Furthermore, events were only scored if they were clinically attributable to RT. With the intention of creating a standardized international scoring system for use in clinical trials, the late effects in normal tissues subjective, objective, management and analytic scales (LENT SOMA) were published by the EORTC and the National Cancer Institute (NCI) funded RTOG in 1995.[32]

In general, adverse events (AEs) during and after cancer treatment are classified and scored according to the Common Terminology Criteria for Adverse Events (CTCAE). This system was initially devised to describe and grade AEs occurring during phase I chemotherapy clinical trials. AEs were defined as any abnormality occurring during or after therapy, whether or not it was thought to be related to therapy. The initial grading scheme, published in 1982, was based on a 4 point scale, with 1 corresponding to mild, and 4 corresponding to life-threatening. The second version, published in 1998, was expanded to include grade 0, which corresponded to no change from baseline, and grade 5, which corresponded to death. The third version (2003) was far more comprehensive, and included chronic changes, making it more applicable to grading of late toxicity following RT. One subsequent revision has been made (version 4, released in 2009),

which introduced MedDRA, a clinically validated international medical terminology system, but which did not include any major changes in AE classification. The period for public comments on the draft of version 5 closed in April 2013; this latest version will be released in late 2013 or 2014. Although the CTCAE system does not classify events as early or late, since release of version 3, there have been enough specific AE categories that most, if not all, radiation effects can be properly classified. The CTCAE system is largely replacing other schemas because most modern clinical trials evaluate multimodal therapy.[33]

Urinary. Radiation-induced injuries of the lower urinary tract include acute and late changes in the urinary bladder, and late toxicities in the urethra and ureters.

As with radiation toxicity in many organs, radiation injury in the urinary bladder is characterized by three clinically distinct phases, including an acute phase, a symptom-free latent period, and a late phase. Symptoms of early and late effects are similar, including dysuria, urgency and increased frequency of micturition, attributable to decreased bladder storage capacity. Unlike radiation injury in many organs, the kinetics of urothelial cell turnover are quite slow and acute bladder injury is not a consequence of stem cell depletion.[34] Rather, early bladder dysfunction is morphologically characterized by hyperemia and edema, which is accompanied by decrease in superficial umbrella cell numbers (but not intermediate or basal cells), loss of apical uroplakin III expression (which is important for barrier protection at the bladder lumen) in the remaining umbrella cells, alteration in the superficial glycosaminoglycan layer (another constituent of the urothelial barrier), and increased expression of cycolooxygenase-2 (COX-2) in the tunica intima and media of bladder blood vessels.[35-37] Transient upregulation of COX-2 expression results in

altered prostaglandin metabolism (particularly prostaglandin E_2), which causes increased detrusor tone and decreased bladder capacity.[38] These acute changes are generally self-limiting, and clinically reversible. Pre-clinical murine data suggests a possible role for non-steroidal anti-inflammatory drugs, such as aspirin, in management of acute bladder toxicity. This is logical since such drugs inhibit prostaglandin synthesis.[38] Antispasmodic drugs, such as oxybutynin, that inhibit the muscarinic effects of acetylcholine can help to relax bladder smooth muscle and relieve symptoms of frequency and urgency.[39]

The incidence of acute toxicity correlates well with development of irreversible late phase radiation-induced bladder injuries, which develop years after completion of RT. This correlation suggests a consequential mechanism (consequential late effects are characterized as having arisen as a result of a severe acute effect), and is supported by that fact that the chronic phase of bladder injury is characterized by progressive mucosal breakdown, which is initiated early after starting RT. The mucosal injury can range from superficial denudation to fistulation; other classic late changes in the bladder include vascular collapse and regional ischemia, mural fibrosis (which causes the decrease in storage capacity) and telangiectasia (which causes bleeding).[35,36] Late radiation effects to the bladder are difficult to manage. Bleeding may be manageable with laser therapy. Severe sequela such as fistulation and bladder contracture may necessitate surgical intervention, and rarely, result in fatality.[39]

Radiation-induced urethral toxicity is less commonly reported than bladder toxicity, but is thought to result from similar pathophysiologic radiation changes, including vascular damage, ischemia, and fibrosis. Urethral stricture is reported in less than 2% of patients undergoing full-

course pelvic irradiation, and approximately 5% of patients receiving combination therapy (radical prostatectomy or brachytherapy plus EBRT).[40] Stenting, urethroplasty and urethrostomy all appear to be viable treatment options for treating late, radiation-induced urethral stricture.[41] A less common, but more severe radiation complication is recto-urethral fistula, which can be also be managed successfully in most cases using urethral and rectal reconstruction.[42]

Acute radiation-induced ureteral toxicity is not recognized, and late toxicity in this organ is quite rare. Ureteral stricture is the most common late effect. In cases of bladder cancer, ureteral stricture can be difficult to distinguish from malignant obstruction; however, the latter is likely far more common. Clinical data describing this adverse event are sparse, and limited to scattered reports in larger studies.[39] Late ureteral injury has been best described in an experimental dog model, where it was shown that the ureteral orifice can tolerate approximately 20 Gy in a single fraction, and that risk of stricture is directly related to both dose and volume or length irradiated.[43,44] In the event of symptomatic stricture of the ureter or ureteral orifice, stenting and or ureteral re-implantation are potential treatment options.

Sexual. Sexual dysfunction is a relatively common complication of pelvic irradiation in both men and women. In both sexes, sexual toxicities are associated with measurable biological changes, as well as psychological issues.

In women, rapid cell turnover in the vaginal and vulvar epithelium render them quite sensitive to the effects of radiation; acute mucosal reactions are common in these organs.[45] Late toxicity is also relatively common, and manifests as decreased vaginal elasticity and stenosis after vaginal

wall thinning and fibrosis.[46] These changes can be accompanied by vaginal bleeding and lack of lubrication. Aside from these physical changes, women frequently report being left with a feeling of lack of femininity, sexual attractiveness and confidence.[47] In premenopausal women, radiation-induced ovarian failure may also contribute to sexual dysfunction. Studies of therapeutic interventions for management of sexual toxicity in women have been limited. Two studies have suggested that women receiving hormone replacement therapy have a lower risk of dysfunction than untreated counterparts.[48,49] There is also some suggestion that vaginal estrogen may positively impact epithelial regeneration.[50,51] Early return to sexual intercourse, or use of a vaginal dilator may help reduce risk of vaginal stenosis.[52,53] Ultimately, the most important intervention with respect to managing risks associated with pelvic irradiation in women is probably appropriate sexual counseling before, during and after irradiation.[54,55]

In men, sexual toxicity is most common after RT for PC, and is characterized by both ejaculatory dysfunction and erectile dysfunction (ED). The mechanism(s) underlying development of these effects are poorly understood, but are believed to be multifactorial and similar regardless of the primary tumor type (i.e., colorectal, bladder or prostate).[47]

Ejaculation is initiated upon stimulation of sensory nerves; the primary sensory input is the dorsal nerve of the penis, which is the distal-most extension of the pudendal nerve and innervates the penis and prepuce. Activation of mechanoreceptors during penile engorgement can also stimulate the sensory tracts. The process of ejaculation requires erection, propulsion of semen and prevention of retrograde seminal flow. During the initial phase of ejaculation, spermatozoa are mixed with seminal fluids, and this mixture is transported into the urethra through smooth

muscle contractions in the accessory sex organs. The expulsion phase requires rhythmic movement of semen through the urethra. This is facilitated by contraction of striated perineal muscles, the bulbocavernosus muscle, ischiocavernosus muscle and external urethral sphincter; motor inputs are derived from the S2 spinal segment, through the pudendal nerve.[56]

Ejaculatory dysfunction is characterized by decreased intensity of orgasm, decreased frequency and rigidity of erections and decreased libido, which are accompanied by decreased volume (or absence) of semen and/or ejaculate and discomfort during ejaculation.[47] The exact cause for ejaculatory dysfunction is unclear. Although serum testosterone levels may transiently drop after prostatic RT, these changes are small and likely of no physiologic consequence; therefore, decreased semen counts following prostatic irradiation are unlikely to be a result of radiation-induced Leydig cell injury.[57-59] Arteriogenic and neurogenic injury may also contribute to ejaculatory dysfunction.[47,60] There are currently no known medical interventions for treatment of ejaculatory dysfunction.

Radiation-induced ED (RI-ED) is a much better studied, though still poorly understood complication of RT. In order to understand ED, it is important to first review normal erectile physiology. There are three types of erection. Reflexogenic erection is produced by tactile stimuli to the genital organs; impulses arise in the penis and reach spinal centers to activate sensory perception and autonomic stimulation of the cavernous nerve. Psychogenic erection results from audiovisual stimuli or fantasy; brain impulses modulate spinal erection centers. Specifically, supraspinal and central neural pathways are important to physiologic erectile function. The medial preoptic area and paraventricular nucleus of the hypothalamus and

hippocampus are important for integrating signaling related to sexual function and penile erection. Visually evoked sexual arousal is associated with three components: perceptual or cognitive, emotional or motivational and physiological. Nocturnal erection occurs during deep, rapid eye movement (REM) sleep.[61]

Both autonomic and somatic innervations play roles in penile erection. Neurons from the spinal cord and peripheral ganglia form the cavernous nerves, which contain sympathetic and parasympathetic fibers. Sympathetic pathways originate from T11 to L2, and travel in the hypogastric nerves to form the pelvic plexus. Parasympathetic pathways arise from S2-4, and pass through the pelvic nerves to join the sympathetic innervation in the pelvic plexus. The cavernous nerves are branches of the pelvic plexus which innervate the penis. Stimulation of the pelvic plexus and cavernous nerves results in parasympathetic stimulation via release of nitric oxide (NO) and acetylcholine, and causes tumescence. Sympathetic stimulation results in inhibition of norepinephrine and causes detumescence. Somatic innervation is largely responsible for sensation and contraction of the bulbocavernosus and ischiocavernosus muscles via release of acetylcholine. Numerous afferent nerve endings are found in the glans penis; these fibers form the dorsal nerve of the penis, which arise from the pudendal nerve (which also innervates the ischiocavernosus and bulbocavernosus muscles and whose parent fibers enter the spinal cord at the S2-4 spinal segments). The dorsal nerve of the penis is not solely somatic though; it also has autonomic components and aids in regulation of erection and ejaculation.[56,61]

The corpora cavernosa is the most prominent of the penile erectile tissues; within this tissue, cavernous smooth musculature and smooth muscles of the arterial walls are most important to

erectile physiology. Both are tonically contracted with low arterial flow rates when the penis is flaccid. However, sexual stimulation leads to release of neurotransmitters (particularly nitric oxide and acetylcholine) from the cavernous nerve endings resulting in smooth muscle relaxation. This is demonstrated by sinusoidal relaxation, arterial dilatation and venous compression. Specifically, smooth muscle relaxation results in dilation of arterioles due to increased blood flow, sinusoidal expansion which results in blood trapping, decreased venous outflow due to compression of subtunical venous plexuses between the tunica albuginea and sinusoids as well as stretching of the tunica to occlude venous outflow. Increased partial pressure of oxygen and increased intracavernous pressure causes the penis to rise from its dependent position, and contractions of the ischiocavernosus and bulbocavernosus muscles result in further spikes in pressure for full tumescence. Arterial flow is similar in the corpus spongiosum and glans penis during erection, though pressures are quite a bit lower than in the copora cavernosa. Detumescence occurs via three stages: transient increases in the intracorporeal pressure, slow drop in the pressure due to reopening of venous channels and return to basal arterial flow, and a fast final drop in pressure to resume normal venous outflow.[56,61]

Erectile dysfunction (ED) can be classified as psychogenic, neurogenic, endocrinologic, arteriogenic, or cavernosal. Radiation-induced ED (RI-ED) is observed in 6-84% of patients following external beam radiotherapy.[62,63] The cause and exact classification of RI-ED are unknown, though cavernosal (abnormal cavernosal distensibility), arteriogenic (low peak penile blood flow rates) and neurogenic (poor response to prostaglandin injections as well as histologic evidence of injury) dysfunction have all been associated with RI-ED.[64]

Distilled down to four necessities, normal penile erection requires functioning cavernous nerves, arterial inflow through the internal pudendal arteries, healthy erectile tissue that is capable of maintaining erection through venocclusion, and pudendal nerves capable of stimulating contraction of perineal musculature.[65] Therefore, RI-ED must be the result of alteration of at least one of these functions.

Ultrasound imaging of the penis in men with RI-ED has demonstrated reduced blood flow in the cavernosal arteries, and venous leakage of the corpora cavernosa.[62,66,67] Although the bulk of the cavernosal tissue is distant from EBRT fields used for treatment of PC, the divergent crura at the base of the penis, and adjacent to the apex of the prostate are continuous with the rest of the corpora cavernosa. Given the proximity of the crura to the prostate, they necessarily receive high dose, which has been significantly correlated with RI-ED in one study, suggesting that radiation injuries in the crura may contribute to altered cavernosal blood flow.[68] This finding is tempered by three other studies which failed to correlate dose to the crura with RI-ED; such negative findings could be due to a true lack of association, or due to small study size and resultant lack of statistical power.[69-71]

Another possible reason for reduced cavernosal arterial blood flow is radiation injury to the internal pudendal arteries.[72,73] The role of internal pudendal arterial injury in RI-ED has not been studied in the clinical setting, but these vessels lie close to the apex of the prostate, and receive significant dose during prostatic irradiation, suggesting a possible role.[72] Furthermore, laboratory studies have suggested that pelvic irradiation causes upregulation of vasoconstrictive

endothelin-1, and that rats with elevated endothelin-1 levels have lower mean maximal intracavernous pressures during erection than normal animals.[74]

There has also been some preclinical work which suggests vascular responses to erectogenic stimuli may be muted by radiation injury to the nervous supply to the cavernosal tissue, rather than injury to that tissue itself. Carrier and colleagues reported reduced numbers of nitric oxide synthase containing fibers in the corpora cavernosa of mice after prostatic irradiation.[75] This could be a result of direct radiation injury to those fibers, or fibers could be reduced in number due to atrophy of the larger parent nerves, lying within the RT field (e.g., those in the NVB).

Injury to the prostatic NVB has been hypothesized to contribute to RI-ED. The prostatic neurovascular bundles are composed of the venous plexus of Santorini (which is the primary drainage of the penis), branches of the internal pudendal artery (which is the primary blood supply for the prostate and penis), as well as nerves originating from the pelvic plexus (the pelvic and hypogastric nerves contribute parasympathetic and sympathetic fibers [respectively] that distribute to the prostate, urethra, seminal vesicles and penile corpora cavernosa). Given the clear role NVB injury plays in loss of potency following radical prostatectomy, and the proximity of the NVB to the prostate, necessitating its inclusion in RT fields, it is logical to think that NVB injury may contribute to RI-ED.[76] However, the only study to link NVB dose with development of ED did so in 3 patients having received prostatic brachytherapy.[77] No larger studies have successfully correlated NVB dose with incidence of RI-ED; as with dose to the crura, negative finding may reflect poor study design, or true lack of biological association.[71,78] The fact that sildenafil effectively alleviates RI-ED in up to 50% of patients with RI-ED further

confuses the potential role of NVB injury in RI-ED, because phosphodiesterase-5 (PDE5) inhibitors are ineffective in men with ED subsequent to NVB damage incurred during prostatectomy.[79-82] PDE5 inhibitors, such as sildenafil and tadalafil, enhance erectile function by preventing degradation of cycloguanosine monophosphate, which decreases intracellular calcium to allow smooth muscle relaxation. If the number of NO synthase containing nerve fibers is decreased in the cavernous tissues, PDE5 inhibitors likely benefit RI-ED patients by enhancing the effectiveness of that NO which remains present. Rather than primary nerve damage, NVB irradiation may also cause vascular injury that is severe enough to cause RI-ED. Such vascular injury could be in the form of injury to the arterial supply of the penis, which enables penile engorgement during erection. Alternatively, vascular damage could comprise injury to the veins which drain the penis, causing venous leakage, and failure of venocclusion.

Finally, just as dose to the crura has been correlated with incidence of RI-ED, so too has dose to the penile bulb.[65,69,71,83,84] The penile bulb is the proximal-most portion of the bulbus spongiosum. Given that it does not play a major role in erectile function, it is unlikely that the penile bulb itself is a critical component in development of RI-ED; rather, it is likely to be a surrogate for another structure whose function is altered when the penile bulb is irradiated (such as the crura or cavernosa). Alternatively, if the irradiation of the bulb itself is responsible for development of RI-ED, it is most likely that this relates to neurogenic injury within the base of the penis, as discussed above.

Gastrointestinal. Early and late radiation-induced complications are observed in the GI tract. Early GI toxicity is common following abdominopelvic irradiation, but is typically mild-to-

moderate, and reversible, with complete resolution of symptoms within weeks. Late GI toxicities are less common, but symptoms are usually moderate-to-severe, and progressive. This section will be limited in scope to the lower GI tract, including colon and rectum.

Acute colorectal toxicity is due to depletion of organ-specific stem cells. Failure of the crypt epithelium to mature causes epithelial denudation. Acute colitis occurs and/or proctitis is expected in upwards of 90% of patients receiving pelvic RT.[85] Signs are most often mild, and rarely severe enough to cause treatment interruption.[86] A strong regenerative response facilitates rapid resolution of symptoms attributable to acute injuries. A large body of work in animal models has described the kinetics of epithelial repopulation following irradiation. Effects have been shown to be dose and fractionation-dependent.[87-90] Withers and Mason described crypt depletion and regeneration, with time to onset of regeneration occurring 3.5 days after initiating RT in mice.[91] They also described shortening of the doubling time of surviving cells as treatment progressed, with a doubling time of 48 hours after 2 days, and 24 hours between 2 and 4 days.[92] In general, prevention and treatment of acute radiation-associated colorectal toxicity is poorly studied. Sucralfate has been used anecdotally for management of acute effects in the GI tract; it has also been evaluated as a prophylactic measure. Its use as a prophylactic should, however, be discouraged, as it may in fact worsen symptoms.[93]

Late GI toxicity is classically thought of as resulting from vascular changes and fibrosis in the submucosal, muscular or serosal layers of the GI tract wall, and is unrelated to previous mucosal injuries in the acute phase of GI toxicity.[94,95] The clinical manifestations of these late injuries include (1) mucosal and mural atrophy, which may lead to chronic, progressive ulceration and/or

perforation secondary to vascular collapse and ischemia in the wall of the gut, (2) chronic colitis secondary to acute inflammatory responses which result from mechanical irritation and bacterial infection subsequent to mucosal atrophy, and (3) luminal stenosis (stricture) due to collagenous proliferation in the wall. Vascular changes may also result in telangiectasia, which predisposes to chronic bleeding. Late colorectal toxicity has been more extensively studied than acute effects. It is well-established that 20 Gy given in a single fraction causes rectal obstruction or death in 50% of animals; furthermore, it is clear that increasing dose is associated with decreased time between irradiation and severe toxicity.[96,97] Bleeding may be treated with topical formaldehyde, electrocoagulation, or argon plasma or laser coagulation. Chronic colitis is managed medically (steroid enemas, aspirin suppositories, antioxidants such as vitamin E, sucralfate, sulfasalazine, etc.), with variable success. Treatment for stricture varies with severity of the lesion, but may include stool softeners or balloon dilation. Surgical intervention is reserved for cases with severe stricture and/or perforation.[98,99]

Consequential late effects (CLE) constitute a less but increasingly commonly recognized form of radiation-induced GI toxicity, for which the time-course and clinical presentation is similar to that of classical late toxicities, though the mechanism of induction differs drastically. CLE's are most common in tissues with barrier or mechanical functions (such as the GI tract), and result from persistence of severe early injuries. Histologically, CLE's look much like classic late effects; however, clinical features can often be used to distinguish between the two processes. For example, classic (or generic) late effects are characterized by modification of vascular function, marked sensitivity to changes in fractionation, little impact due to changes in overall treatment time, and do not correlate with severity of acute effects. Conversely, CLE's rarely

occur in concert with altered vasculature, and as with acute reactions, are insensitive to changes in dose-per-fraction, but are markedly affected by the total treatment time and duration of the interfraction interval.[100] In the GI tract, development of CLE's is supported by intermediate fractionation sensitivity, and treatment time dependency, suggesting a contribution from acute reacting tissues.[88,101-105] Further evidence of a consequential mechanism is the apparently important role that mucosal health and integrity plays in preventing development of late effects.[106-109]

The role of modern technology in limiting the incidence and severity of complications

Radioprotectors. As mentioned earlier, sucralfate is sometimes used for treatment of acute and late GI toxicity; it is not an effective prophylactic intervention for acute toxicity, and its ability to prevent late toxicity has been incompletely evaluated.[93,110,111] Subcutaneous administration of amifostine reduced the risk of severe acute radiation colitis in patients receiving pelvic RT.[112] Statins and angiotensin I-converting enzyme inhibitors have also been shown to decrease severity of gastrointestinal complication scores.[113] Newer chemical radioprotectors are also being investigated. Small-molecule inhibitors of glycogen synthase kinase 3β have been shown to attenuate intestinal injury in murine studies. These compounds work by interfering with Bcl-2, Bax and caspase 3, which are all involved in regulation of radiation-induced apoptosis.[114] While promising in preclinical studies, glycogen synthase kinase inhibitors have not been studied in large animal models or humans.

Aside from these pharmacologic interventions, physical means of radioprotection have also been investigated. In cases of non-GI tract pelvic malignancies, tissue expander devices can be placed

laparoscopically to provide physical separation between the lower urinary tract and GI tract prior to EBRT. This enables delivery of high doses of RT while minimizing risk of GI complications.[115] These devices can become dislodged, and require additional surgery during the course of RT, and invariably require removal from the body after completion of RT. Newer separation devices have been developed, that can be implanted using transabdominal injection, and which naturally biodegrade without need for surgical intervention. For example, hyaluronan gel increases the separation between the prostate and rectum, thereby decreasing rectal dose and improving the therapeutic ratio associated with prostatic irradiation.[116]

IMRT. Intensity-modulated RT (IMRT) is a relatively new technique which delivers nonuniform radiation fluence to optimize dose distributions; IMRT requires a system for both planning and delivering nonuniform fluences. IMRT is generally delivered using linear accelerator-based systems, though highly conformal radiation can also be delivered using arc therapy or tomotherapy. Other systems for delivering highly conformal radiation include robotic radiosurgery and gamma knife technologies; because these are generally reserved for stereotactic irradiation, they are discussed in the next section. IMRT is often referred to as "dose-painting". This refers to the highly conformal nature of IMRT plans. The theoretical benefit of IMRT is improvement of the therapeutic ratio by delivering prescribed doses to the planned target volume (PTV), while minimizing dose delivered to adjacent normal tissues.

Though no phase III clinical trials have been performed to compare rates and severity of toxicity following pelvic IMRT, as compared with 3D-CRT, several recent reports suggest an improved therapeutic ratio for IMRT. Forsythe and colleagues reported greater decreases in urinary quality

of life scores at 3 months for patients receiving 3D-CRT, as compared with IMRT. These scores equalized at a year, suggesting that IMRT mitigates acute toxicity in the urinary tract, but doesn't affect risk of late toxicity. These same investigators also reported lower rates (7% vs. 11%) of moderate-to-severe rectal bleeding in IMRT patients.[117] There has only been one investigation of sexual toxicity following IMRT; after treatment for localized PC, rates of RI-ED were no lower than would be expected for conventional EBRT.[118]

In combination with image-guidance, IMRT can theoretically also be used to spare normal tissues within the PTV. For example, in a dosimetric study, Thomsen and colleagues reported a 17% reduction in urethral dose when a Nickel-Titanium stent was used to facilitate accurate urethral delineation, and IMRT was used to lower radiation dose to the urethra. Calculations of tumor control probabilities suggested no change in predicted tumor control outcomes.[119] These results have not been confirmed through clinical investigations. In fact, the only clinical report of urethral-sparing IMRT for PC showed that this technique failed to improve urinary quality-of-life, and resulted in higher PSA nadirs and inferior biochemical control post-RT.[120] This underscores the importance of rigorously evaluating new therapeutic modalities and techniques before assuming non-inferiority as compared with conventional approaches.

SBRT. Stereotactic body radiation therapy (SBRT) involves the delivery of high doses of ionizing radiation to tumors in 1 to 5 treatment sessions. SBRT is reserved for treatment of well-delineated bulky/macroscopic tumors and relies on accuracy of treatment, which ensures the prescribed dose is delivered to the intended target (PTV) rather than adjacent normal tissues.[121] SBRT generally refers to treatment of tumors within body cavities. Because rigid

immobilization of targets within cavities is difficult, SBRT employs image-guidance (via on-board kilovoltage radiography or computed tomography) and/or real-time tracking systems (involving implantation of transponders that transmit radiofrequency signals to electromagnetic arrays) in order to ensure proper localization of the target prior to and, in some cases, during administration of radiation.

SBRT is a precision technique which has a geometric advantage over conventional EBRT in that it is able to deliver high doses to the target volumes, while sculpting the beam such that normal tissues receive lower dose in comparison to conventional protocols. The physical sparing of normal tissues achieved with SBRT techniques enables frequent administration; radiation fractions are typically administered either daily or every 48 hours, as compared with conventional hypofractionated radiation, where fractions are delivered weekly to allow for repair and in some cases, repopulation, of normal irradiated tissues. Clinically, SBRT prescriptions are thought to have improved biologic effectiveness. Several explanations have been offered for this improvement in effectiveness. First, short SBRT protocols not only avoid accelerated repopulation of tumors, but also limit the effect of normal and expected tumor growth during the course of therapy. Second, in addition to inducing lethal effects via extensive DNA damage leading to chromosomal damage that causes mitotic catastrophe, high dose-per-fraction RT may also cause cell death via generation of ceramide through the acid sphingomyelinase pathway, which activates caspases and leads to apoptosis. Along this vein, murine data suggests that high dose-per-fraction RT induces large amounts vascular endothelial apoptosis, and therefore leads to tumor death by indirect microenvironment changes (hypoxia, pH change, etc.) which alter the tumor cell's ability to complete homologous recombination repair.[122,123] Furthermore, recent

studies suggest that SBRT may have effects outside the defined treatment field.[124-128] As reviewed elsewhere, it has been suggested that "(1) despite steep dose gradients outside the planning target volume, microscopic tumor cells outside the gross tumor volume may receive sufficient dose to inhibit tumor growth, (2) inactivation of cells within the GTV via ablative radiation effects may result in loss of autocrine and paracrine growth stimulants which are needed to support growth of residual tumor cells, (3) bystander effect may mediate cell death within 5-7.5 mm of a cell that has been directly hit, and (4) there may be post-radiation immune responses that either inhibit tumor growth or lead to phagocytosis of residual neoplastic cells."[129]

Potential advantages of SBRT over conventional RT protocols include decreased expense and greater convenience.[130] This, in combination with the fact that PC is thought to have severe fractionation sensitivity (a low α/β ratio) has spurned several investigations into either the safety and/or efficacy of various SBRT protocols for low-to-intermediate risk, localized PC.[131-141] SBRT has also been investigated for use in other pelvic malignancies, including cervical and rectal cancer.[142-144] Overall, these early reports suggest that SBRT is well-tolerated. The incidence of acute GI and GU toxicities appears lower after SBRT than conventionally-fractionated three-dimensional conformal RT. Late GI and GU toxicities are also uncommonly reported after SBRT. This should be interpreted carefully though, as long-term follow-up is clearly lacking, and at least one set of investigators have suggested that the small number of reported severe late toxicities may be just the tip of the iceberg.[135,145] These same investigators have noted significant improvements in rates and severity of GI toxicity when the interfraction interval is longer than 24 hours; this observation suggests a consequential component of the observed toxicities, and is consistent with aforementioned preclinical data.[135,145] The incidence

of sexual toxicity in women has not been well reported. Sexual dysfunction following SBRT for PC has been thoroughly evaluated in one study, suggesting this new RT technique has had little impact on the incidence of RI-ED.[146]

Pelvic irradiation in companion animals

The first reports of pelvic irradiation in the veterinary literature described use of intraoperative RT (IORT) for canine bladder cancer.[147-149] Following a single fraction of 21.9 to 28.9 Gy, local recurrence was common, but 61% of dogs were alive at a year.[148] This compares favorably with dogs managed with medical therapy alone; dogs with transitional cell carcinoma of the urinary bladder that receive cytotoxic chemotherapy and an NSAID have a median survival time of 4.3 to 11 months.[150-153] More recently, EBRT has been used for both bladder cancer and anal sac adenocarcinoma (ASACA) in dogs. Outcomes have been encouraging for dogs receiving fractionated RT for TCC of the bladder.[154,155] Data concerning local tumor control and progression-free survival is lacking in the ASACA literature, however, reported overall survival times for dogs receiving RT as part of their treatment for ASACA are quite high (719-956 days).[156,157]

Despite these promising data, enthusiasm for more rigorous evaluations of EBRT for pelvic tumors in dogs, through prospective and randomized clinical trials, has been limited. This is largely due to the fact that pelvic irradiation has historically been associated with a high rate of severe radiation-associated complications. Following the aforementioned IORT protocols for bladder cancer, dogs experienced increased frequency of micturition (46%), urinary incontinence (46%), cystitis (38%) and stranguria (15%).[148] These signs were attributable to bladder fibrosis,

as well as muscle and nerve injury in the bladder wall.[147] Fractionated RT protocols have also been associated with rates of late GI and/or GU complications exceeding 30%. As expected based upon the pathophysiology underlying development of late effects, Arthur and Anderson have both suggested that large fraction size (≥ 3 Gy) and large field size are risk factors for late pelvic toxicity.[158,159] There are few reports which document the ability of modern irradiation techniques to limit the incidence and/or severity of acute and late radiation-associated toxicities in dogs. Tissue expander devices, together with helical tomotherapy, appear to minimize acute GI and GU toxicity in dogs; sufficiently powered studies have not been performed to know if such techniques affect the risk of developing late effects.[154] Radiation-associated sexual toxicity has not been evaluated in companion animals. It should be noted that most radiation effects in clinical veterinary studies are classified according to a modified version of the RTOG criteria, published by the Veterinary Radiation Therapy Oncology Group.[160] By convention, chemotherapy toxicities in veterinary patients enrolled in prospective clinical trials are scored according to CTCAE version 3.[33]

Statement of the problem

There is a clear role for inclusion of EBRT in management of many human pelvic malignancies. EBRT is also an emerging therapy for management of several pelvic neoplasms in dogs. However, pelvic RT is plagued with a high rate of normal tissue complications. In many cases, development of effective preventative or therapeutic interventions is limited by incomplete understanding of the pathophysiologic changes underlying development of these complications.

The goal of this research was to evaluate outcomes of pelvic irradiation in normal and tumor-bearing dogs. Specifically, we sought to retrospectively evaluate tolerability and effectiveness of full-course, fractionated IMRT combined with image-guidance in the setting of spontaneous GU tract carcinomas in dogs; findings are detailed in Chapter 2. We also sought to develop a canine model for studying the pathophysiology of RI-ED. For this laboratory investigation, prostatic SBRT was delivered to healthy, sexually-intact male dogs. Erectile function, as well as several biomarkers of vascular and neurologic function were evaluated before and after irradiation; findings are presented in Chapter 3. Severe and unexpected colorectal toxicities were observed in dogs receiving high-dose prostatic SBRT as part of the RI-ED study. This spurned investigation of rectal toxicity following pelvic SBRT through a dose-response study; results are detailed in Chapter 4. Concluding thoughts are provided in Chapter 5.

REFERENCES

1. Willett CG, Tepper JE, Cohen AM, et al. Failure patterns following curative resection of colonic carcinoma. *Ann Surg* 1984;200:685-690.
2. Metzger U. Adjuvant therapy for colorectal carcinoma. *World Journal of Surgery* 1991;15:576-582.
3. Hind R, Rew DR, Johnson CD. Surgical excision alone is adequate treatment for primary colorectal cancer. *Annals of the Royal College of Surgeons of England* 1992;74:63-67.
4. Fuchs CS, Mayer RJ. Adjuvant chemotherapy for colon and rectal cancer. *Seminars in Oncology* 1995;22:472-487.
5. Andre T, Boni C, Mounedji-Boudiaf L, et al. Oxaliplatin, fluorouracil, and leucovorin as adjuvant treatment for colon cancer. *New England Journal of Medicine* 2004;350:2343-2351.
6. Braendengen M, Tveit KM, Berglund A, et al. Randomized phase III study comparing preoperative radiotherapy with chemoradiotherapy in nonresectable rectal cancer. *Journal of Clinical Oncology* 2008;26:3687-3694.
7. Gerard JP, Conroy T, Bonnetain F, et al. Preoperative radiotherapy with or without concurrent fluorouracil and leucovorin in T3-4 rectal cancers: Results of FFCD 9203. *Journal of Clinical Oncology* 2006;24:4620-4625.
8. Pettersson D, Holm T, Iversen H, et al. Preoperative short-course radiotherapy with delayed surgery in primary rectal cancer. *British Journal of Surgery* 2012;99:577-583.
9. Mohiuddin M, Marks G. Adjuvant radiation therapy for colon and rectal cancer. *Seminars in Oncology* 1991;18:411-420.
10. Willett CG, Goldberg S, Shellito PC, et al. Does postoperative irradiation play a role in the adjuvant therapy of stage T4 colon cancer? *Cancer Journal from Scientific American* 1999;5:242-247.
11. Jemal A, Siegel R, Ward E, et al. Cancer statistics, 2006. *Ca-a Cancer Journal for Clinicians* 2006;56:106-130.
12. Jin XW, Lipold L, Sikon A, et al. Human papillomavirus vaccine: Safe, effective, underused. *Cleveland Clinic Journal of Medicine* 2013;80:49-60.
13. Fagundes H, Perez CA, Grigsby PW, et al. Distant metastases after irradiation alone in carcinoma of the uterine cervix. *International Journal of Radiation Oncology Biology Physics* 1992;24:197-204.
14. Benedetti-Panici P, Maneschi F, D'Andrea G, et al. Early cervical carcinoma - The natural history of lymph node involvement redefined on the basis of thorough parametrectomy and giant section study. *Cancer* 2000;88:2267-2274.
15. Douple EB, Richmond RC. Review of platinum complex biochemistry suggests a rationale for combined platinum radiotherapy. *International Journal of Radiation Oncology Biology Physics* 1979;5:1335-1339.
16. Green JA, Kirwan JM, Tierney JF, et al. Survival and recurrence after concomitant chemotherapy and radiotherapy for cancer of the uterine cervix: a systematic review and meta-analysis. *Lancet* 2001;358:781-786.
17. McNeal JE. Regional morphology and pathology of prostate. *American Journal of Clinical Pathology* 1968;49:347-&.
18. McNeal JE. Origin and development of carcinoma in prostate. *Cancer* 1969;23:24-&.

19. Partin AW, Kattan MW, Subong ENP, et al. Combination of prostate-specific antigen, clinical stage, and gleason score to predict pathological stage of localized prostate cancer - A multi-institutional update. *Jama-Journal of the American Medical Association* 1997;277:1445-1451.

20. Perrotti M, Pantuck A, Rabbani F, et al. Review of staging modalities in clinically localized prostate cancer. *Urology* 1999;54:208-214.

21. Montie JE, Pienta KJ. Review of the role of androgenic hormones in the epidemiology of benign prostatic hyperplasia and prostate cancer. *Urology* 1994;43:892-899.

22. Gleason DF. Histologic grading of prostate cancer - a perspective. *Human Pathology* 1992;23:273-279.

23. Sylvester JE, Blasko JC, Grimm PD, et al. Ten-year biochemical relapse-free survival after external beam radiation and brachytherapy for localized prostate cancer: The Seattle experience. *International Journal of Radiation Oncology Biology Physics* 2003;57:944-952.

24. Bul M, Zhu XY, Valdagni R, et al. Active surveillance for low-risk prostate cancer worldwide: the PRIAS study. *European Urology* 2013;63:597-603.

25. Kupelian P, Katcher J, Levin H, et al. External beam radiotherapy versus radical prostatectomy for clinical stage T1-2 prostate cancer: Therapeutic implications of stratification by pretreatment PSA levels and biopsy gleason scores. *Cancer Journal from Scientific American* 1997;3:78-87.

26. Damico AV, Whittington R, Kaplan I, et al. Equivalent biochemical failure-free survival after external beam radiation therapy or radical prostatectomy in patients with a pretreatment prostate specific antigen of >4-20 ng/ml. *International Journal of Radiation Oncology Biology Physics* 1997;37:1053-1058.

27. Ischia J, Gleave M. Radical prostatectomy in high-risk prostate cancer. *International Journal of Urology* 2013;20:290-300.

28. Roach M, DeSilvio M, Lawton C, et al. Phase III trial comparing whole-pelvic versus prostate-only radiotherapy and neoadjuvant versus adjuvant combined androgen suppression: Radiation therapy oncology group 9413. *Journal of Clinical Oncology* 2003;21:1904-1911.

29. Hanks GE, Pajak TF, Porter A, et al. Phase III trial of long-term adjuvant androgen deprivation after neoadjuvant hormonal cytoreduction and radiotherapy in locally advanced carcinoma of the prostate: The Radiation Therapy Oncology Group Protocol 92-02. *Journal of Clinical Oncology* 2003;21:3972-3978.

30. Oudard S. Progress in emerging therapies for advanced prostate cancer. *Cancer Treatment Reviews* 2013;39:275-289.

31. Lawton CA, Won MH, Pilepich MV, et al. Long-term treatment sequelae following external beam irradiation for adenocarcinoma of the prostate - analysis of RTOG study 7506 and study 7706. *International Journal of Radiation Oncology Biology Physics* 1991;21:935-939.

32. LENT SOMA tables - table of contents. *Radiotherapy and Oncology* 1995;35:17-60.

33. Trotti A, Colevas AD, Setser A, et al. CTCAE v3.0: Development of a comprehensive grading system for the adverse effects of cancer treatment. *Seminars in Radiation Oncology* 2003;13:176-181.

34. Stewart FA. Mechanism of bladder damage and repair after treatment with radiation and cytostatic drugs. *British Journal of Cancer* 1986;53:280-291.

35. Jaal J, Dorr W. Radiation-induced damage to mouse urothelial barrier. *Radiotherapy and Oncology* 2006;80:250-256.

36. Jaal J, Dorr W. Radiation induced late damage to the barrier function of small blood vessels in mouse bladder. *Journal of Urology* 2006;176:2696-2700.

37. Jaal J, Dorr W. Radiation induced inflammatory changes in the mouse bladder: The role of cyclooxygenase-2. *Journal of Urology* 2006;175:1529-1533.

38. Dorr W, Eckhardt M, Ehme A, et al. Pathogenesis of acute radiation effects in the urinary bladder - Experimental results. *Strahlentherapie Und Onkologie* 1998;174:93-95.

39. Marks LB, Carroll PR, Dugan TC, et al. The response of the urinary bladder, urethra, and ureter to radiation and chemotherapy. *International Journal of Radiation Oncology Biology Physics* 1995;31:1257-1280.

40. Elliott SP, Meng MV, Elkin EP, et al. Incidence of urethral stricture after primary treatment for prostate cancer: Data from CaPSURE. *Journal of Urology* 2007;178:529-534.

41. Glass AS, McAninch JW, Zaid UB, et al. Urethroplasty after radiation therapy for prostate cancer. *Urology* 2012;79:1402-1405.

42. Elliott SP, McAninch JW, Chi T, et al. Management of severe urethral complications of prostate cancer therapy. *Journal of Urology* 2006;176:2508-2513.

43. Sindelar WF, Tepper JE, Kinsella TJ, et al. Late effects of intraoperative radiation therapy on retroperitoneal tissues, intestine, and bile duct in a large animal model. *International Journal of Radiation Oncology Biology Physics* 1994;29:781-788.

44. Deluca AM, Johnstone PAS, Ollayos CW, et al. Tolerance of the bladder to intraoperative radiation in a canine model - a 5-year follow-up. *International Journal of Radiation Oncology Biology Physics* 1994;30:339-345.

45. Abitbol MM, Davenpor.Jh. Irradiated vagina. *Obstetrics and Gynecology* 1974;44:249-256.

46. Grigsby PW, Russell A, Bruner D, et al. Late injury of cancer therapy on the female reproductive tract. *International Journal of Radiation Oncology Biology Physics* 1995;31:1281-1299.

47. Incrocci L, Jensen PT. Pelvic radiotherapy and sexual function in men and women. *Journal of Sexual Medicine* 2013;10:53-64.

48. Ploch E. Hormonal replacement therapy in patients after cervical cancer treatment. *Gynecologic Oncology* 1987;26:169-177.

49. Jensen PT, Groenvold M, Klee MC, et al. Longitudinal study of sexual function and vaginal changes after radiotherapy for cervical cancer. *International Journal of Radiation Oncology Biology Physics* 2003;56:937-949.

50. Pitkin RM, Vanvoorh.Lw. Postirradiation vaginitis - evaluation of prophylaxis with topical estrogen. *Radiology* 1971;99:417-&.

51. Pitkin RM, Bradbury JT. Effect of topical estrogen on irradiated vaginal epithelium. *American Journal of Obstetrics and Gynecology* 1965;92:175-&.

52. Cullen K, Fergus K, DasGupta T, et al. From "sex toy" to intrusive imposition: A qualitative examination of women's experiences with vaginal dilator use following treatment for gynecological cancer. *Journal of Sexual Medicine* 2012;9:1162-1173.

53. Decruze SB, Guthrie D, Magnani R. Prevention of vaginal stenosis in patients following vaginal brachytherapy. *Clinical Oncology* 1999;11:46-48.

54. Krumm S, Lamberti J. Changes in sexual behavior following radiation therapy for cervical cancer. *Journal of Psychosomatic Obstetrics and Gynecology* 1993;14:51-63.

55. Amsterdam A, Carter J, Krychman M. Prevalence of psychiatric illness in women in an oncology sexual health population: A retrospective pilot study. *Journal of Sexual Medicine* 2006;3:292-295.

56. Dimitriadis F, Karakitsios K, Tsounapi P, et al. Erectile function and male reproduction in men with spinal cord injury: a review. *Andrologia* 2010;42:139-165.

57. Zagars GK, Pollack A. Serum testosterone levels after external beam radiation for clinically localized prostate cancer. *International Journal of Radiation Oncology Biology Physics* 1997;39:85-89.

58. Pickles T, Graham P, British Columbia Canc Agency P. What happens to testosterone after prostate radiation monotherapy and does it matter? *Journal of Urology* 2002;167:2448-2452.

59. Nichols RC, Morris CG, Hoppe BS, et al. Proton radiotherapy for prostate cancer is not associated with post-treatment testosterone suppression. *International Journal of Radiation Oncology Biology Physics* 2012;82:1222-1226.

60. Fishel B, Chen J, Alon M, et al. Pudendal nerve conduction to evaluate organic erectile dysfunction. *American Journal of Physical Medicine & Rehabilitation* 2001;80:885-888.

61. Dean RC, Lue TF. Physiology of penile erection and pathophysiology of erectile dysfunction. *Urologic Clinics of North America* 2005;32:379-+.

62. Goldstein I, Feldman MI, Deckers PJ, et al. Radiation-associated impotence - a clinical study of its mechanism. *Jama-Journal of the American Medical Association* 1984;251:903-910.

63. Incrocci L, Slob AK, Levendag PC. Sexual (dys)function after radiotherapy for prostate cancer: A review. *International Journal of Radiation Oncology Biology Physics* 2002;52:681-693.

64. Incrocci L. Sexual function after external-beam radiotherapy for prostate cancer: What do we know? *Critical Reviews in Oncology Hematology* 2006;57:165-173.

65. van der Wielen GJ, Mulhall JP, Incrocci L. Erectile dysfunction after radiotherapy for prostate cancer and radiation dose to the penile structures: A critical review. *Radiotherapy and Oncology* 2007;84:107-113.

66. Mulhall J, Ahmed A, Parker M, et al. The hemodynamics of erectile dysfunction following external beam radiation for prostate cancer. *Journal of Sexual Medicine* 2005;2:432-437.

67. Zelefsky MJ, Eid JF. Elucidating the etiology of erectile dysfunction after definitive therapy for prostatic cancer. *International Journal of Radiation Oncology Biology Physics* 1998;40:129-133.

68. Merrick GS, Butler WM, Wallner KE, et al. Erectile function after prostate brachytherapy. *International Journal of Radiation Oncology Biology Physics* 2005;62:437-447.

69. Merrick GS, Butler WM, Wallner KE, et al. The importance of radiation doses to the penile bulb vs. crura in the development of postbrachytherapy erectile dysfunction. *International Journal of Radiation Oncology Biology Physics* 2002;54:1055-1062.

70. Wright JL, Newhouse JH, Laguna JL, et al. Localization of neurovascular bundles on pelvic CT and evaluation of radiation dose to structures putatively involved in erectile dysfunction after prostate brachytherapy. *International Journal of Radiation Oncology Biology Physics* 2004;59:426-435.

71. Selek U, Cheung R, Lii M, et al. Erectile dysfunction and radiation dose to penile base structures: A lack of correlation. *International Journal of Radiation Oncology Biology Physics* 2004;59:1039-1046.

72. McLaughlin PW, Troyer S, Berri S, et al. Functional anatomy of the prostate: Implications for treatment planning. *International Journal of Radiation Oncology Biology Physics* 2005;63:479-491.

73. McLaughlin PW, Narayana V, Meriowitz A, et al. Vessel-sparing prostate radiotherapy: Dose limitation to critical erectile vascular structures (internal pudendal artery and corpus cavernosum) defined by MRI. *International Journal of Radiation Oncology Biology Physics* 2005;61:20-31.

74. Merlin SL, Brock GB, Begin LR, et al. New insights into the role of endothelin-1 in radiation-associated impotence. *International Journal of Impotence Research* 2001;13:104-109.

75. Carrier S, Hricak H, Lee SS, et al. Radiation-induced decrease in nitric oxide synthase containing nerves in the rat penis. *Radiology* 1995;195:95-99.

76. Ko WJ, Truesdale MD, Hruby GW, et al. Impacting factors for recovery of erectile function within 1 year following robotic-assisted laparoscopic radical prostatectomy. *Journal of Sexual Medicine* 2011;8:1805-1812.

77. DiBiase SJ, Wallner K, Tralins K, et al. Brachytherapy radiation doses to the neurovascular bundles. *International Journal of Radiation Oncology Biology Physics* 2000;46:1301-1307.

78. Merrick GS, Butler WM, Dorsey AT, et al. A comparison of radiation dose to the neurovascular bundles in men with and without prostate brachytherapy-induced erectile dysfunction. *International Journal of Radiation Oncology Biology Physics* 2000;48:1069-1074.

79. Zagaja GP, Mhoon DA, Aikens JE, et al. Sildenafil in the treatment of erectile dysfunction after radical prostatectomy. *Urology* 2000;56:631-634.

80. Incrocci L, Hop WCJ, Slob AK. Efficacy of sildenafil in an open-label study as a continuation of a double-blind study in the treatment of erectile dysfunction after radiotherapy for prostate cancer. *Urology* 2003;62:116-120.

81. Incrocci L, Slagter C, Slob AK, et al. A randomized, double-blind, placebo-controlled, cross-over study to assess the efficacy of tadalafil (Cialis (R)) in the treatment of erectile dysfunction following three-dimensional conformal external-beam radiotherapy. *International Journal of Radiation Oncology Biology Physics* 2006;66:439-444.

82. Incrocci L, Slob AK, Hop WCJ. Tadalafil (Cialis) and erectile dysfunction after radiotherapy for prostate cancer: An open-label extension of a blinded trial. *Urology* 2007;70:1190-1193.

83. Wallner KE, Merrick GS, Benson ML, et al. Penile bulb imaging. *International Journal of Radiation Oncology Biology Physics* 2002;53:928-933.

84. Merrick GS, Wallner K, Butler WM, et al. A comparison of radiation dose to the bulb of the penis in men with and without prostate brachytherapy-induced erectile dysfunction. *International Journal of Radiation Oncology Biology Physics* 2001;50:597-604.

85. Pollack A, Zagars GK, Starkschall G, et al. Conventional vs conformal radiotherapy for prostate cancer: Preliminary results of dosimetry and acute toxicity. *International Journal of Radiation Oncology Biology Physics* 1996;34:555-564.

86. Dewit L, Ang KK, Vanderschueren E. Acute side effects and late complications after radiotherapy of localized carcinoma of the prostate. *Cancer Treatment Reviews* 1983;10:79-&.

87. Cai WB, Roberts SA, Potten CS. The number of clonogenic cells in crypts in three regions of murine large intestine. *International Journal of Radiation Biology* 1997;71:573-579.

88. Dewit L, Oussoren Y, Bartelink H. Early and late damage in the mouse rectum after irradiation and cis-diamminedichloroplatinum(II). *Radiotherapy and Oncology* 1987;8:57-69.

89. Followill DS, Kester D, Travis EL. Histological changes in mouse colon after single dose and split dose irradiation. *Radiation Research* 1993;136:280-288.

90. Northway MG, Scobey MW, Geisinger KR. Radiation proctitis in the rat - sequential changes and effects of anti-inflammatory agents. *Cancer* 1988;62:1962-1969.

91. Withers HR. Regeneration of intestinal mucosa after irradiation. *Cancer* 1971;28:75-&.

92. Withers HR, Mason KA. Kinetics of recovery in irradiated colonic mucosa of mouse. *Cancer* 1974;34:896-903.

93. Hovdenak N, Sorbye H, Dahl O. Sucralfate does not ameliorate acute radiation proctitis: Randomised study and meta-analysis. *Clinical Oncology* 2005;17:485-491.

94. Langberg CW, Hauerjensen M, Sung CC, et al. Expression of fibrogenic cytokines in rat small intestine after fractionated irradiation. *Radiotherapy and Oncology* 1994;32:29-36.

95. Richter KK, Langberg CW, Sung CC, et al. Association of transforming growth factor beta (TGF-beta) immunoreactivity with specific histopathologic lesions in subacute and chronic experimental radiation enteropathy. *Radiotherapy and Oncology* 1996;39:243-251.

96. Hubmann FH. Effect of x-irradiation on the rectum of the rat. *British Journal of Radiology* 1981;54:250-254.

97. Tamou S, Trott KR. The effects of local x-irradiation on the distensibility of the rectum in rats. *British Journal of Radiology* 1995;68:64-69.

98. O'Brien PC. Radiation injury of the rectum. *Radiotherapy and Oncology* 2001;60:1-14.

99. Shadad AK, Sullivan FJ, Martin JD, et al. Gastrointestinal radiation injury: Prevention and treatment. *World Journal of Gastroenterology* 2013;19:199-208.

100. Dorr W, Hendry JH. Consequential late effects in normal tissues. *Radiotherapy and Oncology* 2001;61:223-231.

101. van der Kogel AJ, Jarrett KA, Paciotti MA, et al. Radiation tolerance of the rat rectum to fractionated x-rays and pi-mesons. *Radiotherapy and Oncology* 1988;12:225-232.

102. Dubray BM, Thames HD. Chronic radiation damage in the rat rectum - an analysis of the influences of fractionation, time and volume. *Radiotherapy and Oncology* 1994;33:41-47.

103. Denham JW, Hauer-Jensen M, Kron T, et al. Treatment-time-dependence models of early and delayed radiation injury in rat small intestine. *International Journal of Radiation Oncology Biology Physics* 2000;48:871-887.

104. Langberg CW, Waldron JA, Baker ML, et al. Significance of overall treatment time for the development of radiation-induced intestinal complications - an experimental study in the rat. *Cancer* 1994;73:2663-2668.

105. Langberg CW, Sauer T, Reitan JB, et al. Influence of fractionation schedule on development of intestinal complications following localized irradiation - an experimental study in the rat. *Acta Oncologica* 1994;33:403-408.

106. Trott KR, Breiter N, Spiethoff A. Experimental studies on the pathogenesis of the chronic radiation ulcer of the large bowel in rats. *International Journal of Radiation Oncology Biology Physics* 1986;12:1637-1643.

107. MacNaughton WK, Aurora AR, Bhamra J, et al. Expression, activity and cellular localization of inducible nitric oxide synthase in rat ileum and colon post-irradiation. *International Journal of Radiation Biology* 1998;74:255-264.

108. Francois A, Dublineau I, Lebrun F, et al. Modified absorptive and secretory processes in the rat distal colon after neutron irradiation: In vivo and in vitro studies. *Radiation Research* 1999;151:468-478.

109. Kummermehr J, Trott KR. Chronic radiation damage in the rat rectum - an analysis of the influences of fractionation, time and volume. *Radiotherapy and Oncology* 1994;33:91-92.

110. Sanguineti G, Franzone P, Marcenaro M, et al. Sucralfate versus mesalazine versus hydrocortisone in the prevention of acute radiation proctitis during conformal radiotherapy for prostate carcinoma - A randomized study. *Strahlentherapie Und Onkologie* 2003;179:464-470.

111. Kneebone A, Mameghan H, Bolin T, et al. Effect of oral sucralfate on late rectal injury associated with radiotherapy for prostate cancer: A double-blind, randomized trial. *International Journal of Radiation Oncology Biology Physics* 2004;60:1088-1097.

112. Katsanos KH, Briasoulis E, Tsekeris P, et al. Randomized phase II exploratory study of prophylactic amifostine in cancer patients who receive radical radiotherapy to the pelvis. *Journal of Experimental & Clinical Cancer Research* 2010;29:9.

113. Wedlake LJ, Silia F, Benton B, et al. Evaluating the efficacy of statins and ACE-inhibitors in reducing gastrointestinal toxicity in patients receiving radiotherapy for pelvic malignancies. *European Journal of Cancer* 2012;48:2117-2124.

114. Thotala DK, Geng L, Dickey AK, et al. A new class of molecular targeted radioprotectors: GSK-3 beta inhibitors. *International Journal of Radiation Oncology Biology Physics* 2010;76:557-565.

115. McKay GD, Wong K, Kozman DR. Laparoscopic insertion of pelvic tissue expander to prevent radiation enteritis prior to radiotherapy for prostate cancer. *Radiation Oncology* 2011;6.

116. Wilder RB, Barme GA, Gilbert RF, et al. Cross-linked hyaluronan gel improves the quality of life of prostate cancer patients undergoing radiotherapy. *Brachytherapy* 2011;10:44-50.

117. Forsythe K, Blacksburg S, Stone N, et al. Intensity-modulated radiotherapy causes fewer side effects than three-dimensional conformal radiotherapy when used in combination with brachytherapy for the treatment of prostate cancer. *International Journal of Radiation Oncology Biology Physics* 2012;83:630-635.

118. Brown MW, Brooks JP, Albert PS, et al. An analysis of erectile function after intensity modulated radiation therapy for localized prostate carcinoma. *Prostate Cancer and Prostatic Diseases* 2007;10:189-193.

119. Thomsen JB, Arp DT, Carl J. Urethra sparing - potential of combined Nickel-Titanium stent and intensity modulated radiation therapy in prostate cancer. *Radiotherapy and Oncology* 2012;103:256-260.

120. Vainshtein J, Abu-Isa E, Olson KB, et al. Randomized phase II trial of urethral sparing intensity modulated radiation therapy in low-risk prostate cancer: implications for focal therapy. *Radiation Oncology* 2012;7:9.

121. Benedict SH, Yenice KM, Followill D, et al. Stereotactic body radiation therapy: The report of AAPM Task Group 101. *Medical Physics* 2010;37:4078-4101.

122. Garcia-Barros M, Paris F, Cordon-Cardo C, et al. Tumor response to radiotherapy regulated by endothelial cell apoptosis. *Science* 2003;300:1155-1159.

123. Garcia-Barros M, Lacorazza D, Petrie H, et al. Host acid sphingomyelinase regulates microvascular function not tumor immunity. *Cancer Research* 2004;64:8285-8291.

124. Dhakal S, Corbin KS, Milano MT, et al. Stereotactic body radiotherapy for pulmonary metastases from soft-tissue sarcomas: Excellent local lesion control and improved patient survival. *International Journal of Radiation Oncology Biology Physics* 2012;82:940-945.

125. Roh KW, Jang JS, Kim MS, et al. Fractionated stereotactic radiotherapy as reirradiation for locally recurrent head and neck cancer. *International Journal of Radiation Oncology Biology Physics* 2009;74:1348-1355.

126. Levine AM, Coleman C, Horasek S. Stereotactic radiosurgery for the treatment of primary sarcomas and sarcoma metastases of the spine. *Neurosurgery* 2009;64:A54-A59.

127. Arvidson NB, Mehta MP, Tome WA. Dose coverage beyond the gross tumor volume for various steroetactic body radiotherapy planning techniques reporting similar control for Stage I non-small-cell lung cancer. *International Journal of Radiation Oncology Biology Physics* 2008;72:1597-1603.

128. Sultanem K, Niazi T, Bahoric B, et al. Target volume definition in head and neck IMRT treatment planning: Can we omit high dose clinical target volume (CTV HD)? *International Journal of Radiation Oncology Biology Physics* 2009;75:S416-S416.

129. Nolan M, Griffin L, Custis J, et al. Stereotactic body radiation therapy for treatment of feline injection-site sarcomas: 11 cases (2008-2012). *Journal of the American Veterinary Medical Association*, 2013;In Press.

130. Hodges JC, Lotan Y, Boike TP, et al. Cost-effectiveness analysis of SBRT versus IMRT: An emerging initial radiation treatment option for organ-confined prostate cancer. *American Journal of Managed Care* 2012;18:E186-E192.

131. Madsen BL, Hsi RA, Pham HT, et al. Stereotactic hypofractionated accurate radiotherapy of the prostate (SHARP), 33.5 Gy in five fractions for localized disease: First clinical trial results. *International Journal of Radiation Oncology Biology Physics* 2007;67:1099-1105.

132. Tang CI, Loblaw DA, Cheung P, et al. Phase I/II study of a five-fraction hypofractionated accelerated radiotherapy treatment for low-risk localised prostate cancer: early results of pHART3. *Clinical Oncology* 2008;20:729-737.

133. Aluwini S, van Rooij P, Hoogeman M, et al. CyberKnife stereotactic radiotherapy as monotherapy for low- to intermediate-stage prostate cancer: Early experience, feasibility, and tolerance. *Journal of Endourology* 2010;24:865-869.

134. Katz AJ, Santoro M, Ashley R, et al. Stereotactic body radiotherapy as boost for organ-confined prostate cancer. *Technology in Cancer Research & Treatment* 2010;9:575-582.

135. King CR, Brooks JD, Gill H, et al. Long-term outcomes from a prospective trial of stereotactic body radiotherapy for low-risk prostate cancer. *International Journal of Radiation Oncology Biology Physics* 2012;82:877-882.

136. Friedland JL, Freeman DE, Masterson-McGary ME, et al. Stereotactic body radiotherapy: An emerging treatment approach for localized prostate cancer. *Technology in Cancer Research & Treatment* 2009;8:387-392.

137. McBride SM, Wong DS, Dombrowski JJ, et al. Hypofractionated stereotactic body radiotherapy in low-risk prostate adenocarcinoma. *Cancer* 2012;118:3681-3690.

138. Boike TP, Lotan Y, Cho LC, et al. Phase I dose-escalation study of stereotactic body radiation therapy for low- and intermediate-risk prostate cancer. *Journal of Clinical Oncology* 2011;29:2020-2026.

139. Bolzicco G, Favretto MS, Scremin E, et al. Image-guided stereotactic body radiation therapy for clinically localized prostate cancer: Preliminary clinical results. *Technology in Cancer Research & Treatment* 2010;9:473-477.

140. Kang JK, Cho CK, Choi CW, et al. Image-guided stereotactic body radiation therapy for localized prostate cancer. *Tumori* 2011;97:43-48.

141. Jabbari S, Weinberg VK, Kaprealian T, et al. Stereotactic body radiotherapy as monotherapy or post-external beam radiotherapy boost for prostate cancer: technique, early toxicity and PSA response. *International Journal of Radiation Oncology Biology Physics* 2012;82:228-234.

142. Higginson DS, Morris DE, Jones EL, et al. Stereotactic body radiotherapy (SBRT): Technological innovation and application in gynecologic oncology. *Gynecologic Oncology* 2011;120:404-412.

143. Guckenberger M, Bachmann J, Wulf J, et al. Stereotactic body radiotherapy for local boost irradiation in unfavourable locally recurrent gynaecological cancer. *Radiotherapy and Oncology* 2010;94:53-59.

144. DeFoe SG, Bernard ME, Rwigema JC, et al. Stereotactic body radiotherapy for the treatment of presacral recurrences from rectal cancers. *Journal of Cancer Research and Therapeutics* 2011;7:408-411.

145. King CR, Brooks JD, Gill H, et al. Stereotactic body radiotherapy for localized prostate cancer: interim results of a prospective phase II clinical trial. *International Journal of Radiation Oncology Biology Physics* 2009;73:1043-1048.

146. Wiegner EA, King CR. Sexual function after stereotactic body radiotherapy for prostate cancer: results of a prospective clinical trial. *International Journal of Radiation Oncology Biology Physics* 2010;78:442-448.

147. Withrow SJ, Gillette EL, Hoopes PJ, et al. Intraoperative irradiation of 16 spontaneously occurring canine neoplasms. *Veterinary Surgery* 1989;18:7-11.

148. Walker M, Breider M. Intraoperative radiotherapy of canine bladder cancer. *Veterinary Radiology* 1987;28:200-204.

149. Craig JA, Sigler R, Walker M. Effects of intraoperative irradiation on gastric and urinary bladder incisions in the dog. *American Journal of Veterinary Research* 1985;46:1647-1652.

150. Henry CJ, McCaw DL, Turnquist SE, et al. Clinical evaluation of mitoxantrone and piroxicam in a canine model of human invasive urinary bladder carcinoma. *Clinical Cancer Research* 2003;9:906-911.

151. Marconato L, Zini E, Lindner D, et al. Toxic effects and antitumor response of gemcitabine in combination with piroxicam treatment in dogs with transitional cell carcinoma of the urinary bladder. *Javma-Journal of the American Veterinary Medical Association* 2011;238:1004-1010.

152. Arnold EJ, Childress MO, Fourez LM, et al. Clinical trial of vinblastine in dogs with transitional cell carcinoma of the urinary bladder. *Journal of Veterinary Internal Medicine* 2011;25:1385-1390.

153. Moore AS, Cardona A, Shapiro W, et al. Cisplatin (cisdiamminedichloroplatinum) for treatment of transitional cell carcinoma of the urinary bladder or urethra - a retrospective study of 15 dogs. *Journal of Veterinary Internal Medicine* 1990;4:148-152.

154. Murphy S, Gutierrez A, Lawrence J, et al. Laparoscopically implanted tissue expander radiotherapy in canine transitional cell carcinoma. *Veterinary Radiology & Ultrasound* 2008;49:400-405.

155. Marconato L, Nitzl DB, Melzer-Ruess KJ, et al. Chemotherapy and radiation therapy in 4 dogs with muscle-invasive transitional cell carcinoma of the urinary tract. *Canadian Veterinary Journal-Revue Veterinaire Canadienne* 2012;53:875-879.

156. Turek MM, Forrest LJ, Adams WM, et al. Postoperative radiotherapy and mitoxantrone for anal sac adenocarcinoma in the dog: 15 cases (1991-2001). *Vet Comp Oncol* 2003;1:94-104.

157. Williams LE, Gliatto JM, Dodge RK, et al. Carcinoma of the apocrine glands of the anal sac in dogs: 113 cases (1985-1995). *J Am Vet Med Assoc* 2003;223:825-831.

158. Anderson CR, McNiel EA, Gillette EL, et al. Late complications of pelvic irradiation in 16 dogs. *Veterinary Radiology & Ultrasound* 2002;43:187-192.

159. Arthur JJ, Kleiter MM, Thrall DE, et al. Characterization of normal tissue complications in 51 dogs undergoing definitive pelvic region irradiation. *Veterinary Radiology & Ultrasound* 2008;49:85-89.

160. LaDue T, Klein MK. Toxicity criteria of the veterinary radiation therapy oncology group. *Veterinary Radiology & Ultrasound* 2001;42:475-476.

CHAPTER 2: INTENSITY-MODULATED AND IMAGE-GUIDED RADIATION THERAPY FOR TREATMENT OF GENITOURINARY CARCINOMAS IN DOGS

Brief Overview

Background – External beam radiation therapy can be used to treat pelvic tumors in dogs, but its utility is limited by lack of efficacy data and associated late complications.

Hypothesis/Objectives – The objective of this study was to assess local tumor control, overall survival and toxicosis following intensity-modulated and image-guided radiation therapy (IM/IGRT) for treatment of genitourinary carcinomas (CGUC) in dogs.

Animals – 21 client-owned dogs.

Methods – A retrospective study was performed. Medical records of patients for which there was intent to treat with a course of definitive-intent IM/IGRT for CGUC between 2008 and 2011 were reviewed. Descriptive and actuarial statistics comprised the data analysis.

Results –Primary tumors were located in the prostate (10), urinary bladder (9) or urethra (2). The total radiation dose ranged from 54-58 Gy, delivered in 20 daily fractions. Grade 1 and 2 acute gastrointestinal toxicoses developed in 33% and 5% of dogs, respectively. Grade 1 and 2 acute genitourinary, and grade 1 acute integumentary toxicoses were documented in 5%, 5% and 20% of dogs, respectively. Four dogs experienced late grade 3 gastrointestinal or genitourinary toxicosis. The subjective response rate was 60%. The median event-free survival was 317 days;

the overall median survival time was 654 days. Neither local tumor control nor overall survival were statistically dependent upon location of the primary tumor.

Conclusions and clinical importance – IM/IGRT is generally well-tolerated and provides an effective option for locoregional control of CGUC. As compared with previous reports in the veterinary literature, inclusion of IM/IGRT in multimodal treatment protocols for CGUC can result in superior survival times; controlled prospective evaluation is warranted.

Introduction

Genitourinary carcinomas (CGUC) in dogs, encompassing transitional cell carcinomas, adenocarcinomas and solid carcinomas of the urinary bladder, urethra and prostate, are locally aggressive tumors that have a high propensity for regional and distant metastasis. Death is often attributable to partial or complete urethral, ureteral obstruction, or both; 1-2 month survival times are typical when no therapy is pursued.[1] Palliation of clinical signs is often achievable through urinary diversion.[2-8] Such palliative measures can significantly improve quality of life but are not associated with significantly improved survival. The infiltrative nature of genitourinary carcinomas contributes to difficulties in achieving complete histological margins; as a result, tumors often recur within 3 to 10 months of more aggressive surgical interventions.[9-12] Survival can be extended through the use of non-steroidal anti-inflammatories (NSAIDs); median survival times of approximately 6 months have been reported in dogs that received NSAID monotherapy for CGUC.[13,14] NSAID therapy can also be combined with anti-neoplastic chemotherapy to improve survival and has been associated with survival times ranging from 4.3 to 11 months.[15-18]

Additionally, incorporation of external beam radiation therapy (RT) into multimodal treatment protocols is potentially beneficial for locoregional control of CGUC. Intraoperative RT following surgical cytoreduction, as well as fractionated external beam RT (FRT) for transitional cell carcinomas of the urinary tract have been associated with median survival times ranging from 4 to 15 months.[19-22]

Despite the potential benefits of RT, the high incidence (39-56%) of severe late radiation-associated toxicities (such as chronic colitis, cystitis, rectal perforations and strictures) following pelvico-abdominal radiation has kept definitive RT from inclusion as standard of care therapy in treatment of CGUC. Fraction and field size are known risk factors for development of late complications.[23,24]

In light of these limitations, there have been efforts to create RT protocols that are better tolerated by dogs. Use of laparoscopically-implanted tissue expander RT has been reported in two dogs; although there was clinically important morbidity associated with the surgically-implanted tissue expanders in both dogs, RT was apparently well-tolerated.[25] Helical Tomotherapy allows for delivery of intensity-modulated and image-guided RT (IM/IGRT). Target localization via image-guidance decreases interfraction variability in the position of the target within the patient, and thus enables employment of smaller treatment fields. Use of IMRT increases the conformity of radiation dose, allowing for rapid fall-off of radiation dose outside of target volumes. The use of smaller fields in combination with so-called "dose-painting" limits dose exposures in normal tissues and accounts for the improved tolerability of pelvico-abdominal IM/IGRT as compared with more traditional forms of FRT.

The goals of the present study were to: (1) determine the incidence and severity of both acute and late treatment-associated toxicities and (2) assess local and locoregional tumor control, as well as overall survival, following completion of IM/IGRT for treatment of CGUC. It was hypothesized that treatment-associated toxicities would be mild and self-limiting, and that IM/IGRT would improve local tumor control and survival, as compared with historically reported outcomes.

Methods

A descriptive retrospective analysis of data from dogs for which there was intent to complete IM/IGRT for CGUC at the Animal Cancer Center at Colorado State University (CSU-ACC) between June 2008 and July 2011 was performed. Histologic and/or cytologic evidence of a carcinoma in the genitourinary tract, as well as complete local and systemic staging (including complete blood count, serum biochemical profile, urinalysis, three-view thoracic radiographs, abdominal ultrasound and computed tomography of the pelvis) were requisite for inclusion.

A medical records review was performed. Information relating to patient demographics, oncologic histories, details of RT plans, response to treatment, local tumor control, toxicity and overall survival was extracted. Timing of follow-up examinations and restaging lacked uniformity; when possible, information about extent and duration of tumor responses, normal tissue toxicities and overall survival was obtained through review of medical records, and verbal follow-up with primary care veterinarians and pet owners.

A standardized and anonymous written questionnaire was administered to owners of dogs in this study, with the intent of determining the impact of RT on pets and pet owners; questions related to challenges and/or difficulties associated with the logistics of treatment (cost, travel, duration of therapy, etc), quality of life during and after completion of RT, overall outcomes and client satisfaction. Institutional Review Board approval for research involving human subjects was obtained prior to releasing this survey. Surveys were sent to owners whose pets completed RT prior to June 2011 (18/21 cases); although much of the information gathered through this survey could have been applied to the three cases with shorter follow-up times, protocol approval did not allow for prospective data collection. Likewise, the retrospective nature of case identification did not allow for a standard temporal relationship between the time of RT and the time of questionnaire administration.

Radiation Therapy. Computerized three-dimensional treatment planning was utilized in all cases. Simulation CT scans were obtained before and after intravenous administration of iodinated contrast medium, with patients positioned in lateral, dorsal or sternal recumbency. The current preference is to immobilize dogs in a Vac-Lok™ cushion, while positioned in lateral recumbency, with an Accu-Form™ cushion between their pelvic limbs to minimize interfraction variability of target tissue localization and maximize separation between the urinary and gastrointestinal tracts.[26] Dogs were positioned in right lateral recumbency in 68% of these cases. Grossly evident tumor was delineated using the CT scan and defined as the gross tumor volume (GTV). Radiation fields were extended 2 cm in all directions, but confined to the urogenital tract to encompass potential microscopic extension of local disease (clinical target volume, CTV). A final uniform field expansion of 0.5 cm comprised the planning target volume (PTV) and

accounted for possible intra- and interfraction variations in target position, shape and size. A second target within the IMRT field was created to include lymph nodes (plus a margin of 1 cm) when there was clinical or tomographic suspicion of lymph node metastasis (14/22 cases, confirmed by cytology or histopathology in 4/22); one patient's lymph nodes were irradiated prophylactically. Inverse planning was performed at an Eclipse^{TM} (v8.6) treatment planning workstation. Prescriptions for initial courses of IM/IGRT ranged from 54-58 Gy delivered in 20 daily fractions on a Monday to Friday basis (2.7–2.85 Gy per fraction administered over 28-31 days); lymph node prescriptions ranged from 28-54 Gy in 20 fractions. Institutional standards for radiation prescriptions in IMRT plans were applied; the prescribed isodose was normalized such that it covered at least 95% of the PTV, with the maximum global dose being 110% of the prescribed dose. Treatment plans typically involved 6-9 isocentrically-placed coplanar 6 or 10 MV X-ray beams which were shaped using dynamic multileaf collimation in a sliding-window fashion to achieve intensity-modulation. Plans were constructed using iterative inverse-planning with heterogeneity corrections to meet specified goals for both tumor/target volumes and organs at risk (OAR). OAR included colon, urethra, ureters and urinary bladder. Dose constraints varied during the development of our institutional IM/IGRT program, but generally adhered to our current standard, which is to constrain all OAR lying within the PTV to a maximum dose of 57 Gy, with no more than 54 Gy delivered to the colon lying outside of the PTV. Data regarding treatment volumes, prescriptions and normal tissue exposures are summarized in Tables 2.1 and 2.2, and Figure 2.1. A conformity index (CI) was calculated as follows: $CI = \frac{TV_{PIV}^2}{TV * PIV}$, where TV_{PIV} is volume of the target (PTV) covered by the prescription isodose, TV is 95% of the target volume and PIV is the prescription isodose volume. This index expresses the relationship between a fraction of the tumor volume covered by the prescription isodose and the

volume delineated by that isodose, thereby quantifying both coverage of the delineated target volumes and the dose gradient outside that volume. Thus, the conformity index provides an absolute score; this score is complementary to dose-volume histogram and dose-distribution data and adds to the armamentarium upon which overall RT plan quality can be judged, but should not be used alone for plan evaluation.[27,28] The mean value of the conformity index was 0.77 +/- 0.13 (range: 0.54 – 1.05). Individual treatment plan review was performed by an American College of Veterinary Radiology board-certified veterinary radiation oncologist and an American Board of Radiology certified therapeutic medical physicist. Patient specific plan quality assurance was performed for each field comprising the treatment plan using gamma analysis comparing treatment plan data to that measured using the Varian portal dosimetry system. A minimum of 95% gamma for a 3 mm distance to agreement and a 3% absolute dose difference was defined as a passing QA score.

Table 2.1: Absorbed dose within the target volumes

	GTV		**CTV**		**PTV**		**Lymph Nodes**	
	Vol (cc)	D_{99}	*Vol (cc)*	D_{99}	*Vol (cc)*	D_{95}	*Vol (cc)*	D_{95}
Min.	2.3	49.6	4.7	49.8	18.1	48.3	4.4	29.1
Max.	130.4	57.9	130.4	57.9	339.4	56.6	30.5	53.8
Median	16.6	54.9	23.6	55.6	60	54.1	43.3	40.9
Mean	25.1	54.7	31.6	54.7	83.9	53.9	39.7	40.2
Std. Dev.	29.5	2.6	27.7	2.5	71.3	1.7	17.3	8.3

Average size of and dose delivered to treatment volumes are detailed above. D_x refers to the radiation dose (in Gray) delivered to X% of the respective treatment volume.

Table 2.2: Absorbed dose within organs at risk

		Colon	Urethra	Ureters
D_{max} (Gy)	*Median*	58.2	56.8	56.4
	Mean	58.2	56.8	47.1
	Std. Dev.	1.5	2.1	17.1
$D_{X\ cc}$ (Gy)	*Median*	52.3	54.9	41.5
	Mean	51.4	52.2	37.5
	Std. Dev.	1.5	10.7	20.2
$V_{54\ Gy}$ (cc)	*Median*	2.9	0.7	0.1
	Mean	3.4	1.8	0.3
	Std. Dev.	2.7	2.5	0.4

Average values of the maximum dose (D_{max}) delivered to an organ at risk, minimum dose delivered to the X cubic centimeters of an organ at risk which are receiving the highest dose (D_x), and volume of an organ at risk exceeding 54 Gy (V_{54}). X = 4 cc for rectum, 0.5 cc for urethra, 0.25cc for ureters.

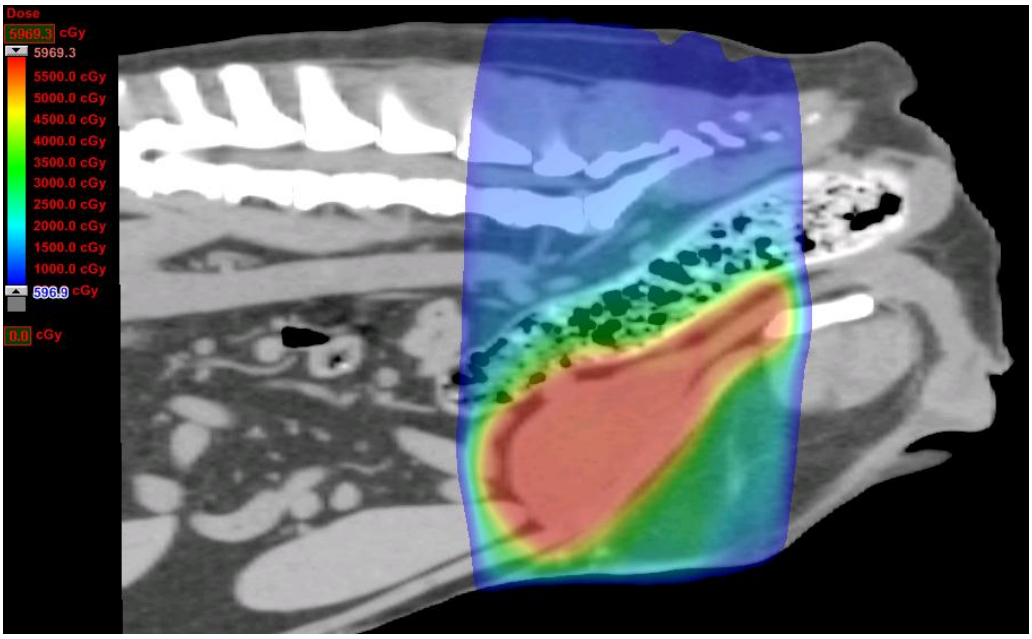

Figure 2.1: Typical dose distribution for IM/IGRT. Typical dose distribution for IM/IGRT, depicted as a color-wash superimposed over the simulation CT. A steep dose gradient between target volumes and organs at risk is shown with areas of relatively high dose in red and orange, and lower doses in yellow, green and blue.

All dogs were anesthetized for treatment; protocols varied, but generally included opioid premedications, followed by intravenous propofol and benzodiazepine induction and inhaled isoflurane maintenance. Daily image-guided patient position verification was performed with an

on-board kilovoltage cone-beam CT (kV-CBCT, Figure 2). Aside from lateral positioning, additional measures were employed to minimize interfraction variations in the size and shape of target tissues (especially important when treatment fields include all or part of the urinary bladder), which enabled conformity to the standard established by the 0.5cm PTV expansion. These measures included adherence to rigid dietary habits (meal size and times were as consistent as possible) and standardization of urination and defecation habits (patients were taken for a walk at a specific time each day, and then confined to a small living space or cage until anesthetic induction and RT, which occurred at approximately the same time each day). Diet, but not urinary habits were typically instituted prior to CT simulation. In patients with adequate cardiovascular function, modest intravenous crystalloid boluses were used to enlarge the bladder when bladder size was significantly smaller than planned. In these cases, small bladder size was defined as the bladder walls being at least 1 cm from the PTV margin. In such cases, judicious use of fluid therapy was a successful means of managing treatment volumes and minimizing radiation exposures in normal tissues. Due to variable patient size and variable bladder size in relation to the PTV margin, there was no standard intravenous fluid bolus size. Kilovoltage CBCT was repeated for position verification approximately 10 minutes after completing fluid administration. In cases where bladder size initially exceeded that allowed for by the PTV expansion, gentle manual expression of the urinary bladder and/or temporary urethral catheterization was performed to remove urine from the bladder; in such cases, kV-CBCT was also repeated after manipulation. Following position verification, IMRT was delivered using a Varian Trilogy^{TM} linear accelerator.

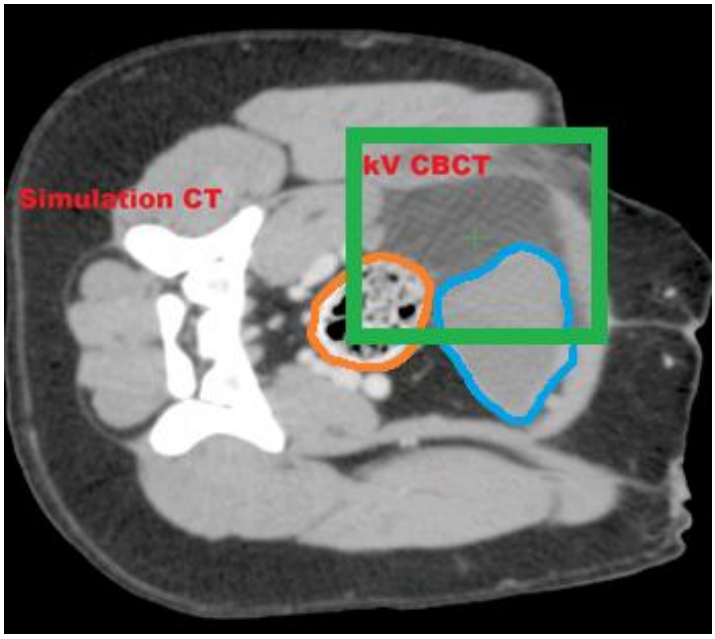

Figure 2.2: Example of patient position verification via three-dimensional imaging. The larger image is derived from a simulation CT scan; the smaller image (within the green box) is a representative example of a daily kV-CBCT for this patient. The colon (orange) and bladder (blue) are outlined. This demonstrates the high level of target and normal tissue reproducibility which is possible when employing three-dimensional image-guidance.

Offline dynamic adaptive RT (DART) was utilized in 6 of 22 of the presently described RT plans; RT plans were adapted once in 4 of the 6 cases and twice in 2 of the 6 cases. Plans were adapted when the PTV was deemed inappropriate; in all cases in this series, an inappropriate PTV was defined by the PTV margin being larger than what was needed to encompass the CTV for each daily fraction.

Data Analysis. Toxicity was graded according to the criteria for acute and late radiation morbidity, as defined by the Veterinary Radiation Therapy and Oncology Group.[29] Toxicity data were analyzed using descriptive statistics. Tumor control was reported according to RECIST criteria. Survival was defined as the time from the first fraction of RT until the time of first event or death. Local tumor control was described with Kaplan-Meier survival analysis of event

free survival (EFS). Events were defined as disease progression, late radiation-associated toxicity, death from any cause, or loss to follow-up; patients who had not experienced an event were censored at the time of data analysis. Overall survival was studied in a similar manner. Death from any cause was considered an event, and living dogs were censored at the time of Kaplan-Meier survival analysis. Log-rank analysis was employed to compare survival times between groups. All statistical analyses were performed using a commercial software package (SigmaStat© *v*3.5). A *P* value of < 0.05 was considered significant for all analyses.

Results

Patient Demographics and Oncologic Histories. Twenty-two treatment protocols were undertaken in 21 dogs, and 19 dogs completed 20 courses of IM/IGRT (Table 2.3). Seven of 21 dogs were female and 14 were male; all were neutered. Sixteen dogs had localized disease ($T_{2\text{-}3}N_0M_0$), four had locoregional lymph node metastases ($T_{2\text{-}3}N_1M_0$) and one had pulmonary metastases ($T_3N_0M_1$) at initiation of IM/IGRT. Two dogs failed to complete therapy; these dogs were included in the survival analysis. The first of these patients died of suspected paraneoplastic polyradiculoneuropathy prior to completion of IM/IGRT; no gross or histopathologic CNS abnormalities were identified on necropsy. The second patient had undergone ureteronephrectomy prior to starting IM/IGRT and developed a partial ureteral obstruction during RT; radiotherapy was discontinued prior to completion of the prescribed course, and the patient succumbed to acute renal failure secondary to complete ureteral obstruction 86 days after initiation of RT. Another dog completed a second course of IM/IGRT (49.5 Gy, delivered to the bladder, prostate and sublumbar lymph nodes, in 22 fractions) upon

local disease progression, which occurred 776 days after completion of the first course; this patient died 1043 days after initiation of the first course of IM/IGRT. This dog's overall survival time was included in analysis; however, tumor control and toxicity data were only analyzed for the first course of radiation, as the second course had an altered fractionation scheme.

Table 2.3: Location of index tumors. Twenty-one treatment protocols were initiated in 22 patients. Two dogs failed to complete therapy and another dog completed a second course upon local failure two years after completing the first course. In all, nineteen dogs completed twenty courses of IM/IGRT. Locations of index/primary tumor are detailed in this table.

Site of primary Tumor	**# dogs with intent to treat**	**# dogs that completed treatments**	**Total # of completed courses of treatment**
Bladder	9	7	8
*Prostate**	10	10	10
*Urethra***	2	2	2
Total	21	19	20

* or prostatic urethra; ** in female patients.

Neoadjuvant therapy included NSAID administration in 14 dogs, MTD chemotherapy (that which is delivered to the "maximally tolerated dose") in six dogs and surgery in three dogs prior to RT. Neoadjuvant antineoplastic drugs included carboplatin (2/6) and mitoxantrone (4/6). Four of these patients received both an NSAID and MTD chemotherapy prior to RT, whereas 10 had only an NSAID and 2 had only MTD chemotherapy. Surgical procedures performed prior to administration of RT included cytoreductive debulking (2/3) and ureteronephrectomy (1/3). All dogs treated with neoadjuvant therapy had local progression/recurrence prior to presentation, and all had macroscopic carcinomas present at the time they started IM/IGRT. NSAIDs were used in the adjuvant setting in twelve dogs. Adjuvant MTD chemotherapy was also utilized in twelve dogs, and included carboplatin (3/12), mitoxantrone (8/12), doxorubicin (2/12) and vinorelbine (2/12); some dogs received more than one antineoplastic drug after completing RT. No dog

received a multi-agent MTD chemotherapy protocol; dogs that received multiple chemotherapeutic drugs were switched from one agent to another upon detection of progressive disease. Of those dogs receiving adjuvant therapy, 8 had both an NSAID and chemotherapy following RT, whereas 4 had only an NSAID and 4 had only chemotherapy. None of these dogs received concurrent MTD chemotherapy and RT.

Toxicity. Acute radiation-associated gastrointestinal complications were most common. One dog (5%) suffered grade 2 colitis, while seven (33%) others experienced grade 1 colitis. Acute urinary complications presented as hematuria (grade 1) in one (5%) patient and stranguria (grade 2) in another patient (5%). Integumentary changes were limited to mild erythema and/or pigmentary changes, which developed in 4 patients (in all, 19% developed grade 1 acute integumentary toxicity). Regardless of body system involved, all acute radiation toxicoses were mild to moderate and self-limiting.

Delayed signs of radiation intoxication was less common, though severe when documented. Late radiation-associated complications were manifested as rectal (1), ureteral (1) and urethral (2) strictures. Overall, 4/21 (19%) developed grade 3 late GI or GU toxicity. Each presented 6-18 months after completion of IM/IGRT, and was successfully palliated with either stenting or surgery. Ureteral transposition was performed in one patient who was presented with ureteral obstruction which, based on unremarkable imaging studies and grossly normal appearance, was presumably due to radiation-induced fibrosis; a urethral stent was placed one month after the initial procedure due to partial urethral obstruction, which again was presumably due to radiation-induced fibrosis. Another dog had a rectal stent placed ten months after IM/IGRT due

to rectal stenosis; a urethral stent was later placed in the same patient to relieve obstruction caused by local tumor progression. A urethral stent was placed in one other dog to relieve clinical signs associated with malignant urethral obstruction six months after completion of IM/IGRT. There was no correlation between radiation prescription, delivered dose, overall radiation field size, plan adjustment via dynamic adaptive radiation therapy or calculated CI, and incidence of late toxicity.

Outcomes. Seventy-eight percent of pet owners responded to a standardized questionnaire; the responses suggested that treatment was associated with improved quality of life in the majority of patients. Sixty percent of respondents reported improved, and 30% reported unchanged quality of life after completion of IM/IGRT. Therefore, the subjective response rate, defined as those with improved quality of life (and therefore a reasonable substitution for objective response rate which would reflect those patients with partial and complete responses) was 60%. Because several patients initiated RT without clinical signs attributable to their lower urinary tract disease, the combination of dogs with demonstrable clinical responses (60%) and those with unchanged quality of life (30%) following completion of RT suggests the presently described treatment protocol was associated with potential clinical benefit in 90% of patients. The questionnaire was anonymous; therefore, the outcomes described by individual respondents cannot be correlated with known clinical data, including initial stage, neoadjuvant or adjuvant therapy, toxicoses or tumor control (Table 2.4).

Table 2.4: Summary of results from a standardized client questionnaire

Difficulties/challenges of radiation treatment:

	Extremely difficult or challenging	Very difficult or challenging	Moderately difficult or challenging	Minimally difficult or challenging	Not difficult or challenging
Cost*	1 (7.1%)	3 (21.4%)	8 (57.1%)	-	2 (14.3%)
Duration of treatment	1 (7.1%)	3 (21.4%)	4 (28.6%)	4 (28.6%)	2 (14.3%)
Distance traveled	1 (7.1%)	6 (42.9%)	2 (14.3%)	2 (14.3%)	3 (21.4%)

How informed did you feel you were about the:

	Very inadequately informed	Inadequately informed	Adequately informed	Very adequately informed
Potential side effects?	1 (7.1%)	1 (7.1%)	4 (28.6%)	8 (57.1%)
Expected outcome (tumor control and prognosis)?	2 (14.3%)	1 (7.1%)	7 (50.0%)	4 (28.6%)

Overall, how would you rate you pet's quality of life during or immediately following RT?

Much worse than before RT	Worse than before RT	Unchanged	Better than before RT	Much better than before RT
--	2 (15.4%)	5 (38.5%)	2 (15.4%)	4 (30.8%)

How often did your pet experience the following potential side effects since completing RT?

	Always	Most of the time	Some of the time	Infrequently	Never
Pain while defecating	1 (7.7%)	1 (7.7%)	4 (30.8%)	3 (23.1%)	4 (30.8%)
Difficulty defecating when he/she seems to desire to go	1 (7.7%)	3 (23.1%)	3 (23.1%)	2 (15.4%)	4 (30.8%)
Pain while urinating	1 (7.7%)	1 (7.7%)	2 (15.4%)	4 (30.8%)	5 (38.5%)
Difficulty urinating when he/she seems to desire to go	1 (8.3%)	2 (16.7%)	2 (16.7%)	3 (25%)	4 (33.3%)

Overall rating of pet's quality of life since radiation therapy:

Much worse than it was before RT	Worse than it was before RT	Unchanged	Better than it was before RT	Much better than it was before RT
--	1 (10.0%)	3 (30.0%)	1 (10.0%)	5 (50.0%)

Given what you know today, how likely would you be to:

	Very likely	Likely	Neutral	Not likely	Very unlikely
Still have opted to treat your pet's tumor with radiation:	13 (92.9%)	--	--	--	1 (7.1%)
Recommend radiation to a family member or friend who has a pet with similar problems:	11 (78.6%)	2 (14.3%)	--	--	1 (7.1%)

* The average cost of consultation, CT simulation, RT planning and IM/IGRT delivery for management of CGUC ranges from $5,500 to $6,000 at CSU-ACC.

The median time to first event in all patients was 317 days. Although there was a trend toward improved survival in dogs with primary prostatic disease (median EFS of 317 days) as compared to those with primary bladder disease (median EFS of 226 days), this difference was not statistically significant.

The median overall survival time (OST) was 654 days; as with EFS, there was no significant difference based upon site of primary disease.

Six patients were censored from the EFS analysis, and 8 were censored from OST analysis. Median follow-up time for censored patients was 310 days (range 142-632 for EFS and 142-688 for OST). Thirty-three percent (7/21) of patients experienced confirmed local disease progression (confirmed via imaging, or pathologic evaluation of tumor tissue). Two of seven dogs had a geographic miss, with local disease progression proximal and distal to the site of the primary urethral disease. The remaining five dogs suffered in-field progression of CGUC. Two of these seven patients also developed regional lymph node metastases after completing IM/IGRT. The first of these dogs had tomographically normal lymph nodes which were prophylactically irradiated; 29.1 Gy was delivered to 95% of the planning target volume for the sublumbar/pelvic nodal bed. The second dog with local lymph node metastases also had tomographically normal lymph nodes at initial staging; this dog did not have nodal irradiation. The dog presented with local recurrence (in-field progression) as well as local lymph node metastases 776 days after completing the first course of IM/IGRT. A second course of RT was completed and 49 Gy was delivered to 95% of the PTV for the recurrent primary disease as well as the sublumbar/pelvic nodal bed. There were no clinically-detectable adverse events

attributable to either course of radiation. The patient was euthanized 267 days after completion of the second course of RT and 1043 days after completion of the first course of RT due to progressive azotemia associated with bilateral ureteral obstruction. The ureter had been stented one month prior to euthanasia due to suspected ureteral stricture. Though there was mild left-sided peri-ureteral fibrosis detected on necropsy, gross and histologic findings were consistent with malignant obstruction due to in-field disease progression, rather than functional obstruction due to ureteral fibrosis and stricture. An additional 14% (3/21) of patients in this series experienced distant (pulmonary) metastases prior to death; one of these patients was euthanized due to clinical signs associated with these distant lesions, whereas the other two patients were euthanized due to progressive locoregional disease.

Discussion

Inclusion of IM/IGRT in multimodal treatment protocols for CGUC was well-tolerated. Acute toxicoses were generally limited to grade 1 or 2 GI toxicosis which was self-limiting. Late grade 3 GI or GU toxicoses occurred in 19% of dogs, but were typically well-managed and occurred late in the course of disease.

Although direct and statistically-valid comparisons cannot be made between this data and those reported in historical literature, outcomes in this study appear superior to previously reported data. The median event-free survival time in this study was 317 days (10.4 months), and the median overall survival time was 654 days (21.6 months). This compares favorably with the aforementioned outcomes for dogs receiving no treatment (where survival has been reported to

range from 0.7 to 3 months), surgery alone (3.5 – 8.2 months), NSAIDs (approximately 6 months), chemotherapy (4.3-11 months) and multimodal protocols including palliative and/or intraoperative RT (3.8-15 months).[1,13-22]

Limitations of this study include the small and retrospective nature of the case series. Inherent to such study design was considerable variability in neoadjuvant and adjuvant therapy, as well as post-treatment monitoring. Complete restaging data was not available for all subjects. This, in combination with the inherent difficulties in determining responses using traditional restaging methods such as abdominal ultrasonography, make it impossible to report an accurate and/or reliable objective response rate.[30] In lieu of this deficiency, a subjective response rate (60%) was determined using owner-reported changes in quality of life. Overall, 93% of respondents were satisfied with outcomes of treatment, and would opt for such treatment if another pet were affected by CGUC. Most would also recommend such therapy to friends or family if their pet was thusly afflicted, lending further support to the reported potential clinical benefit in 90% of patients. And although follow-up was incomplete, data nears maturity, with 8 of 21 patients alive at the time of submission and a median follow-up time of 310 days for the censored patients.

Despite these limitations, improved survival with limited morbidity makes it clear that there may be an important role for inclusion of IM/IGRT in treatment of CGUC. However, with 7 of 21 (33%) dogs suffering locoregional failure, it is important to evaluate the patterns of failure in order to improve the efficacy of RT. In all, 5 of 7 dogs experienced in-field local recurrence and

2 failed due to presumed geographic misses; 2 of these dogs also had lymph node metastases at the time of necropsy.

Because in-field recurrence appears to be the most important reason for locoregional failure following completion of IM/IGRT, dose-escalation should be considered as a potential means for improving the efficacy of this therapy. It has been suggested that dynamic-adaptive RT (DART) is one potential means for safely escalating dose.[31,32] Plan adaptation can be performed as a daily on-line or off-line procedure. Whichever technique is used, the goal of DART is to minimize normal tissue exposures by adapting PTV margins to reflect a particular dog's anatomy. In this case series, all plan adaptations were performed via offline DART. In each case, the plan was adapted because bladder size was smaller than planned, enabling use of a smaller than originally planned PTV.

While DART can limit dose to nearby tissues, its limitation lies in the inability to physically spare normal tissues that lie within the PTV. Because it has been suggested that CGUC behaves like a late-responding tissue (i.e., it has a low α/β ratio), finer fractionation cannot be exploited to spare normal tissues without decreasing the probability of local tumor control.[33] With this in mind, preemptive stenting of the urethra and/or ureters might allow for escalation of prescribed dose without increasing the risk of clinically-manifested late radiation-associated complications.[7,8,34] Morbidity associated with stent placement is an important consideration, and preemptive stenting should likely be reserved for those experiencing partial or complete ureteral or urethral obstruction at the time of initial presentation.

Another potential mechanism for improving local tumor control is the combination of RT with either neoadjuvant or concurrent chemotherapy. The goal of neoadjuvant chemotherapy would be cytoreductive downstaging of local disease prior to initiation of RT, with the aim of reducing the number of tumor clonogens in order increase tumor control probability, rather than physical reduction in the size of macroscopic tumor. Concurrent chemoradiotherapy may also provide a cytoreductive advantage. However, the true benefit of concurrent therapy would likely lie in radiosensitization of tumor cells. Neoadjuvant chemotherapy and/or concurrent chemoradiation protocols have proven beneficial in bladder-sparing treatment of human muscle-invasive bladder cancer (MIBC); inclusion of platinum-based and/or gemcitabine therapies can improve local tumor control by 5-9% without potentiating either acute or late radiation-associated toxicosis.[35-37]

It is important to consider the role of chemotherapy not only in the neoadjuvant/concurrent setting (as previously discussed), but also in the adjuvant setting. MTD chemotherapy is often used to grossly evident CGUC, and such therapy is typically not discontinued until there is demonstrable disease progression in the face of chemotherapy. However, this practice should be reconsidered in patients having received definitive local therapy for CGUC; in this setting, it may be adequate to prescribe a finite course of MTD chemotherapy to address potentially occult micrometastatic disease. Frequent restaging of local disease is recommended for patients receiving such therapy and local disease recurrence/progression should be aggressively managed with additional local and/or systemic therapy. When considering the need for additional local therapy it is imperative to consider the clinical response to initial therapy. Because neoplastic cell kill can be slow in the post-RT setting and remodeling/resorption of tumor stroma is often incomplete, a partial response or stable disease may signify adequate local tumor control in the

post-RT setting. Due to risk for significant treatment-associated morbidity, aggressive re-treatment should be reserved for patients with clear evidence of progressive disease.

Appropriate case selection is an important factor in determining how likely a dog is to: (1) complete therapy and (2) realize clinical benefit from therapy. Adequate bladder capacity is perhaps the most important selection criterion. Dogs with pollakiuria due to diminished bladder filling capacity secondary to neoplastic infiltration of the entire urinary bladder or associated chronic inflammation and fibrosis are unlikely to experience normalization of frequency of urination even if 100% local tumor control is attained.

Finally, because 64.3% of clients at CSU-ACC found the duration of treatment and the distance they had to travel for IM/IGRT to be at least moderately challenging, and because most veterinary RT centers do not have direct access to either image-guided or intensity-modulated RT, it is important to consider how definitive RT may be safely applied in the setting of less sophisticated radiation planning and delivery systems. First, dogs should be positioned in lateral recumbency, and a PTV margin of at least 1 cm should be utilized to ensure adequate target coverage if position verification is being performed using two-dimensional kilovoltage or megavoltage portal imaging rather than a three-dimensional soft tissue-target localization system (such as CBCT, surgically implanted fiducial markers or electromagnetic tracking).[26] Second, in the absence of IMRT, it is essential to limit the risk for late radiation-associated complications by limiting the dose per fraction to less than 3 Gy.[23] Finally, size of the radiation field should be considered as another risk factor for late complications.[24] Therefore, inclusion of lymph node beds in the portal may increase the risk for adverse effects such as chronic colitis and rectal,

ureteral or urethral stricture. Bladder size will also affect the size of the portal, and so, efforts should be made to treat a small bladder. The authors have also considered use of rectal balloon catheters to limit the volume of rectum receiving high radiation doses, and facilitate repeatable positioning of the rectum and prostate. However, this is not employed in our practice because bowel preparation and insertion of the balloon is associated with physical mucosal trauma that can exacerbate radiation-associated acute colitis/proctitis.

In conclusion, this study has demonstrated that IM/IGRT is generally well-tolerated and provides an effective treatment option for locoregional control of CGUC. These findings support the need for prospective evaluation of definitive RT in the setting of locoregionally-extensive CGUC; they also suggest that although IM/IGRT can be utilized to maximize survival in affected patients, there is still room for improvement in local therapy for CGUC.

REFERENCES

1. Sorenmo KU, Goldschmidt MH, Shofer FS, et al. Evaluation of cyclooxygenase-1 and cyclooxygenase-2 expression and the effect of cyclooxygenase inhibitors in canine prostatic carcinoma. *Vet Comp Oncol* 2004;2:13-23.

2. Montgomery RD, Hankes GH. Ureterocolonic anastomosis in a dog with transitional cell carcinoma of the urinary bladder. *Journal of the American Veterinary Medical Association* 1987;190:1427-1429.

3. Stone EA, Withrow SJ, Page RL, et al. Ureterocolonic anastamosis in 10 dogs with transitional cell carcinoma. *Veterinary Surgery* 1988;17:147-153.

4. Smith JD, Vaden SL, Stone EA, et al. Management and complications following trigonal-colonic anastomosis in a dog: Five-year evaluation. *Journal of the American Animal Hospital Association* 1996;32:29-35.

5. Mann FA, Barrett RJ, Henderson RA. Use of a retained urethral catheter in 3 dogs with prostatic neoplasia. *Veterinary Surgery* 1992;21:342-347.

6. Smith JD, Stone EA, Gilson SD. Placement of a permanent cystostomy catheter to relieve urine outflow obstruction in dogs with transitional cell carcinoma. *Journal of the American Veterinary Medical Association* 1995;206:496-499.

7. Weisse C, Berent A, Todd K, et al. Evaluation of palliative stenting for management of malignant urethral obstructions in dogs. *Javma-Journal of the American Veterinary Medical Association* 2006;229:226-234.

8. Berent AC, Weisse C, Beal MW, et al. Use of indwelling, double-pigtail stents for treatment of malignant ureteral obstruction in dogs: 12 cases (2006-2009). *Javma-Journal of the American Veterinary Medical Association* 2011;238:1017-1025.

9. Liptak JM, Brutscher SP, Monnet E, et al. Transurethral resection in the management of urethral and prostatic neoplasia in 6 dogs. *Veterinary Surgery* 2004;33:505-516.

10. Stone EA, George TF, Gilson SD, et al. Partial cystectomy for urinary bladder neoplasia: Surgical technique and outcome in 11 dogs. *Journal of Small Animal Practice* 1996;37:480-&.

11. Norris AM, Laing EJ, Valli VEO, et al. Canine bladder and urethral tumors - a retrospective study of 115 cases (1980-1985). *Journal of Veterinary Internal Medicine* 1992;6:145-153.

12. Helfand SC, Hamilton TA, Hungerford LL, et al. Comparison of 3 treatments for transitional cell carcinoma of the bladder in the dog. *Journal of the American Animal Hospital Association* 1994;30:270-275.

13. Knapp DW, Richardson RC, Chan TCK, et al. Piroxicam therapy in 34 dogs with transitional cell carcinoma of the urinary bladder. *Journal of Veterinary Internal Medicine* 1994;8:273-278.

14. McMillan SK, Boria P, Moore GE, et al. Antitumor effects of deracoxib treatment in 26 dogs with transitional cell carcinoma of the urinary bladder. *Javma-Journal of the American Veterinary Medical Association* 2011;239:1084-1089.

15. Henry CJ, McCaw DL, Turnquist SE, et al. Clinical evaluation of mitoxantrone and piroxicam in a canine model of human invasive urinary bladder carcinoma. *Clinical Cancer Research* 2003;9:906-911.

16. Marconato L, Zini E, Lindner D, et al. Toxic effects and antitumor response of gemcitabine in combination with piroxicam treatment in dogs with transitional cell carcinoma of

the urinary bladder. *Javma-Journal of the American Veterinary Medical Association* 2011;238:1004-1010.

17. Arnold EJ, Childress MO, Fourez LM, et al. Clinical trial of vinblastine in dogs with transitional cell carcinoma of the urinary bladder. *Journal of Veterinary Internal Medicine* 2011;25:1385-1390.

18. Moore AS, Cardona A, Shapiro W, et al. Cisplatin (cisdiamminedichloroplatinum) for treatment of transitional cell carcinoma of the urinary bladder or urethra - a retrospective study of 15 dogs. *Journal of Veterinary Internal Medicine* 1990;4:148-152.

19. Turrel JM. Intraoperative radiotherapy of carcinoma of the prostate gland in 10 dogs. *Journal of the American Veterinary Medical Association* 1987;190:48-52.

20. Walker M, Breider M. Intraoperative radiotherapy of canine bladder cancer. *Veterinary Radiology* 1987;28:200-204.

21. Withrow SJ, Gillette EL, Hoopes PJ, et al. Intraoperative irradiation of 16 spontaneously occurring canine neoplasms. *Veterinary Surgery* 1989;18:7-11.

22. Poirier VJ, Forrest LJ, Adams WM, et al. Piroxicam, mitoxantrone, and coarse fraction radiotherapy for the treatment of transitional cell carcinoma of the bladder in 10 dogs: A pilot study. *Journal of the American Animal Hospital Association* 2004;40:131-136.

23. Anderson CR, McNiel EA, Gillette EL, et al. Late complications of pelvic irradiation in 16 dogs. *Veterinary Radiology & Ultrasound* 2002;43:187-192.

24. Arthur JJ, Kleiter MM, Thrall DE, et al. Characterization of normal tissue complications in 51 dogs undergoing definitive pelvic region irradiation. *Veterinary Radiology & Ultrasound* 2008;49:85-89.

25. Murphy S, Gutierrez A, Lawrence J, et al. Laparoscopically implanted tissue expander radiotherapy in canine transitional cell carcinoma. *Veterinary Radiology & Ultrasound* 2008;49:400-405.

26. Nieset JR, Harmon JF, LaRue SM. Use of cone-beam computed tomography to characterize daily urinary bladder variations during fractionated radiotherapy for canine bladder cancer. *Veterinary Radiology & Ultrasound* 2011;52:580-588.

27. Feuvret L, Noel G, Mazeron JJ, et al. Conformity index: A review. *International Journal of Radiation Oncology Biology Physics* 2006;64:333-342.

28. Paddick I, Lippitz B. A simple dose gradient measurement tool to complement the conformity index. *Journal of Neurosurgery* 2006;105:194-201.

29. LaDue T, Klein MK. Toxicity criteria of the veterinary radiation therapy oncology group. *Veterinary Radiology & Ultrasound* 2001;42:475-476.

30. Hume C, Seiler G, Porat-Mosenco Y, et al. Cystosonographic measurements of canine bladder tumours. *Veterinary and Comparative Oncology* 2010;8:122-126.

31. Vestergaard A, Sondergaard J, Petersen JB, et al. A comparison of three different adaptive strategies in image-guided radiotherapy of bladder cancer. *Acta Oncologica* 2010;49:1069-1076.

32. Murthy V, Master Z, Adurkar P, et al. 'Plan of the day' adaptive radiotherapy for bladder cancer using helical tomotherapy. *Radiotherapy and Oncology* 2011;99:55-60.

33. Parfitt SL, Milner RJ, Salute ME, et al. Radiosensitivity and capacity for radiation-induced sublethal damage repair of canine transitional cell carcinoma (TCC) cell lines. *Veterinary and Comparative Oncology* 2011;9:232-240.

34. Liatsikos E, Kyriazis I, Kallidonis P, et al. Ureteric response to abdominal radiotherapy and metallic double-pigtail ureteric stents: a pig model. *Bju International* 2009;104:862-866.

35. Choudhury A, Swindell R, Logue JP, et al. Phase II study of conformal hypofractionated radiotherapy with concurrent gemcitabine in muscle-invasive bladder cancer. *Journal of Clinical Oncology* 2011;29:733-738.

36. Bono AV, Goebell PJ, Groshen S, et al. Adjuvant chemotherapy in invasive bladder cancer: A systematic review and meta-analysis of individual patient data. *European Urology* 2005;48:189-201.

37. Abol-Enein H, Bassi P, Boyer M, et al. Neoadjuvant chemotherapy in invasive bladder cancer: Update of a systematic review and meta-analysis of individual patient data. *European Urology* 2005;48:202-206.

CHAPTER 3: CHARACTERIZATION OF RADIATION-INDUCED ERECTILE DYSFUNCTION IN A CANINE MODEL

Brief Overview

Introduction: Erectile dysfunction (ED) is a common complication in men having received radiation therapy for prostate cancer. The etiopathology of radiation-induced ED (RI-ED) is poorly understood. Purported mechanisms include cavernosal, arteriogenic and neurogenic injuries. Radiation dose to the posterolateral prostatic neurovascular bundles (NVB) and penile bulb (PB) have been associated with RI-ED. This manuscript describes a canine model that has been developed to study the pathogenesis of RI-ED.

Methods: Stereotactic body radiotherapy (SBRT) was used to irradiate the prostate gland, NVB and/or PB of purpose-bred, intact male dogs. Manual evaluation was used to characterize erectile function and quality. B-mode and Doppler ultrasound of the internal pudendal arteries, prostate and penis, dynamic contrast enhanced MRI of the NVB, prostate and penis, and electrophysiology of sensory and motor nerves as well as muscle were performed before and after irradiation. Results of these assays were compared with results of physical evaluations to identify non-invasive functional assays to quantify arteriogenic and neurogenic changes associated with incidence of RI-ED. Gross necropsy and histopathology was also performed.

Results: Erectile dysfunction was a repeatable finding in subjects for whom the prostate, neurovascular bundles and penile bulb were irradiated with 50 Gy, as documented via subjective and objective manual evaluations following SBRT. Irradiated dogs were found to have a

decreased extravascular, extracellular volume in the glans penis, longer systolic rise times in the pudendal artery following papaverine injection, abnormal spontaneous EMG activity in the bulbocavernosus muscle, and slower pudendal nerve motor conduction velocities.

Discussion/Conclusions: ED occurs following SBRT in dogs. Radiation dose-dependent changes in internal pudendal arterial function and dysfunction of the pudendal nerve due to axonal loss may contribute to RI-ED. Measurable endpoints have been developed for evaluation of RI-ED in dogs, that should be used in future studies to refine this novel animal model and perform additional studies aimed at further elucidating the etiopathologic processes underlying RI-ED.

Introduction

Erectile dysfunction (ED) is a common complication of treatment for localized prostate cancer. While nerve-sparing prostatectomies have greatly reduced the risk of post-operative ED,[1,2] modern irradiation techniques such as intensity-modulated radiation therapy (IMRT) and stereotactic body radiation therapy (SBRT) seem to have had little impact on the incidence of radiation-induced ED (RI-ED).[3,4]

ED is generally classified as psychogenic, neurogenic, endocrinologic, arteriogenic, or cavernosal.[5] The cause and exact classification of RI-ED are unknown, though cavernosal (abnormal cavernosal distensibility), arteriogenic (low peak penile blood flow rates) and neurogenic (poor response to prostaglandin injections as well as histologic evidence of injury)

dysfunction have all been associated with RI-ED.[6-9] Irradiation of the bulbus penis, posterolateral neurovascular bundles and/or pudendal nerves have been inconsistently implicated in RI-ED.[10-13]

Poor understanding of the mechanisms underlying development of RI-ED is a major hindrance to development of methods which may reduce the risk of RI-ED. Historically, the only animal models available for studying RI-ED have involved delivery of single or multiple fractions of large pelvic radiation fields to rats, which were often associated with significant normal tissue toxicity.[14-16] The rat model has recently been improved through use of SBRT, which allows targeted irradiation of the prostate, and has minimized apparent toxicosis. Briefly, young adult male Sprague-Dawley rats are irradiated with a single fraction of 20 Gray (Gy), delivered using highly conformal, image-guided SBRT. In a pilot study, 5 of 5 irradiated rats had decreased intracavernosal pressure (ICP), area under the curve (AUC) and mean arterial pressure ratios following direct stimulation of the cavernosal nerve as compared with unirradiated control animals. The bioassay also involves recording of erection frequency after administration of apomorphine, which is used as a direct measure of erectile function.[17] Time- and dose-dependency have been demonstrated in this model; various physiologic and histologic endpoints have been correlated with results of the bioassay, providing functional evidence of RI-ED.[18,19]

Despite improvements in the models available for investigation of the etiopathology of RI-ED, several limitations still exist. For example, none of the rat irradiation protocols mimic clinical prostatic irradiation protocols. Also, apomorphine administration results in activation of selective postsynaptic dopaminergic (D2) receptors which in turn activate pro-erectile central

neurologic pathways, involving nitric oxide (NO) signaling and ultimately inducing penile erection.[20,21] This system of inducing and measuring centrally-mediated erections may not be as efficient at recapitulating the disturbances in erectile physiology which result in RI-ED in irradiated human prostate cancer patients, as would a system involving measurement and study of locally-induced penile erections.

Therefore, the purpose of the present study was to develop a complementary animal model. Despite limitations common to most large animal models, such as cost and space limitations,[22] dogs were considered a reasonable candidate for several reasons. First, volumes irradiated are similar to those of humans, which is important when assessing toxicity data, as risk and severity of many late radiation toxicoses are related to the volume of tissue irradiated; furthermore, similar size allows for study endpoints to be similar to those assays which might be clinically meaningful in evaluation of humans with RI-ED. Second, the lifespan of dogs is long enough to assess late radiation effects. Third, dogs are easily trainable, so erectile function can be evaluated following local induction of penile erection via manual stimulation. And if the goal is to distinguish between neurogenic and vascular causes of ED, methods for doing so are well described in dogs. For example, dogs are the preferred model for nerve-sparing radical prostatectomy research and training,[23,24] where intracavernous pressures can be directly measured following direct stimulation of the cavernous nerves within the NVB, and changes in peak intracavernous pressures reported as a percent of mean arterial pressure serve as a marker of changes in erectile function.[25] The vasoactive effects can be studied following intracorporeal injection of papaverine, which results in smooth muscle relaxation, causing increase in cavernous artery diameter, maximization of peak systolic velocity and intracavernous blood pressures

equaling or exceeding diastolic pressures, resulting in near zero blood velocities within the penis.[26,27] Finally, the unique anatomy of dogs may also be beneficial for studying RI-ED. While their penile anatomy is quite similar to that of humans, there is physical separation, several centimeters in magnitude, between the prostate and penile bulb. This should allow for selective irradiation of those two structures to clarify the role that irradiation of the penile bulb plays in development of RI-ED.

With this in mind, SBRT (50 Gy) was delivered to the prostate, NVB and PB of five dogs, over 5 consecutive days to determine whether or not RI-ED could be observed in dogs. This protocol was chosen based upon promising results of a recent phase I clinical trial.[28] A variety of bioassays were developed to quantify functional, physiologic, hormonal and histologic correlates to the measurable ED. These assays were then used to quantify vascular and neurologic changes after specific geographic irradiation of tissues which have previously been implicated in the pathogenesis of RI-ED, namely the NVB and PB. This canine model was further characterized through a dose-response study.

Methods

Animals

Twenty-two healthy, approximately one year old, intact male mixed breed hound dogs, weighing 24.9 - 40.4 kg, were purchased from a commercial breeding facility,[3] and transported to the Colorado State University Veterinary Teaching Hospital, Fort Collins, Colorado, USA. Dogs were housed in individual enclosures, and fed a commercially-manufactured dry dog chow and

[3] Antech, Inc, Barnhart, MO

water ad libitum. Two weeks were allotted for environmental acclimation. All studies were conducted in accordance with a protocol approved by the Colorado State University Institutional Animal Care and Use Committee. Tissues from four additional 2 to 4 year old dogs of mixed breed were used as unirradiated controls; these dogs were not subject to IACUC oversight for this project, as they were euthanized as part of an unrelated study.

Erectile Function Testing

During the 2-6 weeks following acclimation, and prior to commencing radiation therapy, dogs were subjected to erectile function evaluation training. Initial training involved use of a combination of pheromones, exposure to bitches in estrus, and rhythmic manual stimulation; ultimately evaluations in all dogs could be performed with manual stimulation alone. Erection quality was quantified by size of erection (measured as the maximal transverse diameter of the penis at the level of the bulbus penis), and firmness of erection (subjectively graded on a 4 point scale, with zero corresponding to a lack of erection, 1 being a minimally firm erection with lack of turgidity, 2 being moderate firmness, and 3 being very firm and fully engorged). Time to ejaculation was also noted. Dogs were deemed fully-trained and ready for irradiation upon demonstrating repeatable induction of measurable erection with grade 3 firmness. Evaluations were repeated at least once each month following completion of radiotherapy. Subjects were deemed to exhibit erectile dysfunction if they demonstrated a lack of change in diameter of the penis upon manual stimulation, accompanied by a firmness score no greater than 1; these findings had to be noted during two evaluations performed at least one week apart, in the absence of clinically identifiable pelvico-abdominal pain during physical examination, including digital rectal palpation of the prostate.

Radiation Therapy

Radiation simulation and dose fractions were delivered while the dogs where under general anesthesia. Dogs were fasted for 12 hours and received a warm, soapy enema prior to anesthesia. Dogs were given acepromazine[4] (0.01 mg/kg), atropine[5] (0.04 mg/kg) and hydromorphone[6] (0.05 mg/kg) subcutaneously 15-20 minutes before anesthetic induction, which was achieved with intravenous midazolam[7] (0.2 mg/kg) and propofol[8] (4-6 mg/kg). The dogs were then intubated and anesthesia was maintained using isoflurane gas[9] (1-3% in 100% O_2). Dogs were monitored with electrocardiography, invasive blood pressure measurement, and pulse oximetry. The mean arterial blood pressure was maintained above 65 mmHg; intravenous crystalloid fluid therapy and inotropic support (constant rate infusion of dopamine, 5-10 μg/kg/min) were used in hypotensive subjects. A sterile 8-Fr Foley urinary catheter was placed, as was a rectal balloon[10] that was insufflated with 30 cubic centimeters (cc) of air. Dogs were placed in dorsal recumbency in a standard foam trough, with their feet into the gantry. Their stifles were immobilized with a foam wedge, which was attached to the trough.

Computed tomography (CT) and magnetic resonance imaging (MRI) were performed for radiation therapy planning. Pre- and post-contrast CT scans of the pelvis and caudal abdomen were obtained with 1 mm slice thickness, using a 512 x 512 mm matrix before and after

[4] PromAce® Injectable; Fort Dodge Animal Health, Fort Dodge, IA
[5] Atropine Sulfate (0.54 mg/mL); Vedco Inc, St. Joseph, MO
[6] Hydromorphone HCl Injection USP (2 mg/mL); West-Ward, Eastontown, NJ
[7] Midazolam Injection USP (5 mg/mL); Hospira Inc, Lake Forest, IL
[8] NovaPlus® (propofol injectable emulsion USP, 1%); AAP Pharmaceuticals LLC, Schaumburg, IL
[9] Isoflurane USP; Piramal HealthCare, Andhra Pradesh, India
[10] Immobilizer Treatment Device (REF RB-100F); RadiaDyne, Houston, TX

intravenous administration of contrast material (159.1 mg/kg iohexol IV).[11] The treatment planning MRI study consisted of transverse T2, T1 series obtained before and after intravenous administration of contrast material (21.3 mg/kg gadopentetate dimeglumine IV),[12] as well as dorsal and sagittal T1 post-contrast weighted images of the pelvis and caudal abdomen. Images were manually fused using the image registration function on the radiation treatment planning software.[13] The prostate, bilateral prostatic neurovascular bundles (NVB) and penile bulb (PB) were delineated as the gross target volume (GTV). The planning target volume (PTV) was represented by a 0.5 cm expansion of the prostatic and neurovascular bundle volumes, and a 0.7 cm expansion of the penile bulb volume; the rectal wall was excluded from PTV's. The total prescribed radiation dose and treated tissue volume varied (Table 3.1 and Figures 3.1-3.3), but always

Table 3.1. Prescription information

Treatment Group	**n**	**Total dose (Gy)**	**Total treatment time (days)**	**Treated volume**		
				Prostate	**NVB**	**PB**
A	5	50	5	x	x	x
B	4	50	11	x	x	x
C	4	50	11		x	
D	3	50	11			x
E	3	40	11	x	x	x
F	3	30	11	x	x	x

[11] Omnipaque 350™; GE Healthcare, Broomfield, CO
[12] Magnevist; Bayer HealthCare Pharmaceuticals Inc, Wayne, NJ
[13] Eclipse™ (v8.6); Varian Medical Systems Inc, Palo Alto, CA

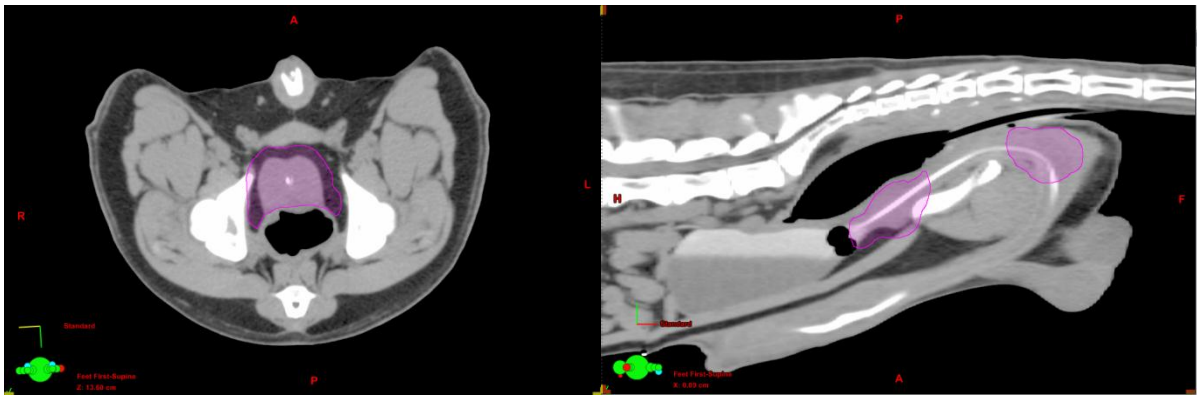

Figure 3.1. Treated volumes for Groups A, B, E and F. The image on the left is a transverse view through the pelvis, at the level of the prostate gland, with the PTV for the prostate and NVB highlighted in magenta. The image on the right is a parasagittal view of the caudal abdomen and pelvis, with the PTV's for the prostate, NVB and PB highlighted in magenta.

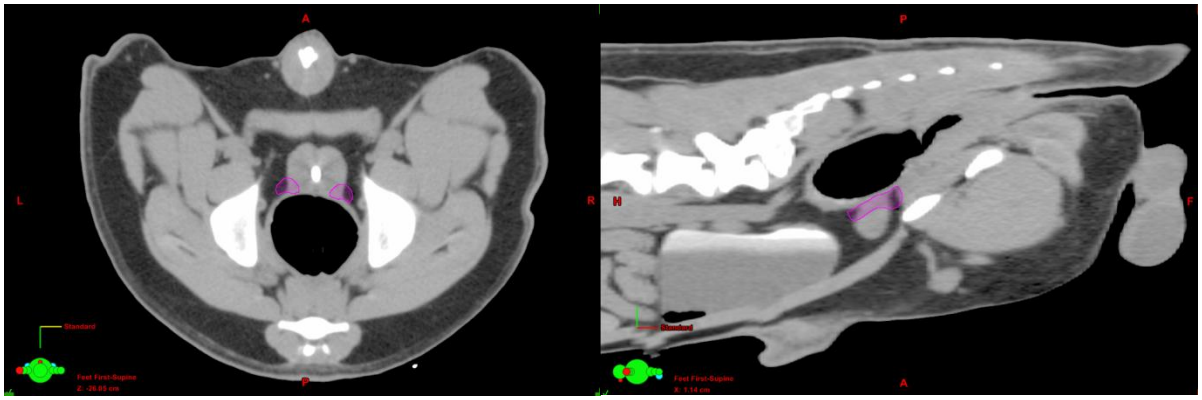

Figure 3.2. Treated volumes for Group C. The image on the left is a transverse view through the pelvis, at the level of the prostate gland, with the PTV for the NVB highlighted in magenta. The image on the right is a parasagittal view of the caudal abdomen and pelvis, with the PTV for the NVB highlighted in magenta.

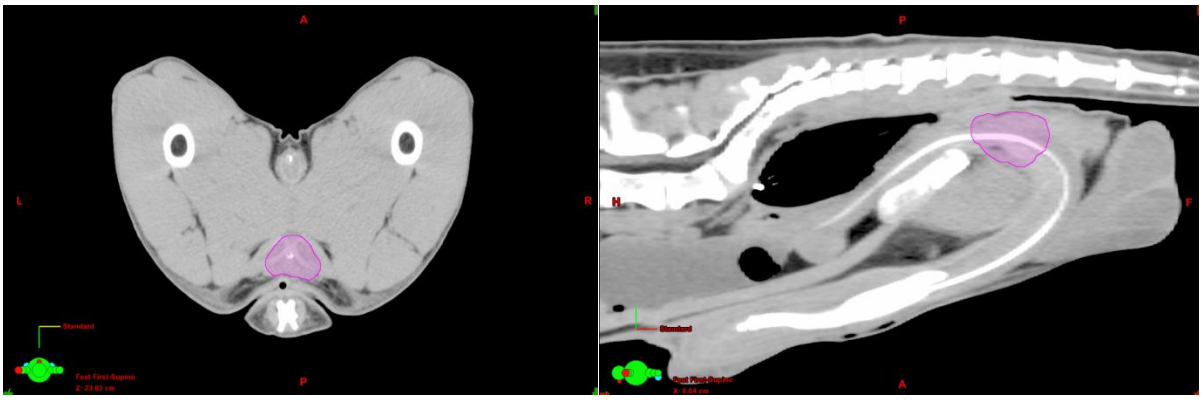

Figure 3.3. Treated volumes for Group D. The image on the left is a transverse view through the perineum, at the level of the PB, with the PTV for the PB highlighted in magenta. The image on the right is a parasagittal view of the perineum, with the PTV for the PB highlighted in magenta.

involved delivery of 95% of the prescribed dose to the PTV, in five equal fractions, administered over either 5 (daily fractions) or 11 days (with an interfraction interval of no less than 48 hours). Treatment plans involved 7-9 isocentrically-placed coplanar 6 and 10 MV X-ray beams which were shaped using dynamic multileaf collimation in a sliding-leaf fashion to achieve intensity-modulation. Plans were constructed using iterative inverse-planning with heterogeneity corrections to meet specified goals for both target volumes and organs at risk (Table 3.2). Individual treatment plan review was performed by an American College of Veterinary Radiology board-certified veterinary radiation oncologist and an American College of Radiology board-certified medical physicist. Beam output was verified for each plan using gamma analysis of data generated from an electronic portal dosimeter. For quality-assurance purposes, a minimum of 95% gamma for a 3-mm distance to agreement and a 3% absolute dose difference was defined as a passing score. Daily image-guided patient position verification was performed

Table 3.2. Dose-volume limits for organs at risk

Organ	Volume	Dose
Femoral heads	Less than 1 cc	> 30 Gy
Peri-prostatic anterior rectal wall	Maximum point dose	105% of Rx
Peri-prostatic lateral rectal wall	Maximum point dose Less than 0.3 cc cumulative (both sides)	100% of Rx > 90% of Rx
Peri-prostatic posterior rectal wall	Maximum point dose	45% of Rx
Skin	Maximum point dose	20 Gy
Small intestine	Maximum point dose Less than 1 cc	29 Gy > 19.5 Gy
Spinal cord	Maximum point dose Less than 0.8 cc	22 Gy > 20 Gy
Urethra	Maximum point dose	105% of Rx
Urinary bladder	Maximum point dose Less than 1 cc	105% of Rx > 18.3 Gy

with on-board kilovoltage cone-beam CT. Following position verification, intensity-modulated SBRT was delivered using a Varian Trilogy™ linear accelerator.[14]

Follow-up Evaluations

In addition to weekly erectile function testing, endocrine evaluation, ultrasonography, dynamic contrast-enhanced MRI and electrophysiologic evaluations were performed in most dogs prior to radiotherapy and repeated 4 months after completion of radiotherapy, and immediately prior to termination. Dogs were monitored daily for toxicity. Toxicity was scored according to the Radiation Therapy Oncology Group (RTOG) urinary and rectal toxicity scale.[29] Subjects were humanely euthanized via intravenous injection of propofol (6 mg/kg) and pentobarbital[15] (18 mg/kg) within three weeks of reaching any of the following endpoints: (1) confirmation of erectile dysfunction, (2) development of clinically-evident grade 3 or higher enterocolonic or

[14] Varian Trilogy™; Varian Medical Systems Inc, Palo Alto, CA

[15] Beuthanasia-D Special (pentobarbital 390 mg/mL, with phenytoin 50 mg/mL); Schering-Plough Animal Health Corp, Union, NJ

genitourinary toxicity that was not responsive to aggressive medical therapy, or (3) 1 year after commencing radiotherapy. Post-mortem examination was performed on all dogs.

Endocrine Testing

Serum concentrations of testosterone and luteinizing hormone (LH) were determined using radioimmunoassay techniques. Radio-iodinated testosterone tyrosyl methyl ester (^{125}I-TEST-TME) and luteinizing hormone (^{125}I-LH) functioned in their respective radioimmunoassays. Activity counts were performed with a gamma spectrometer calibrated using ^{125}I sources. The reference range for intact dogs in our laboratory for testosterone is 0.5 to 9.0 ng/mL, and for LH is 0.8 to 11.2 ng/mL. The lower limit of detection for testosterone is 0.02 ng/mL, the intra-assay coefficient of variance is 7.3 to 14.6%, and the intra-assay coefficient of variance is 21.3 to 14.8%. The mean lower limit of detection for LH is 1.08 ng/mL, the intra-assay coefficient of variance is 4.4 to 8.9%, and the inter-assay coefficient of variance is 17.4 to 20.0%.

Dynamic Contrast-Enhanced Magnetic Resonance Imaging

In addition to the aforementioned anatomic imaging, dynamic contrast-enhanced MRI (DCE-MRI) was performed to assess prostatic and penile vascularity and permeability. DCE-MRI was be done by intravenous injection of gadolinium DTPA (0.1 mmol/kg by controlled injector at 3 ml/sec) while the prostate was repeatedly scanned using 3D Spoiled Gradient (TR 6.8, TE 3.06, NEX 0.75 with 30 degree flip, 3 mm slice thickness, 22 cm FOV and 256 x 128 matrix), run as two continuous series. Temporal resolution was 10-12 seconds per phase for a total of 4 minutes and 36 seconds of scanning.

Quantitative kinetic parameters were derived from gadolinium concentration versus time curves that were fitted to the two-compartment model proposed by Toft's et al.[30] Specifically, the volume transfer coefficient (K^{trans}), rate constant (k_{ep}), fractional plasma volume (v_p), extravascular extracellular fractional volume (v_e) and instantaneous area under the gadolinium concentration curve (iAUGC; measured with a 120 second time interval) were determined, in conjunction with an arterial input function (AIF), derived from either the left or right internal iliac artery, to minimize influence of the rate of contrast medium injection or patient-to-patient variations in baseline blood flow. AIF's were selected by drawing a bounding box around each internal pudendal artery, and assessing the associated signal intensity curve. This was done by interactively moving the bounding box and either selecting or deselecting individual voxels of information that were contributing to the averaged curve. This selection process was performed to optimize the peak intensity and uptake slope of the resultant curve. See the appendix for a brief description of the Toft's model. All DCE-MRI analyses were performed using a commercial software package.[16]

Ultrasonography

Both the penis and prostate were subjectively evaluated and described using B-mode imaging. The diameter of the penis was measured mid-shaft, at its widest point. These tissues were also subjectively evaluated using color and power Doppler ultrasound; this imaging was systematically performed by starting at the distal end of the penis and working proximally. Pulsed-wave Doppler was used to evaluate the internal pudendal arteries; the terminal aorta was also assessed, and functioned as an internal control. Flow measurements were made in the

[16] MIStar; Apollo Medical Imaging Technology Pty Ltd., North Melbourne, Australia

internal pudendal artery using a long-axis view; these measurements were the basis for objective determination of the systolic rise time (SRT). SRT is the time measured from the start of systolic acceleration to the peak forward frequency on a Doppler waveform; reported SRT values are the average of three repeated measurements. The above imaging was then repeated five minutes after intracorporeal injection of 45 mg of papaverine.[17] All images were obtained using a linear, high frequency transducer.[18]

Electrophysiology

Electrodiagnostic testing was performed. Electromyography (EMG) was performed on the bulbospongiosus muscles and results were noted as normal or abnormal, with description of any spontaneous activity. Motor nerve conduction velocity (MNCV) studies of the pudendal nerve were obtained by recording compound muscle action potentials (CMAP) from the bulbospongiosus muscle; pudendal motor conduction velocities were calculated and compound CMAP amplitudes were recorded. Sensory nerve conduction velocity (SNCV) studies of the dorsal nerve of the penis were obtained by recording conduction velocities from the pudendal nerve as it travels between the coccygeus muscle and the superficial gluteal muscle; nerve conduction velocities were calculated. Cord dorsum potential (CDP) analysis was performed via stimulation of the dorsal nerve of the penis and recording off the spinal cord at the L4-L5 interarcuate ligament. All studies were performed under general anesthesia (as detailed above), and dogs were paralyzed with intravenous administration of atracurium[19] (0.1 – 0.2 mg/kg,

[17] Papaverine hydrochloride injection USP (30 mg/mL); American Reagent Inc, Shirley, NY
[18] VFX 9-4 MHz transducer; Siemens, Malvern, PA
[19] Tracrium (10 mg/mL); GlaxoSmithKline, Parma, Italy

repeated as needed; depth of neuromuscular blockade was assessed via train-of-four monitoring) during sensory conduction studies.

Post-Mortem Examination

Gross necropsy examination was performed after humane euthanasia. The entire lower genitourinary tract (urinary bladder, urethra, prostate and penis) was removed and preserved in 10% neutral buffered formalin and processed for histologic evaluation, as were the NVB and peri-prostatic rectum. All histologic evaluations were also performed on age-matched, un-irradiated intact male dogs that served as negative control subjects. These dogs had been euthanized subsequent to an unrelated experiment which did not involve manipulation of the either the lower gastrointestinal or urinary tracts.

All specimens were routinely processed and embedded in paraffin, then sectioned at 5 μm. Sections of prostate, colon, NVB and penis were stained with hematoxylin and eosin (H&E) for morphologic evaluation, and Masson's trichrome for evaluation of fibrosis. Verhoeff-van Gieson (VVG) staining was performed on prostate and NVB for assessment of intimal vascular changes. Immunohistochemical staining (IHC) for vascular endothelium was performed. Briefly, sections were deparaffinized and then rehydrated with descending alcohol concentrations to buffer. Heat-induced epitope retrieval with low-pH buffer (pH 6.0) at 125C in a steamer for 1 minute was followed by endogenous peroxidase blocking with 3% hydrogen peroxide and incubation with the primary antibody at 4C for 10 hours. The primary antibody was a monoclonal mouse anti-human CD31 antibody[20] at a 1:50 dilution. A pre-dilute horseradish

[20] Dako (Clone JC70A); Agilent Technologies, Carpinteria, CA, USA

peroxidase-conjugated secondary antibody[21] was applied for 30 minutes followed by application of a DAB peroxidase substrate[22] to detect the immunoreactive complexes. The slides were then counterstained with Mayer's hematoxylin QS,[23] dehydrated and mounted in xylene based mounting medium. Neurofilament protein was also detected in paraffin embedded tissues, following enzymatic antigen retrieval, using a mouse monoclonal IgG1 antibody specific to neurofilament protein structural epitopes,[24] and a peroxidase enzyme conjugated polymer labeling system,[25] and DAB+ chromogen. IHC protocols were applied to prostate and penis.

Various semi-quantitative image analyses were performed. Microvascular density (MVD) was evaluated in three separate regions of the prostate: (1) the periurethral stroma, (2) dorsomedial prostate and capsule, as well as the (3) glandular prostatic parenchyma of the central and peripheral zones). Microvessel counts were performed using a modification of previously described techniques.[31] Briefly, 5 nonoverlapping areas from each of the aforementioned regions of the prostate were selected from the CD31-treated sections, and photographed at 200 times magnification (20X objective and 10X ocular). Manual vessel counts were performed, and averaged over the 5 fields; any brown-staining endothelial cell or cluster of endothelial cells which was clearly separate from adjacent connective tissue or glandular prostate was counted as a single microvessel; neither vessel lumens nor red blood cells were required to define a structure as a microvessel. MVD was also quantified via semiautomatic morphometric analysis to determine the average percentage of CD31 positive pixels in the photomicrographs. Prostatic

[21] Dako (Clone K4061); Agilent Technologies, Carpinteria, CA, USA
[22] SK-4100; Vector Laboratories; Burlingame, CA, USA
[23] H-3404; Vector Laboratories; Burlingame, CA, USA
[24] Dako (clone 2F11); Agilent Technologies, Carpinteria, CA, USA
[25] Envision+ mouse HRP; Dako; Agilent Technologies, Carpinteria, CA, USA

collagen content was determined by counting the number of blue pixels, and reporting results as a percentage of total surface area in transverse sections of the prostate. Nerve density was determined using a "hotspot" technique, wherein a photomicrograph was obtained, at 100 times magnification, from a random area within each of three distinct neuronal hotspots in the dorsal capsular tissue of the prostate gland, identified using neurofilament IHC. Image analysis software was used to count the percentage of pixels staining positive for neurofilament expression per field. Changes in the percent of neurofilament and collagen within nerves were evaluated in the prostate and penis. Fifteen to 20 nerves were imaged in the dorsomedial prostate and prostatic capsule, as well as the penis from each dog. Neurofilament expression and fibrosis were quantified, for each nerve, as the number of positively stained pixels (on neurofilament IHC and Masson's trichrome, respectively) divided by the total area of the nerve. Arterial patency was performed by measuring the cross-sectional surface area of the patent lumen, as a percentage of cross-sectional surface area of the whole vessel, in 10 medium to large arteries in the NVB. Image analysis was performed using commercial software packages.[26,27,28] Slides were examined microscopically without prior knowledge of the radiation site (prostate, NVB and/or PB), prescription (30, 40 or 50 Gy) or schedule (5 fractions over 5 or 11 days).

Statistical Analysis

Due to small sample size in the study, a non-parametric approach was undertaken to perform comparisons between the categories of interest in the DCE-MRI and ultrasound variables. A 'Friedman's test for non-parametric measures ANOVA' was used, which also accounted for

[26] AxioVision; Carl-Zeiss Microscopy GmbH, Jena, Germany
[27] ImageJ; U.S. National Institutes of Health, Bethesda, MD, USA
[28] BioQuant; BIOQUANT Image Analysis Corporation, Nashville, TN, USA

repeated measurements on the same subject over time. Means were reported for description of the data. A p-value of 0.05 was considered to determine statistical significance; a p-value of 0.1 was also considered in interpretation of data to avoid committing type II error. Pathology data was studied using the Kruskal-Wallis test; Dunn's test was performed for multiple comparisons. Statistical software was used for all data analyses.[29,30]

Results

Feasibility of a Canine Model of SBRT, and Impact of the Interfraction Interval

Erectile Function Testing

ED was observed in 2 of the 5 dogs treated in group A; the time from commencing SBRT to development of ED was 158 and 192 days. The 3 dogs not developing ED were euthanized 99, 104 and 151 days after commencing SBRT, as a result of developing grade IV colorectal toxicity. Due to the high rate of severe colorectal toxicity in group A, the fractionation schedule was altered for all remaining irradiations, such that SBRT was delivered over 11 days, with a minimum interfraction interval of 48 hours. Two of 4 dogs treated with 50 Gy to all 3 sites in 11 days (group B) developed ED, at 216 and 325 days, respectively. The remaining two dogs were euthanized at 125 and 396 days, with grade III and IV colorectal toxicity, respectively.

Endocrine Testing

Table 3.3 enumerates the serum concentrations of testosterone and luteinizing hormone measured at each timepoint for all dogs in this study.

[29] SAS v 9.3, SAS Institute Inc., Cary, NC, USA
[30] Prism 6 for Windows, GraphPad, La Jolla, CA, USA

Table 3.3. Serum testosterone and luteinizing hormone concentrations

Treatment Group/Dog ID	Testosterone (ng/mL)			Luteinizing hormone (ng/mL)		
	Pre-SBRT	4 months post-SBRT	12 months post-SBRT	Pre-SBRT	4 months post-SBRT	12 months post-SBRT
A/1	nm	0.346	nm	nm	20.75	nm
A/2	nm	1.3	nm	nm	18.11	nm
A/4	2.65	nm	nm	1.64	nm	nm
A/5	nm	4.99	nm	nm	8.45	nm
A/6	nm	5.51	0.95	nm	8.05	ND
B/7	3.09	nm	0.74	1.93	nm	ND
B/8	0.48	2.43	1.28	4.73	8.12	13.2
B/9	0.54	0.88	1.24	ND	1.4	ND
B/13	0.49	0.8	3.73	4.65	ND	2.49
C/10	3.6	1.83	0.37	5.22	1.92	1.14
C/11	0.48	nm	nm	4.06	nm	nm
C/12	4.97	nm	1.97	6.37	nm	4.87
C/17	1.17	0.49	2.14	23.73	ND	4.59
D14	2.51	3.28	nm	2.62	2.62	nm
D15	2.07	1.85	2.02	2.11	ND	0.578
D16	0.68	nm	1.29	1.22	ND	1.55
E18	1.2	1	2.46	0.88	ND	5.27
E19	0.89	1.54	2.52	2.08	ND	12.47
E20	0.24	1.85	3.91	1.39	ND	4.7
F21	0.9	4.26	2.73	ND	8.91	28.23
F22	1.36	3.05	2.09	ND	5.92	5.73
F23	0.48	0.47	3.50	ND	0.21	11.52

Treatment Group	Pre-SBRT	4 months post-SBRT	12 months post-SBRT	p*	p**
Testosterone (ng/mL)					
A	1.54 +/- 1.33	3.04 +/- 2.59	0.95 +/- 0.00	> 0.9999	> 0.9999
B		1.37 +/- 0.92	1.75 +/- 1.34	> 0.9999	> 0.9999
C		1.16 +/- 0.95	1.49 +/- 0.98	> 0.9999	> 0.9999
D		2.57 +/- 1.01	1.65 +/- 0.52	> 0.9999	> 0.9999
E		1.46 +/- 0.43	2.96 +/- 0.82	> 0.9999	0.4932
F		2.59 +/- 1.94	2.77 +/- 0.71	> 0.9999	0.6868
Luteinizing hormone (ng/mL)					
A	4.47 +/- 5.80	13.84 +/- 6.55	--	0.0842	--
B		4.76 +/- 4.75	7.85 +/- 7.57	> 0.9999	> 0.9999
C		1.92 +/- 0.00	3.53 +/- 2.08	> 0.9999	> 0.9999
D		2.62 +/- 0.00	1.064 +/- 0.69	> 0.9999	> 0.9999
E		--	7.48 +/- 4.33	--	> 0.9999
F		5.01 +/- 4.42	15.16 +/- 11.68	> 0.9999	0.2324

*Comparing pooled pre-SBRT testosterone with 4 month post-SBRT concentrations; ** Comparing pooled pre-SBRT testosterone with 12 month post-SBRT concentrations; ND = below the limit of detection; nm = not measured

Magnetic Resonance Imaging

Serial (pre- and post-irradiation) DCE-MRI data for the prostatic ROI of dogs in groups A and B are summarized in Table 3.4. Similar data for the ROI encompassing the glans penis are presented in Table 3.5, and data for the left and right NVB are in Figures 3.6 and 3.7.

Ultrasound

The unirradiated prostate is generally of homogeneous echogenicity, and is hyperechoic as compared with surrounding tissues. It has mild, multifocal flow, evident on color and power Doppler, and which may increase in response to intracavernosal administration of papaverine. The penis also has mild to moderate basal flow which increases in response to papaverine.

Post-irradiation ultrasound was performed in two dogs (both of whom had clinical evidence of ED) from group A, both of whose prostates became hypoechoic to surrounding tissues. The prostate enlarged (8.3%) in one, and remained stable in size in the other. Prostatic flow was either unchanged or decreased in response to papaverine; penile blood flow increased after papaverine administration in both dogs. Post-irradiation ultrasound was performed in all four dogs in group B, two of whom had evidence of ED at their terminal examination. The prostate became hypoechoic to surrounding tissues in 2 of these 4 dogs, and hyperechoic in the others (the prostate of one dog with ED became hypoechoic after SBRT, the other became hyperechoic). Prostate size varied in these dogs, becoming smaller in 2, and larger in 2 after SBRT (again, incidence of ED did not predict the direction of prostatic size change in these dogs). Prostatic flow was either unchanged or decreased in response to papaverine; all four dogs

Table 3.4. Interfraction interval study: Mean outcome variables and overall summary statistics for DCE-MRI of the prostate gland.

	0 months (Baseline)	**4 months**	**12 months**	***p**** ***(0 vs. 4m)***	***p**** ***(0 vs. 12m)***	***p**** ***(4 vs. 12m)***
K^{trans} (min^{-1})						
Group A (q24h)	723.1	--	507.0	--	*0.14*	--
Group B (q48h)	622.3	744.0	461.2	*0.96*	*0.29*	*0.70*
*p***	*0.26*	--	*0.88*			
k_{ep} (min^{-1})						
Group A (q24h)	2998.2	--	1799.0	--	*0.25*	--
Group B (q48h)	2465.3	589.4	960.7	*< 0.0001*	*< 0.0001*	*0.05*
*p***	*0.29*	--	*0.56*			
v_p (unitless)						
Group A (q24h)	15.7	--	40.7	--	*0.79*	--
Group B (q48h)	99.3	9.0	54.4	*< 0.0001*	*0.21*	*0.0005*
*p***	*0.05*	--	*0.63*			
v_e (unitless)						
Group A (q24h)	273.6	--	339.9	--	*0.001*	--
Group B (q48h)	382.6	1762.7	834.0	*0.001*	*< 0.0001*	*0.59*
*p***	*0.03*	--	*<0.0001*			
iAUGC (mM/min)						
Group A (q24h)	525.8	--	562.9	--	*0.25*	--
Group B (q48h)	743.7	1120.2	624.2	*0.001*	*0.65*	*0.001*
*p***	*0.13*	--	*1*			

*This is the p-value comparing individual timepoints.

**This is the p-value comparing outcomes between groups at given timepoints.

Table 3.5. Interfraction interval study: Mean outcome variables and overall summary statistics for DCE-MRI of the glans penis.

	0 months (Baseline)	**4 months**	**12 months**	***p**** ***(0 vs. 4m)***	***p**** ***(0 vs. 12m)***	***p**** ***(4 vs. 12m)***
K^{trans} (min^{-1})						
Group A (q24h)	144.8	--	108.1	--	*0.03*	--
Group B (q48h)	188.2	257.5	105.1	*0.96*	*0.12*	*0.02*
*p***	*0.97*	--	*0.85*			
k_{ep} (min^{-1})						
Group A (q24h)	427.4	--	585.4	--	*0.25*	--
Group B (q48h)	407.0	342.3	547.5	*0.29*	*0.06*	*0.82*
*p***	*0.75*	--	*0.96*			
v_p (unitless)						
Group A (q24h)	5.5	--	5.8	--	*0.30*	--
Group B (q48h)	12.2	7.1	11.0	*0.06*	*0.58*	*0.02*
*p***	*0.13*	--	*0.07*			
v_e (unitless)						
Group A (q24h)	438.2	--	250.6	--	*0.002*	--
Group B (q48h)	607.4	1390.2	372.8	*0.01*	*0.04*	*0.01*
*p***	*0.92*	--	*0.097*			
iAUGC (mM/min)						
Group A (q24h)	123.5	--	111.4	--	*0.03*	--
Group B (q48h)	258.8	364.1	124.8	*0.44*	*0.25*	*0.01*
*p***	*0.16*	--	*0.49*			

*This is the p-value comparing individual timepoints.
**This is the p-value comparing outcomes between groups at given timepoints.

Table 3.6. Interfraction interval study: Mean outcome variables and overall summary statistics for DCE-MRI of the left neurovascular bundle.

	0 months (Baseline)	**4 months**	**12 months**	***p**** ***(0 vs. 4m)***	***p**** ***(0 vs. 12m)***	***p**** ***(4 vs. 12m)***
K^{trans} (min^{-1})						
Group A (q24h)	96.5	--	121.7	--	*0.35*	--
Group B (q48h)	132.4	280.6	174.4	*0.075*	*0.01*	*0.14*
*p***	*0.42*	--	*0.41*			
k_{ep} (min^{-1})						
Group A (q24h)	611.2	--	800.0	--	*0.82*	--
Group B (q48h)	778.6	665.8	675.9	*0.39*	*0.84*	*0.59*
*p***	*0.72*	--	*0.73*			
v_p (unitless)						
Group A (q24h)	19.5	--	23.7	--	*0.56*	--
Group B (q48h)	31.1	6.7	18.7	*0.03*	*0.34*	*0.53*
*p***	*0.31*	--	*0.17*			
v_e (unitless)						
Group A (q24h)	175.9	--	227.1	--	*0.35*	--
Group B (q48h)	390.0	1177.0	437.4	*0.02*	*0.04*	*0.24*
*p***	*0.67*	--	*0.079*			
iAUGC (mM/min)						
Group A (q24h)	166.4	--	213.2	--	*0.25*	--
Group B (q48h)	232.7	468.6	243.1	*0.04*	*0.45*	*0.05*
*p***	*0.15*	--	*0.81*			

*This is the p-value comparing individual timepoints.
**This is the p-value comparing outcomes between groups at given timepoints.

Table 3.7. Interfraction interval study: Mean outcome variables and overall summary statistics for DCE-MRI of the right neurovascular bundle.

	0 months (Baseline)	**4 months**	**12 months**	***p**** ***(0 vs. 4m)***	***p**** ***(0 vs. 12m)***	***p**** ***(4 vs. 12m)***
K^{trans} (min^{-1})						
Group A (q24h)	198.3	--	162.6	--	*0.64*	--
Group B (q48h)	256.9	379.2	157.9	*0.62*	*0.65*	*0.04*
*p***	*0.36*	--	*0.88*			
k_{ep} (min^{-1})						
Group A (q24h)	1126.5	--	852.0	--	*0.25*	--
Group B (q48h)	1547.4	705.0	718.9	*0.007*	*< 0.0001*	*0.82*
*p***	*0.56*	--	*0.66*			
v_p (unitless)						
Group A (q24h)	13.8	--	51.1	--	*0.64*	--
Group B (q48h)	59.1	1.8	13.2	*0.02*	*0.39*	*0.07*
*p***	*0.47*	--	*0.005*			
v_e (unitless)						
Group A (q24h)	200.5	--	248.9	--	*0.35*	--
Group B (q48h)	304.6	1598.6	367.5	*0.001*	*0.14*	*0.59*
*p***	*0.95*	--	*0.12*			
iAUGC (mM/min)						
Group A (q24h)	245.3	--	301.8	--	*0.42*	--
Group B (q48h)	384.2	523.3	220.8	*0.16*	*0.0497*	*0.01*
*p***	*0.06*	--	*0.097*			

*This is the p-value comparing individual timepoints.

**This is the p-value comparing outcomes between groups at given timepoints.

had evidence of increased penile blood flow in response to papaverine. Ultrasonographically determined arterial blood velocity data for the interfraction interval study are summarized in Table 3.8.

Electrophysiology

Electromyography of the bulbospongiosus muscle was performed before and after SBRT in 2 dogs from group A (both of whom developed clinically-evident ED) and 3 of the 4 dogs in group B. All of the dogs had a normal electromyogram prior to SBRT and exhibited spontaneous activity after SBRT. The majority of the abnormal activity was characterized by fibrillation potentials and positive sharp waves. MNCV was calculated and CMAP amplitude was recorded for these dogs, and is reported in Table 3.9 and Figure 3.4, respectively. There were no statistically detectable changes in MNCV or CMAP with time within either group, nor were there differences between the groups at any point in time. The numerical values of MNCV at 12 months were however lower than baseline in 4 of these 5 subjects. The post-irradiation CMAP amplitude was lower than baseline in all cases. Sensory nerve action potentials were not elicited in any of the dogs. There were no cord dorsum potentials that were successfully recorded in this set of dogs.

Post-Mortem Examination

The prostate gland of dogs from groups A and B was generally small and firm. The majority of dogs in these groups had deep colonic ulcers with umbilicated edges, and/or full-thickness perforations adjacent to the prostate gland, with fibrinonecrotic membranes in the ulcer bed. In dogs with perforations, there were fibrous adhesions between the dorsal surface of the prostate

Table 3.8. Interfraction interval study: Summary statistics for ultrasonographic evaluation of systolic rise times in the internal pudendal artery.

	Pre-Papaverine Systolic Rise Time (s)			*p**		
	Baseline	**4 months**	**12 months**	**Baseline to 4 months**	**Baseline to 12 months**	**4 to 12 months**
Group A (q24h)	0.12	--	0.11	--	*0.21*	--
Group B (q48h)	0.11	0.09	0.08	*0.03*	*0.02*	*0.24*
*p***	*0.22*	--	*0.039*			
	Change in Systolic Rise Time after Papaverine Administration (%)			*p**		
	Baseline	**4 months**	**12 months**	**Baseline to 4 months**	**Baseline to 12 months**	**4 to 12 months**
Group A (q24h)	-29.8	--	11.66	--	*0.16*	--
Group B (q48h)	-25.93	7.74	33.34	*0.046*	*0.08*	*0.08*
*p***	*0.64*	--	*0.56*			

*This is the p-value for overall analysis of temporal change in an outcome variable within a treatment group; comparison of individual timepoints was also performed, and relevant results are summarized in the text.
**This is the p-value comparing outcomes between groups A and B at a given timepoint.

Table 3.9. Interfraction interval study: Motor nerve conduction velocities (MNCV) before and after SBRT

Treatment Group/ Dog ID	**MNCV (m/s)**		
	Pre-SBRT	**4 months post-SBRT**	**12 months post-SBRT**
A/1	52	NDA	32
A/2	NDA	NDA	N/A
A/4	47	NDA	N/A
A/5	NDA	NDA	N/A
A/6	45	NDA	31
B/7	56	59	37
B/8	51	NDA	45
B/9	58	64	67
B/13	67	NDA	N/A

N/A = dog euthanized earlier than this point in time; NDA = no data available

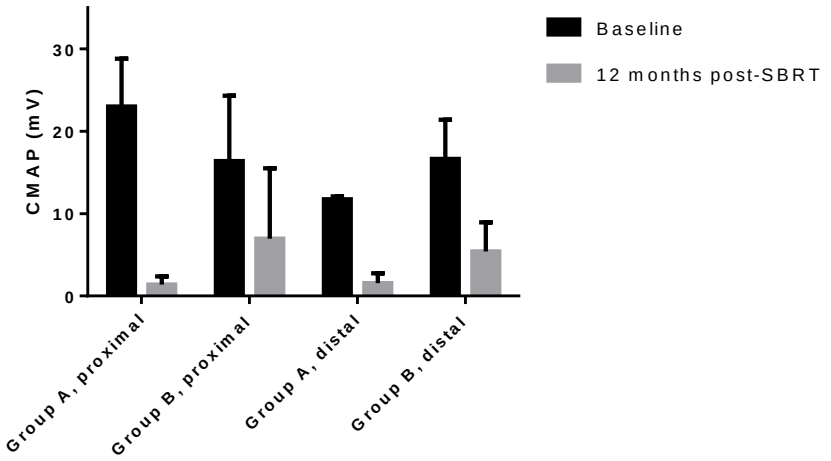

Figure 3.4. Interfraction interval study: Compound muscle action potentials (CMAP) before and after SBRT at proximal and distal recording sites

and the ventral peritoneal surface of the colon. The neurovascular bundles were severely thickened with fibrous connective tissue. Localized caudal abdominal and/or intrapelvic hemorrhagic peritonitis was present in several of the dogs with colonic perforations. The penis was grossly normal.

The prostate gland was transected at mid-body; in unirradiated control dogs it consisted of active, organized prostatic glands, with a central urethra surrounded by loose connective tissue, and occasional loose, multifocal periurethral lymphoid aggregates. There was a fibrous capsule which was contiguous with a dorsomedial zone of dense connective tissue along a median cleft (where the bilateral lobes meet), which contained small peripheral nerves, ganglia, arteries and veins; this dorsomedial capsular zone also contains the ejaculatory ducts. The neurovascular plexuses were sectioned longitudinally and contain large arteries, veins, medium to large peripheral nerves and ganglia within a thin layer of fibrofatty connective tissue. The penis was transected at the level of the bulbus glandis. The penile urethra and os penis lie in the middle of

the sections, and were surrounded by cavernous tissue lined by vascular endothelium; this was all surrounded by an epidermal tissue layer, including subcuticular loose connective tissue, containing small arteries, veins and nerves. Most nerves of the prostate and penis were unmyelinated (confirmed in representative prostate sections, using an osmium tetroxide preparation which was counterstained with toluidine blue), though a small number of myelinated fibers were present in the penis.

The prostate from dogs in groups A and B showed marked reduction in the number of glands, with abundant replacement fibrosis; in dogs euthanized within the first 6 months post-irradiation, more relatively normal glands persisted at the periphery of the organ. The remnant glands were ectatic, and often contained sloughed and rounded epithelial cells. There was mild to moderate, multifocal to diffuse lymphocytic inflammation within the fibrosis, and around the urethra. The capsule was thickened; there was lymphocytic cuffing of arteries, veins and nerves in several of the dogs. Medium-sized arteries were sclerotic, with prominent reorganizing thrombi, particularly in dogs euthanized more than 6 months post-irradiation. Ganglia and nerves appeared to have increased interstitial collagen. Within the neurovascular plexuses in dogs from both groups, there was hyaline change in small arteries and arterioles, reactive perivascular fibrosis, widespread interstitial fibrosis and atrophy of peripheral nerves, with moderate axon loss. The glans penis was histologically normal in all dogs from groups A and B.

A summary of outcomes and statistics from semiquantitative pathologic evaluations is presented in Tables 3.10 and 3.11.

Table 3.10. Interfraction interval study: Summary statistics for semiquantitative pathology data

	Median Values			Statistics	
	50 Gy in 5 days (A)	**50 Gy in 11 days (B)**	**Control (0 Gy)**	**Comparisons**	**Corrected P-value**
MVD (vessel count), whole prostate	12.87 vessels/field	6.00 vessels/field	23.00 vessels/field	Control vs. 50 Gy in 5 days Control vs. 50 Gy in 11 days 50 Gy in 5 vs. 11 days	0.1765 0.0021 0.3266
MVD (pixel count), whole prostate	0.362%	0.0850%	1.863%	Control vs. 50 Gy in 5 days Control vs. 50 Gy in 11 days 50 Gy in 5 vs. 11 days	0.4530 0.0046 0.2077
Collagen content, prostate	20.90%	17.80%	10.41%	Control vs. 50 Gy in 5 days Control vs. 50 Gy in 11 days 50 Gy in 5 vs. 11 days	0.1671 0.6114 > 0.9999
Nerve density, prostatic capsule	3.042%	4.537%	3.524%	Kruskal-Wallis test	0.5100
Neurofilament content, prostatic nerves	61.73%	64.01%	76.75%	Control vs. 50 Gy in 5 days Control vs. 50 Gy in 11 days 50 Gy in 5 vs. 11 days	0.0196 0.4780 0.7406
Collagen content, prostatic nerves	21.73%	24.74%	48.16%	Control vs. 50 Gy in 5 days Control vs. 50 Gy in 11 days 50 Gy in 5 vs. 11 days	0.1483 0.3635 > 0.9999
Neurofilament content, penile nerves	41.95%	43.78%	75.51%	Control vs. 50 Gy in 5 days Control vs. 50 Gy in 11 days 50 Gy in 5 vs. 11 days	0.0658 0.1551 >0.9999
Collagen content, penile nerves	31.15%	27.09%	67.70%	Control vs. 50 Gy in 5 days Control vs. 50 Gy in 11 days 50 Gy in 5 vs. 11 days	0.4142 0.0285 0.9390
Arterial patency, NVB	23.30%	21.00%	32.40%	Kruskal-Wallis test	0.2027

Table 3.11. Interfraction interval study: Summary statistics for prostatic microvascular density data

	Median Values			Statistics	
	50 Gy in 5 days (A)	**50 Gy in 11 days (B)**	**Control (0 Gy)**	**Comparisons**	**Corrected P-value**
MVD (vessel count), Periurethral	15.0 vessels/field	5.5 vessels/field	17.2 vessels/field	Control vs. 50 Gy in 5 days Control vs. 50 Gy in 11 days 50 Gy in 5 vs. 11 days	0.9774 0.0093 0.1269
MVD (pixel count), Periurethral	15.00%	5.50%	17.20%	Control vs. 50 Gy in 5 days Control vs. 50 Gy in 11 days 50 Gy in 5 vs. 11 days	0.9774 0.0093 0.1269
MVD (vessel count), Capsular	9.4 vessels/field	4.2 vessels/field	9.2 vessels/field	Control vs. 50 Gy in 5 days Control vs. 50 Gy in 11 days 50 Gy in 5 vs. 11 days	> 0.9999 0.0277 0.0506
MVD (pixel count), Capsular	0.226%	0.092%	1.091%	Control vs. 50 Gy in 5 days Control vs. 50 Gy in 11 days 50 Gy in 5 vs. 11 days	0.3374 0.0083 0.4036
MVD (vessel count), Parenchymal	16.8 vessels/field	7.3 vessels/field	37.0 vessels/field	Control vs. 50 Gy in 5 days Control vs. 50 Gy in 11 days 50 Gy in 5 vs. 11 days	0.1239 0.0040 0.5988
MVD (pixel count), Parenchymal	0.254%	0.046%	1.429%	Control vs. 50 Gy in 5 days Control vs. 50 Gy in 11 days 50 Gy in 5 vs. 11 days	0.5994 0.0111 0.2254

Differences in Outcomes After Geographic Irradiation

One of four dogs in group C (irradiation of the NVB only) developed ED, at 105 days post-SBRT. Two dogs in that group were euthanized at days 110 and 118 due to grade IV colorectal toxicity, and the fourth dog was euthanized at 398 days with grade III colorectal toxicity. None of the dogs in group D developed ED; all were euthanized one year post-SBRT without evidence of colorectal toxicity.

Endocrinology

See Table 3.3.

Magnetic Resonance Imaging

Serial (pre- and post-irradiation) DCE-MRI data for the prostatic ROI of dogs in groups B, C and D are summarized in Table 3.12. Similar data for the ROI encompassing the glans penis are presented in Table 3.13, and data for the left and right NVB are in Figures 3.14 and 3.15.

Table 3.12. Geographic irradiation study: Mean outcome variables and overall summary statistics for DCE-MRI of the prostate.

	0 months (Baseline)	**4 months**	**12 months**	*p* (0 vs. 4m)*	*p* (0 vs. 12m)*	*p* (4 vs. 12m)*
K^{trans} (min^{-1})						
Group B (all sites)	612.3	820.0	337.3	*0.96*	*0.29*	*0.70*
Group C (NVB)	380.4	745.9	679.3	*0.03*	*0.002*	*0.65*
Group D (PB only)	605.3	680.0	560.2	*0.001*	*0.04*	*0.047*
*p** - Group B vs. D*	*0.95*	*0.27*	*0.12*			
*p** - Group C vs. D*	*0.87*	*0.52*	*0.08*			
*p** - Group B vs. C*	*0.91*	*0.52*	*0.098*			
k_{ep} (min^{-1})						
Group B (all sites)	2465.3	589.4	960.7	*< 0.0001*	*< 0.0001*	*0.05*
Group C (NVB)	1492.4	1560.7	675.5	*0.20*	*0.002*	*0.002*
Group D (PB only)	1165.2	1504.1	2763.1	*0.87*	*< 0.0001*	*< 0.0001*
*p** - Group B vs. D*	*0.0003*	*0.0002*	*<0.0001*			
*p** - Group C vs. D*	*0.003*	*0.001*	*<0.0001*			
*p** - Group B vs. C*	*0.05*	*0.002*	*0.098*			
v_p (unitless)						
Group B (all sites)	93.4	15.3	54.7	*< 0.0001*	*0.21*	*0.001*
Group C (NVB)	64.5	29.9	19.1	*0.62*	*0.002*	*0.002*
Group D (PB only)	6.5	4.1	5.5	*0.04*	*0.83*	*0.25*
*p** - Group B vs. D*	*<0.0001*	*0.15*	*<0.0001*			
*p** - Group C vs. D*	*0.001*	*<0.0001*	*<0.0001*			
*p** - Group B vs. C*	*0.19*	*0.004*	*0.03*			
v_e (unitless)						
Group B (all sites)	382.6	1762.7	834.0	*0.001*	*< 0.0001*	*0.59*
Group C (NVB)	727.0	625.7	1221.8	*0.55*	*0.002*	*0.002*
Group D (PB only)	618.6	678.0	221.4	*0.75*	*< 0.0001*	*< 0.0001*
*p** - Group B vs. D*	*0.001*	*0.01*	*<0.0001*			
*p** - Group C vs. D*	*0.0003*	*0.01*	*<0.0001*			
*p** - Group B vs. C*	*0.001*	*0.005*	*0.06*			
iAUGC (mM/min)						
Group B (all sites)	743.7	1120.2	624.2	*0.001*	*0.65*	*0.001*
Group C (NVB)	760.8	696.2	967.0	*0.16*	*0.002*	*0.002*
Group D (PB only)	732.3	753.7	395.0	*0.02*	*0.003*	*0.04*
*p** - Group B vs. D*	*0.28*	*0.34*	*0.0003*			
*p** - Group C vs. D*	*0.84*	*0.22*	*<0.0001*			
*p** - Group B vs. C*	*0.42*	*0.06*	*0.003*			

*This is the p-value comparing individual timepoints.

**This is the p-value comparing outcomes between groups at given timepoints.

Table 3.13. Geographic irradiation study: Mean outcome variables and summary statistics for DCE-MRI of the glans penis.

	0 months (Baseline)	**4 months**	**12 months**	*p* (0 vs. 4m)*	*p* (0 vs. 12m)*	*p* (4 vs. 12m)*
K^{trans} (min^{-1})						
Group B (all sites)	188.2	257.5	105.1	*0.96*	*0.12*	*0.02*
Group C (NVB)	433.4	183.7	383.4	*0.0002*	*0.65*	*0.004*
Group D (PB only)	278.9	277.2	173.8	*0.81*	*0.002*	*0.02*
*p** - Group B vs. D*	*0.055*	*0.86*	*0.36*			
*p** - Group C vs. D*	*0.0004*	*0.17*	*0.003*			
*p** - Group B vs. C*	*0.0004*	*0.13*	*0.001*			
k_{ep} (min^{-1})						
Group B (all sites)	407.0	342.3	547.5	*0.29*	*0.06*	*0.82*
Group C (NVB)	669.4	695.8	358.7	*0.27*	*0.004*	*0.004*
Group D (PB only)	405.7	435.2	935.7	*0.13*	*< 0.0001*	*0.05*
*p** - Group B vs. D*	*0.93*	*0.2*	*0.004*			
*p** - Group C vs. D*	*0.28*	*0.01*	*0.0001*			
*p** - Group B vs. C*	*0.13*	*0.01*	*0.06*			
v_p (unitless)						
Group B (all sites)	12.2	7.1	11.0	*0.06*	*0.58*	*0.02*
Group C (NVB)	9.1	7.9	1.0	*0.37*	*0.01*	*0.002*
Group D (PB only)	3.2	3.5	9.3	*0.29*	*0.0002*	*< 0.0001*
*p** - Group B vs. D*	*<0.0001*	*0.059*	*0.46*			
*p** - Group C vs. D*	*<0.0001*	*0.01*	*0.0003*			
*p** - Group B vs. C*	*0.38*	*0.37*	*0.0004*			
v_e (unitless)						
Group B (all sites)	607.4	1390.2	372.8	*0.01*	*0.04*	*0.01*
Group C (NVB)	1117.6	625.3	1406.1	*0.03*	*0.002*	*0.004*
Group D (PB only)	799.0	986.3	165.5	*0.94*	*< 0.0001*	*< 0.0001*
*p** - Group B vs. D*	*0.02*	*0.08*	*0.002*			
*p** - Group C vs. D*	*0.01*	*0.004*	*<0.0001*			
*p** - Group B vs. C*	*0.004*	*0.003*	*0.0003*			
iAUGC (mM/min)						
Group B (all sites)	258.8	364.1	124.8	*0.44*	*0.25*	*0.01*
Group C (NVB)	599.9	225.0	550.3	*< 0.0001*	*0.18*	*0.002*
Group D (PB only)	438.4	386.5	169.7	*0.63*	*< 0.0001*	*< 0.0001*
*p** - Group B vs. D*	*0.01*	*0.89*	*0.44*			
*p** - Group C vs. D*	*0.0002*	*0.03*	*0.0004*			
*p** - Group B vs. C*	*0.0002*	*0.03*	*0.0003*			

*This is the p-value comparing individual timepoints.

**This is the p-value comparing outcomes between groups at given timepoints.

Table 3.14. Geographic irradiation study: Mean outcome variables and overall summary statistics for DCE-MRI of the left neurovascular bundle.

	0 months (Baseline)	**4 months**	**12 months**	*p* (0 vs. 4m)*	*p* (0 vs. 12m)*	*p* (4 vs. 12m)*
K^{trans} (min^{-1})						
Group B (all sites)	132.4	280.6	174.4	*0.08*	*0.01*	*0.14*
Group C (NVB)	183.5	217.8	98.3	*0.69*	*0.03*	*0.02*
Group D (PB only)	208.9	273.3	37.1	*0.04*	*< 0.0001*	*< 0.0001*
*p** - Group B vs. D*	*0.17*	*0.76*	*<0.0001*			
*p** - Group C vs. D*	*0.09*	*0.55*	*<0.0001*			
*p** - Group B vs. C*	*0.02*	*0.43*	*0.07*			
k_{ep} (min^{-1})						
Group B (all sites)	778.6	665.8	675.9	*0.39*	*0.84*	*0.59*
Group C (NVB)	802.8	769.7	97.2	*0.92*	*0.002*	*0.002*
Group D (PB only)	643.5	798.9	530.0	*0.57*	*0.28*	*0.21*
*p** - Group B vs. D*	*0.94*	*0.1*	*0.4*			
*p** - Group C vs. D*	*0.87*	*0.21*	*0.001*			
*p** - Group B vs. C*	*0.69*	*0.54*	*0.004*			
v_p (unitless)						
Group B (all sites)	36.6	10.6	23.4	*0.03*	*0.34*	*0.53*
Group C (NVB)	27.8	27.1	12.9	*0.73*	*0.57*	*0.80*
Group D (PB only)	12.9	9.8	5.4	*0.63*	*0.16*	*0.52*
*p** - Group B vs. D*	*0.005*	*0.84*	*0.03*			
*p** - Group C vs. D*	*0.01*	*0.02*	*0.1*			
*p** - Group B vs. C*	*0.43*	*0.01*	*0.31*			
v_e (unitless)						
Group B (all sites)	390.0	1177.0	437.4	*0.02*	*0.04*	*0.24*
Group C (NVB)	600.8	820.0	1073.6	*0.004*	*0.002*	*0.002*
Group D (PB only)	391.1	498.8	38.3	*0.57*	*< 0.0001*	*< 0.0001*
*p** - Group B vs. D*	*0.06*	*0.21*	*<0.0001*			
*p** - Group C vs. D*	*0.04*	*0.14*	*<0.0001*			
*p** - Group B vs. C*	*0.02*	*0.97*	*0.003*			
iAUGC (mM/min)						
Group B (all sites)	232.7	468.6	243.1	*0.04*	*0.45*	*0.05*
Group C (NVB)	297.0	344.7	214.7	*0.69*	*0.28*	*0.75*
Group D (PB only)	331.6	376.5	40.7	*0.23*	*< 0.0001*	*< 0.0001*
*p** - Group B vs. D*	*0.14*	*0.84*	*<0.0001*			
*p** - Group C vs. D*	*0.12*	*0.96*	*<0.0001*			
*p** - Group B vs. C*	*0.04*	*0.89*	*0.81*			

*This is the p-value comparing individual timepoints.

**This is the p-value comparing outcomes between groups at given timepoints.

Table 3.15. Geographic irradiation study: Mean outcome variables and overall summary statistics for DCE-MRI of the right neurovascular bundle.

	0 months (Baseline)	**4 months**	**12 months**	*p* (0 vs. 4m)*	*p* (0 vs. 12m)*	*p* (4 vs. 12m)*
K^{trans} (min^{-1})						
Group B (all sites)	256.9	379.2	157.9	*0.62*	*0.65*	*0.04*
Group C (NVB)	424.9	336.7	206.5	*0.06*	*0.002*	*0.11*
Group D (PB only)	315.7	404.6	76.6	*0.02*	*0.001*	*< 0.0001*
*p** - Group B vs. D*	*0.42*	*0.72*	*0.005*			
*p** - Group C vs. D*	*0.07*	*0.81*	*0.0004*			
*p** - Group B vs. C*	*0.02*	*0.8*	*0.19*			
k_{ep} (min^{-1})						
Group B (all sites)	1547.4	705.0	718.9	*0.01*	*0.45*	*0.82*
Group C (NVB)	1095.4	909.6	204.0	*0.92*	*0.002*	*0.02*
Group D (PB only)	766.2	1313.5	920.0	*0.09*	*0.83*	*0.15*
*p** - Group B vs. D*	*0.04*	*0.04*	*0.66*			
*p** - Group C vs. D*	*0.14*	*0.1*	*0.002*			
*p** - Group B vs. C*	*0.24*	*0.43*	*0.01*			
v_p (unitless)						
Group B (all sites)	55.6	4.9	25.4	*0.02*	*0.39*	*0.07*
Group C (NVB)	21.4	13.4	5.8	*0.92*	*0.13*	*0.40*
Group D (PB only)	3.6	6.4	11.1	*0.20*	*0.0001*	*0.14*
*p** - Group B vs. D*	*0.005*	*0.11*	*0.32*			
*p** - Group C vs. D*	*0.01*	*0.11*	*0.087*			
*p** - Group B vs. C*	*0.04*	*0.06*	*0.06*			
v_e (unitless)						
Group B (all sites)	304.6	1598.6	367.5	*0.001*	*0.14*	*0.59*
Group C (NVB)	659.5	734.9	1212.1	*0.37*	*0.002*	*0.05*
Group D (PB only)	477.0	506.2	53.2	*0.63*	*< 0.0001*	*< 0.0001*
*p** - Group B vs. D*	*0.001*	*0.03*	*<0.0001*			
*p** - Group C vs. D*	*0.0001*	*0.06*	*<0.0001*			
*p** - Group B vs. C*	*0.0002*	*0.26*	*0.001*			
iAUGC (mM/min)						
Group B (all sites)	384.2	523.3	220.8	*0.16*	*0.05*	*0.01*
Group C (NVB)	523.0	430.0	361.7	*0.003*	*0.06*	*0.95*
Group D (PB only)	419.0	466.3	79.2	*0.01*	*< 0.0001*	*< 0.0001*
*p** - Group B vs. D*	*0.49*	*0.86*	*0.001*			
*p** - Group C vs. D*	*0.04*	*0.92*	*<0.001*			
*p** - Group B vs. C*	*0.01*	*0.54*	*0.098*			

*This is the p-value comparing individual timepoints.

**This is the p-value comparing outcomes between groups at given timepoints

Ultrasound

Post-irradiation ultrasound was performed in all four dogs from group C (one of which had clinical evidence of ED), the prostate was and continued to be hyperechoic to surrounding tissues in all. The prostate enlarged in one, and decreased in diameter in the other 3. Following irradiation, prostatic flow was either unchanged (3 of 4) or increased (1 of 4) in response to papaverine; penile blood flow increased after papaverine administration in all dogs. There was no subjective difference in ultrasonographic appearance or flow pattern in the one dog with erectile dysfunction. The prostate of all dogs in group D also was and continued to be hyperechoic to surrounding tissues following SBRT in all dogs. The prostate became smaller in one, and enlarged in the other 2 dogs in this group. In the dog with a shrinking prostate, prostatic flow increased in response to papaverine, as did penile flow. Penile flow increased in response to papaverine in the other two, as well, but after irradiation, prostatic blood flow was unaltered by intracavernosal administration of that drug. Results of the ultrasonographic evaluation of arterial blood velocity for the geographic irradiation study are summarized in Table 3.16.

Electrophysiology

Electromyography of the bulbospongiosus muscle was performed before and after SBRT in 3 of the 4 dogs in group B, 2 of the 3 dogs in group C and all three subjects in group D. All of the dogs had a normal electromyogram prior to SBRT and exhibited spontaneous activity after. Again, the majority of the abnormal activity was characterized by fibrillation potentials and positive sharp waves. MNCV was calculated for these dogs, and is reported in Table 3.17; mean data for CMAP amplitudes are reported in Figure 3.5. There were no statistically detectable

Table 3.16. Geographic irradiation study: Summary statistics for ultrasonographic evaluation of systolic rise times in the internal pudendal artery.

	Pre-Papaverine Systolic Rise Time (s)			*p**		
	Baseline	**4 months**	**12 months**	**Baseline to 4 months**	**Baseline to 12 months**	**4 to 12 months**
Group B (all sites)	0.11	0.09	0.08	*0.057*	*0.019*	*0.24*
Group C (NVB)	0.11	0.09	0.08	*0.0026*	*0.046*	*0.26*
Group D (PB only)	0.12	0.08	0.07	*0.02*	*0.0009*	*0.003*
*p** - Group B vs. D*	*0.73*	*0.20*	*0.69*			
*p** - Group C vs. D*	*0.47*	*0.97*	*0.11*			
*p** - Group B vs. C*	*0.88*	*0.68*	*0.64*			
	Change in Systolic Rise Time after Papaverine Administration (%)			*p**		
	Baseline	**4 months**	**12 months**	**Baseline to 4 months**	**Baseline to 12 months**	**4 to 12 months**
Group B (all sites)	-27.26	7.74	33.34	*0.046*	*0.08*	*0.08*
Group C (NVB)	-21.63	-1.13	-42.92	*0.32*	*0.32*	*0.32*
Group D (PB only)	-31.42	-27.85	-32.64	*0.56*	*0.56*	*0.08*
*p** - Group B vs. D*	*0.72*	*0.03*	*0.0495*			
*p** - Group C vs. D*	*0.48*	*0.0497*	*0.65*			
*p** - Group B vs. C*	*0.39*	*0.56*	*0.18*			

*This is the p-value for overall analysis of temporal change in an outcome variable within a treatment group; comparison of individual timepoints was also performed, and relevant results are summarized in the text.
**This is the p-value comparing outcomes between groups at given timepoints.

changes in MNCV with time in either group, nor were there differences between the groups at any point in time. The numerical values of MNCV post-irradiation were however lower than baseline in 2 of 3 subjects in group B, and all three subjects in group D. The MNCV was higher than baseline in both subjects in group C, for whom serial measurements were made. CMAP amplitudes were measured in two dogs from group C, and were higher at the proximal and distal sites at the terminal examination than at baseline in one subject, and lower in the other. Sensory nerve action potentials were not elicited in any of the dogs. There were no cord dorsum potentials that were successfully recorded in this set of dogs.

Post-Mortem Examination

Grossly, the prostate gland, neurovascular bundles and colon from dogs in group C were similar to those in group B. Those tissues were grossly unremarkable in dogs from group D. The penis was normal in all dogs from these treatment groups.

The prostate from dogs in group C showed marked glandular atrophy and replacement fibrosis, with moderate, diffuse lymphocytic interstitial inflammation dorsally. There was marked axonal vacuolization, and moderate coagulative necrosis of the interstitium of the dorsal prostatic capsule in one dog from this group. The ventral prostatic glands retained more normal features, though there was moderate interstitial fibrosis, and mild, diffuse lymphocytic inflammation. The neurovascular bundles from dogs in group C displayed the same histologic abnormalities as those in groups A and B. No histologic abnormalities were noted in the penis of dogs from group C.

Table 3.17. Geographic irradiation study: Motor nerve conduction velocities before and after SBRT

Treatment Group/ Dog ID	MNCV (m/s)		
	Pre-SBRT	4 months post-SBRT	12 months post-SBRT
B/7	56	59	37
B/8	51	NDA	45
B/9	58	64	67
B/13	67	NDA	N/A
C/10	50	63	68
C/11	65	68	N/A
C/12	66	NDA	N/A
C/17	64	47	N/A
D/14	60	42	NDA
D/15	65	69	44
D/16	63	NDA	49

N/A = dog euthanized earlier than this point in time; NDA = no data available

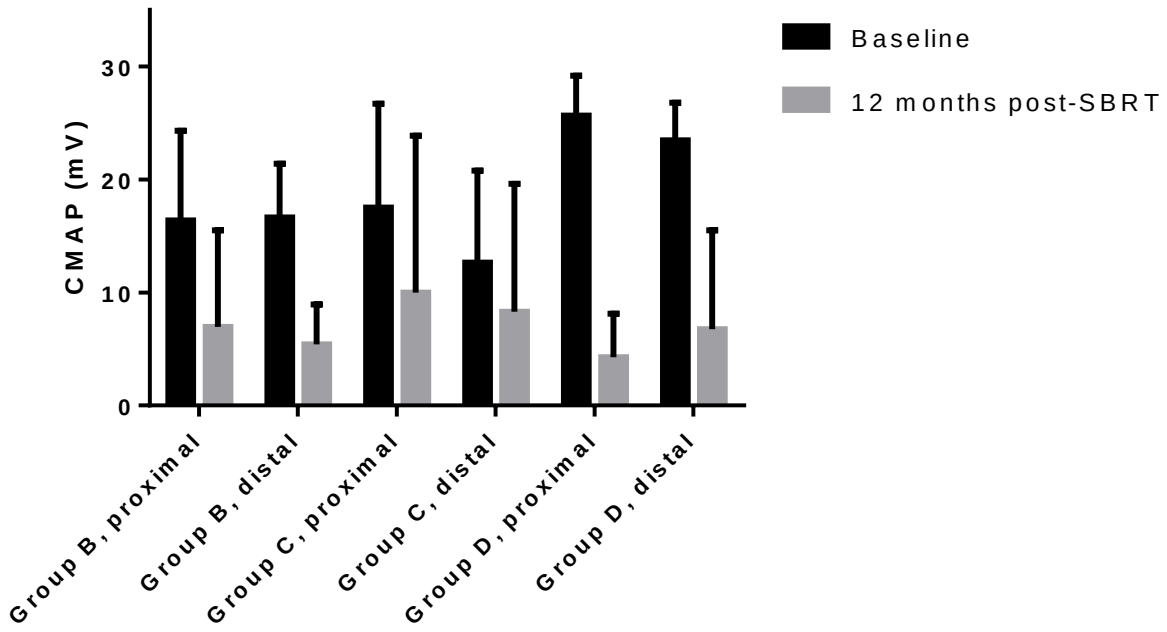

Figure 3.5. Geographic irradiation study: Compound muscle action potentials (CMAP) before and after SBRT at proximal and distal recording sites

The prostate from dogs in group D showed no evidence of glandular atrophy or fibrosis. Nerves and vessels appeared normal. The neurovascular bundles and penis from dogs in this group were also histologically unremarkable.

A summary of outcomes and statistics from semiquantitative pathologic evaluations is presented in Tables 3.18 and 3.19.

Dose-Response Assay

Although increasing the minimum duration of the interfraction interval from 24 to 48 hours improved complication rates, the incidence of grade III and IV colorectal toxicity in dogs whose prostates and/or NVBs were treated with 50 Gy was still too high to allow continued use of the canine model of RI-ED. Therefore a dose de-escalation study was performed to characterize the dose-responsiveness of measurable ED, and associated outcome measures. No subjects in groups E or F developed measurable ED during the study period (1 year after completion of SBRT). No subject in either of these groups experienced clinical evidence of colorectal toxicity.

Endocrinology

See Table 3.3.

Magnetic Resonance Imaging

Serial (pre- and post-irradiation) DCE-MRI data for the prostatic ROI of dogs in groups B, E and F are summarized in Table 3.20. Similar data for the ROI encompassing the glans penis are presented in Table 3.21, and data for the left and right NVB are in Tables 3.22 and 3.23.

Table 3.18. Geographic irradiation study: Summary statistics for semiquantitative pathology data

	Median Values				Statistics	
	All sites (A)	**NVB (C)**	**PB (D)**	**Control**	**Comparisons**	**Corrected P-value**
MVD (vessel count)	6.00	10.27	17.00	23.00	Control vs. All Control vs. NVB Control vs. PB All vs. NVB All vs. PB NVB vs. PB	0.0026 0.1134 > 0.9999 > 0.9999 0.3433 > 0.9999
MVD (pixel count)	0.085%	0.390%	0.793%	1.863%	Control vs. All Control vs. NVB Control vs. PB All vs. NVB All vs. PB NVB vs. PB	0.0100 0.4939 > 0.9999 > 0.9999 0.1771 > 0.9999
Collagen content, prostate	17.80%	41.00%	19.20%	10.41%	Control vs. All Control vs. NVB Control vs. PB All vs. NVB All vs. PB NVB vs. PB	> 0.9999 0.0341 > 0.9999 0.4923 > 0.9999 0.9863
Nerve density, prostatic capsule	4.537%	2.016%	1.764%	3.524%	Control vs. All Control vs. NVB Control vs. PB All vs. NVB All vs. PB NVB vs. PB	> 0.9999 0.9509 0.9043 0.0905 0.1536 > 0.9999
Neurofilament content in prostatic nerves	64.01%	68.43%	73.43%	76.75%	Control vs. All Control vs. NVB Control vs. PB All vs. NVB All vs. PB NVB vs. PB	0.2329 > 0.9999 > 0.9999 > 0.9999 0.1318 0.9731
Collagen content in prostatic nerves	24.74%	41.50%	43.82%	48.16%	Kruskal-Wallis test	0.1234
Neurofilament content in penile nerves	43.78%	61.66%	56.71%	75.51%	Control vs. All Control vs. NVB Control vs. PB All vs. NVB All vs. PB NVB vs. PB	0.0235 > 0.9999 > 0.9999 0.2751 > 0.9999 > 0.9999
Collagen content in penile nerves	27.09%	64.12%	62.11%	67.70%	Control vs. All Control vs. NVB Control vs. PB All vs. NVB All vs. PB NVB vs. PB	0.0470 > 0.9999 > 0.9999 0.1080 0.5114 > 0.9999
Arterial patency, NVB	21.00%	24.90%	28.00%	32.40%	Kruskal-Wallis test	0.3237

Table 3.19. Geographic irradiation study: Summary statistics for prostatic microvascular density data

	Median Values				Statistics	
	All sites (A)	**NVB (C)**	**PB (D)**	**Control**	**Comparisons**	**Corrected P-value**
MVD (vessel count), Periurethral	5.5 vessels/field	10.2 vessels/field	15.0 vessels/field	17.2 vessels/field	Control vs. All Control vs. NVB Control vs. PB All vs. NVB All vs. PB NVB vs. PB	0.0100 0.4939 > 0.9999 > 0.9999 0.1771 > 0.9999
MVD (pixel count), Periurethral	5.5%	10.2%	15.0%	17.2%	Control vs. All Control vs. NVB Control vs. PB All vs. NVB All vs. PB NVB vs. PB	0.0100 0.4939 > 0.9999 > 0.9999 0.1771 > 0.9999
MVD (vessel count), Capsular	4.2 vessels/field	5.9 vessels/field	8.8 vessels/field	9.2 vessels/field	Control vs. All Control vs. NVB Control vs. PB All vs. NVB All vs. PB NVB vs. PB	0.0359 0.5008 > 0.9999 > 0.9999 0.3161 > 0.9999
MVD (pixel count), Capsular	0.092%	0.224%	0.514%	1.091%	Control vs. All Control vs. NVB Control vs. PB All vs. NVB All vs. PB NVB vs. PB	0.0228 0.1395 > 0.9999 > 0.9999 0.2774 0.8931
MVD (vessel count), Parenchymal	7.3 vessels/field	12.3 vessels/field	26.4 vessels/field	37.0 vessels/field	Control vs. All Control vs. NVB Control vs. PB All vs. NVB All vs. PB NVB vs. PB	0.0019 0.1389 > 0.9999 > 0.9999 0.2917 > 0.9999
MVD (pixel count), Parenchymal	0.046%	0.312%	0.929%	1.429%	Control vs. All Control vs. NVB Control vs. PB All vs. NVB All vs. PB NVB vs. PB	0.0094 0.3470 > 0.9999 > 0.9999 0.1587 > 0.9999

Table 3.20. Dose-response study: Mean outcome variables and overall summary statistics for DCE-MRI of the prostate.

	0 months (Baseline)	**4 months**	**12 months**	*p* (0 vs. 4m)*	*p* (0 vs. 12m)*	*p* (4 vs. 12m)*
K^{trans} (min^{-1})						
Group B (50 Gy)	622.34	743.98	461.21	*0.96*	*0.29*	*0.70*
Group E (40 Gy)	894.15	386.67	224.22	*0.15*	*< 0.0001*	*< 0.0001*
Group F (30 Gy)	906.47	436.30	353.94	*0.003*	*< 0.0001*	*0.87*
*p** - Group B vs. F*	*0.015*	*0.0038*	*0.22*			
*p** - Group E vs. F*	*0.84*	*0.52*	*0.21*			
*p** - Group B vs. E*	*0.017*	*0.0036*	*0.0001*			
k_{ep} (min^{-1})						
Group B (50 Gy)	2465.25	589.37	960.69	*< 0.0001*	*< 0.0001*	*0.05*
Group E (40 Gy)	2460.03	681.89	646.41	*< 0.0001*	*< 0.0001*	*0.64*
Group F (30 Gy)	1510.85	1371.86	1376.68	*0.33*	*0.40*	*0.21*
*p** - Group B vs. F*	*0.003*	*0.002*	*0.34*			
*p** - Group E vs. F*	*< 0.0001*	*0.0088*	*0.0015*			
*p** - Group B vs. E*	*0.55*	*0.41*	*0.025*			
v_p (unitless)						
Group B (50 Gy)	93.36	15.35	54.73	*< 0.0001*	*0.14*	*0.0005*
Group E (40 Gy)	45.02	28.65	20.44	*0.02*	*0.43*	*0.64*
Group F (30 Gy)	46.82	103.67	31.95	*0.0001*	*0.21*	*0.0006*
*p** - Group B vs. F*	*0.0284*	*< 0.0001*	*0.01*			
*p** - Group E vs. F*	*0.87*	*< 0.0001*	*0.87*			
*p** - Group B vs. E*	*0.056*	*0.05*	*0.0004*			
v_e (unitless)						
Group B (50 Gy)	382.61	1762.72	833.97	*0.001*	*< 0.0001*	*0.59*
Group E (40 Gy)	429.82	636.33	482.69	*< 0.0001*	*0.09*	*0.27*
Group F (30 Gy)	626.09	326.66	256.47	*0.0002*	*0.002*	*0.009*
*p** - Group B vs. F*	*0.03*	*< 0.0001*	*< 0.0001*			
*p** - Group E vs. F*	*0.004*	*< 0.0001*	*0.0001*			
*p** - Group B vs. E*	*0.20*	*0.004*	*0.008*			
iAUGC (mM/min)						
Group B (50 Gy)	743.71	1120.21	624.23	*0.001*	*0.65*	*0.0005*
Group E (40 Gy)	783.97	566.73	328.68	*0.23*	*0.005*	*0.0001*
Group F (30 Gy)	1125.00	576.33	194.80	*< 0.0001*	*< 0.0001*	*< 0.0001*
*p** - Group B vs. F*	*< 0.0001*	*0.0079*	*< 0.0001*			
*p** - Group E vs. F*	*0.0027*	*0.85*	*0.0098*			
*p** - Group B vs. E*	*0.94*	*0.0041*	*0.0001*			

*This is the p-value comparing individual timepoints.

**This is the p-value comparing outcomes between groups at given timepoints.

Table 3.21. Dose-response study: Mean outcome variables and overall summary statistics for DCE-MRI of the glans penis.

	0 months (Baseline)	**4 months**	**12 months**	*p* (0 vs. 4m)*	*p* (0 vs. 12m)*	*p* (4 vs. 12m)*
K^{trans} (min^{-1})						
Group B (50 Gy)	219.64	228.51	98.71	*0.47*	*0.14*	*0.024*
Group E (40 Gy)	228.24	39.87	40.50	*< 0.0001*	*< 0.0001*	*0.38*
Group F (30 Gy)	341.64	122.97	21.95	*< 0.0001*	*< 0.0001*	*< 0.0001*
*p** - B vs. F*	*0.058*	*0.017*	*< 0.0001*			
*p** - E vs. F*	*0.016*	*0.12*	*0.03*			
*p** - B vs. E*	*0.51*	*< 0.0001*	*0.0004*			
k_{ep} (min^{-1})						
Group B (50 Gy)	427.47	309.91	557.50	*0.47*	*0.063*	*0.94*
Group E (40 Gy)	463.47	435.02	183.47	*1.00*	*< 0.0001*	*0.0007*
Group F (30 Gy)	505.10	522.72	267.91	*0.33*	*0.009*	*0.0034*
*p** - B vs. F*	*0.29*	*0.096*	*< 0.0001*			
*p** - E vs. F*	*0.61*	*0.54*	*0.03*			
*p** - B vs. E*	*0.21*	*0.05*	*0.0015*			
v_p (unitless)						
Group B (50 Gy)	14.04	5.38	10.17	*0.001*	*0.51*	*0.0008*
Group E (40 Gy)	7.20	8.08	7.25	*0.11*	*0.43*	*0.96*
Group F (30 Gy)	11.72	12.98	7.02	*0.38*	*0.85*	*0.006*
*p** - B vs. F*	*0.42*	*0.007*	*0.05*			
*p** - E vs. F*	*0.69*	*0.40*	*0.65*			
*p** - B vs. E*	*0.17*	*0.056*	*0.0995*			
v_e (unitless)						
Group B (50 Gy)	644.02	1417.89	365.39	*0.001*	*0.0497*	*0.0005*
Group E (40 Gy)	757.17	126.67	353.37	*< 0.0001*	*< 0.0001*	*< 0.0001*
Group F (30 Gy)	879.69	217.55	95.66	*< 0.0001*	*< 0.0001*	*< 0.0001*
*p** - B vs. F*	*0.02*	*< 0.0001*	*0.0001*			
*p** - E vs. F*	*0.27*	*0.0056*	*< 0.0001*			
*p** - B vs. E*	*0.04*	*< 0.0001*	*0.82*			
iAUGC (mM/min)						
Group B (50 Gy)	303.75	324.89	114.61	*0.96*	*0.58*	*0.0102*
Group E (40 Gy)	296.61	55.08	49.74	*< 0.0001*	*< 0.0001*	*0.23*
Group F (30 Gy)	521.77	160.79	34.74	*< 0.0001*	*< 0.0001*	*0.0001*
*p** - B vs. F*	*0.013*	*0.003*	*< 0.0001*			
*p** - E vs. F*	*0.0012*	*0.15*	*0.034*			
*p** - B vs. E*	*0.59*	*< 0.0001*	*0.0004*			

*This is the p-value comparing individual timepoints.

**This is the p-value comparing outcomes between groups at given timepoints.

Table 3.22. Dose-response study: Mean outcome variables and overall summary statistics for DCE-MRI of the left neurovascular bundle.

	0 months (Baseline)	**4 months**	**12 months**	*p* (0 vs. 4m)*	*p* (0 vs. 12m)*	*p* (4 vs. 12m)*
K^{trans} (min^{-1})						
Group B (50 Gy)	129.17	299.76	173.07	*0.062*	*0.0015*	*0.70*
Group E (40 Gy)	256.47	98.13	21.63	*0.069*	*0.0007*	*0.0003*
Group F (30 Gy)	248.71	67.21	11.50	*0.0017*	*< 0.0001*	*0.036*
*p** - Group B vs. F*	*0.087*	*< 0.0001*	*< 0.0001*			
*p** - Group E vs. F*	*0.81*	*0.058*	*0.05*			
*p** - Group B vs. E*	*0.10*	*0.001*	*< 0.0001*			
k_{ep} (min^{-1})						
Group B (50 Gy)	897.05	619.53	556.62	*0.27*	*0.42*	*0.14*
Group E (40 Gy)	859.20	231.04	378.08	*0.039*	*0.059*	*0.19*
Group F (30 Gy)	768.97	634.34	339.97	*0.28*	*0.012*	*0.28*
*p** - Group B vs. F*	*0.98*	*0.49*	*0.13*			
*p** - Group E vs. F*	*0.94*	*0.04*	*0.55*			
*p** - Group B vs. E*	*0.92*	*0.28*	*0.26*			
v_p (unitless)						
Group B (50 Gy)	35.13	7.20	24.44	*0.014*	*0.65*	*0.04*
Group E (40 Gy)	26.84	16.64	6.91	*0.28*	*0.047*	*0.025*
Group F (30 Gy)	21.84	23.67	3.03	*0.56*	*0.0002*	*0.0008*
*p** - Group B vs. F*	*0.22*	*0.0079*	*0.0007*			
*p** - Group E vs. F*	*0.66*	*0.36*	*0.04*			
*p** - Group B vs. E*	*0.59*	*0.11*	*0.007*			
v_e (unitless)						
Group B (50 Gy)	331.66	1231.09	535.19	*0.004*	*0.003*	*0.024*
Group E (40 Gy)	365.99	564.34	63.51	*0.008*	*0.001*	*< 0.0001*
Group F (30 Gy)	348.97	121.71	8.38	*0.003*	*< 0.0001*	*0.0011*
*p** - Group B vs. F*	*0.027*	*0.0003*	*< 0.0001*			
*p** - Group E vs. F*	*0.91*	*< 0.0001*	*0.0044*			
*p** - Group B vs. E*	*0.07*	*0.80*	*< 0.0001*			
iAUGC (mM/min)						
Group B (50 Gy)	215.01	487.91	264.27	*0.0026*	*0.25*	*0.024*
Group E (40 Gy)	322.19	168.22	36.49	*0.021*	*0.0002*	*< 0.0001*
Group F (30 Gy)	349.98	122.81	14.35	*0.0009*	*< 0.0001*	*0.0006*
*p** - Group B vs. F*	*0.07*	*0.0005*	*< 0.0001*			
*p** - Group E vs. F*	*0.75*	*0.08*	*0.05*			
*p** - Group B vs. E*	*0.049*	*0.0069*	*< 0.0001*			

*This is the p-value comparing individual timepoints.

**This is the p-value comparing outcomes between groups at given timepoints.

Table 3.23. Dose-response study: Mean outcome variables and overall summary statistics for DCE-MRI of the right neurovascular bundle.

	0 months (Baseline)	**4 months**	**12 months**	*p* (0 vs. 4m)*	*p* (0 vs. 12m)*	*p* (4 vs. 12m)*
K^{trans} (min^{-1})						
Group B (50 Gy)	317.81	305.73	153.96	*0.27*	*0.39*	*0.07*
Group E (40 Gy)	415.50	152.57	36.84	*0.11*	*0.0003*	*< 0.0001*
Group F (30 Gy)	571.30	123.15	17.58	*< 0.0001*	*< 0.0001*	*0.0011*
*p** - Group B vs. F*	*0.012*	*0.003*	*< 0.0001*			
*p** - Group E vs. F*	*0.50*	*0.07*	*0.0005*			
*p** - Group B vs. E*	*0.36*	*0.02*	*0.0002*			
k_{ep} (min^{-1})						
Group B (50 Gy)	1682.36	464.28	771.28	*0.0017*	*0.39*	*0.70*
Group E (40 Gy)	1053.11	285.65	343.33	*0.039*	*0.0039*	*0.50*
Group F (30 Gy)	1121.53	753.65	362.73	*0.096*	*0.033*	*0.036*
*p** - Group B vs. F*	*0.67*	*0.16*	*0.007*			
*p** - Group E vs. F*	*0.55*	*0.0014*	*0.83*			
*p** - Group B vs. E*	*0.21*	*0.59*	*0.0019*			
v_p (unitless)						
Group B (50 Gy)	58.16	3.83	22.66	*0.09*	*0.24*	*0.12*
Group E (40 Gy)	46.69	22.88	10.19	*0.06*	*0.046*	*0.085*
Group F (30 Gy)	26.57	32.55	6.76	*0.77*	*0.06*	*0.0008*
*p** - Group B vs. F*	*0.08*	*< 0.0001*	*0.05*			
*p** - Group E vs. F*	*0.29*	*0.25*	*0.0319*			
*p** - Group B vs. E*	*0.63*	*0.0015*	*0.31*			
v_e (unitless)						
Group B (50 Gy)	303.21	1680.72	372.58	*0.001*	*0.12*	*0.24*
Group E (40 Gy)	461.88	699.46	141.38	*0.004*	*< 0.0001*	*< 0.0001*
Group F (30 Gy)	533.77	171.44	22.84	*< 0.0001*	*< 0.0001*	*< 0.0001*
*p** - Group B vs. F*	*0.0015*	*< 0.0001*	*< 0.0001*			
*p** - Group E vs. F*	*0.11*	*< 0.0001*	*< 0.0001*			
*p** - Group B vs. E*	*0.002*	*0.59*	*0.0003*			
iAUGC (mM/min)						
Group B (50 Gy)	442.98	471.39	208.02	*0.89*	*0.0041*	*0.024*
Group E (40 Gy)	504.94	284.45	64.03	*0.029*	*< 0.0001*	*< 0.0001*
Group F (30 Gy)	726.73	191.68	26.11	*< 0.0001*	*< 0.0001*	*0.0001*
*p** - Group B vs. F*	*0.0015*	*0.0097*	*< 0.0001*			
*p** - Group E vs. F*	*0.048*	*0.044*	*< 0.0001*			
*p** - Group B vs. E*	*0.35*	*0.17*	*0.004*			

*This is the p-value comparing individual timepoints.

**This is the p-value comparing outcomes between groups at given timepoints.

Ultrasound

The prostate of all dogs in groups E and F became less echogenic after irradiation. The majority (2 of 3 in group E and 3 of 3 in group F) had prostatic shrinkage after irradiation. Subjectively, prostatic blood flow failed to change in response to papaverine after irradiation in all dogs from groups E and F. Penile blood flow continued to increase in response to papaverine administration in each of these dogs post-irradiation. Results of ultrasonographic evaluations of arterial blood velocity, for the dose-response study are summarized in Table 3.24.

Electrophysiology

Electromyography of the bulbospongiosus muscle was performed before and after SBRT in 3 of the 4 dogs in group B, and all three subjects in groups E and F. All of the dogs had a normal electromyogram prior to SBRT and exhibited spontaneous activity after. Again, the majority of the abnormal activity was characterized by fibrillation potentials and positive sharp waves. MNCV was calculated for these dogs, and is reported in Table 3.25; baseline MNCV was not available for 2 of the three dogs in group E. There were no statistically detectable changes in MNCV with time in either group, nor were there differences between the groups at any point in time. Again, the numerical values of MNCV post-irradiation were however lower than baseline in 2 of 3 subjects in group B; there was also a temporal decline in MNCV in all three subjects in group E, and temporal declines were noted in all 3 subjects in group F. Mean CMAP amplitude data is presented in Figure 6. Briefly, there was a temporal decline in 2 of 3 dogs from group E; there was a temporal increase in 2 of 3 dogs from group F. Sensory nerve action potentials were not elicited in any of the dogs. There were no cord dorsum potentials that were successfully recorded in this set of dogs.

Table 3.24. Dose-response study: Summary statistics for ultrasonographic evaluation of systolic rise times in the internal pudendal artery.

	Pre-Papaverine Systolic Rise Time (s)			*p**		
	Baseline	**4 months**	**12 months**	**Baseline to 4 months**	**Baseline to 12 months**	**4 to 12 months**
Group B (50 Gy)	0.11	0.09	0.08	*0.057*	*0.019*	*0.24*
Group E (40 Gy)	0.08	0.08	0.07	*0.57*	*0.003*	*0.0007*
Group F (30 Gy)	0.09	0.08	0.07	*0.30*	*0.15*	*0.01*
*p** - Group B vs. F*	*0.01*	*0.099*	*0.35*			
*p** - Group E vs. F*	*0.86*	*0.14*	*0.75*			
*p** - Group B vs. E*	*0.0028*	*0.52*	*0.37*			
	Change in Systolic Rise Time after Papaverine Administration (%)			*p**		
	Baseline	**4 months**	**12 months**	**Baseline to 4 months**	**Baseline to 12 months**	**4 to 12 months**
Group B (50 Gy)	-27.26	7.74	33.34	*0.05*	*0.08*	*0.08*
Group E (40 Gy)	-27.92	-21.11	-14.76	*0.08*	*0.08*	*0.56*
Group F (30 Gy)	-24.96	-33.32	-10.30	*0.08*	*0.56*	*0.56*
*p** - Group B vs. F*	*0.72*	*0.03*	*0.0495*			
*p** - Group E vs. F*	*0.51*	*0.0495*	*0.51*			
*p** - Group B vs. E*	*0.72*	*0.03*	*0.0495*			

*This is the p-value for overall analysis of temporal change in an outcome variable within a treatment group; comparison of individual timepoints was also performed, and relevant results are summarized in the text.
**This is the p-value comparing outcomes between groups at given timepoints.

Table 3.25. Dose-response study: Motor Nerve Conduction Velocity before and after SBRT

Treatment Group/ Dog ID	**MNCV (m/s)**		
	Pre-SBRT	**4 months post-SBRT**	**12 months post-SBRT**
B/7	56	59	37
B/8	51	NDA	45
B/9	58	64	67
B/13	67	NDA	N/A
E/18	70	43	42
E/19	NDA	58	46
E/20	NDA	69	52
F/21	45	48	39
F/22	89	55	46
F/23	58	52	32

N/A = dog euthanized earlier than this point in time; NDA = no data available

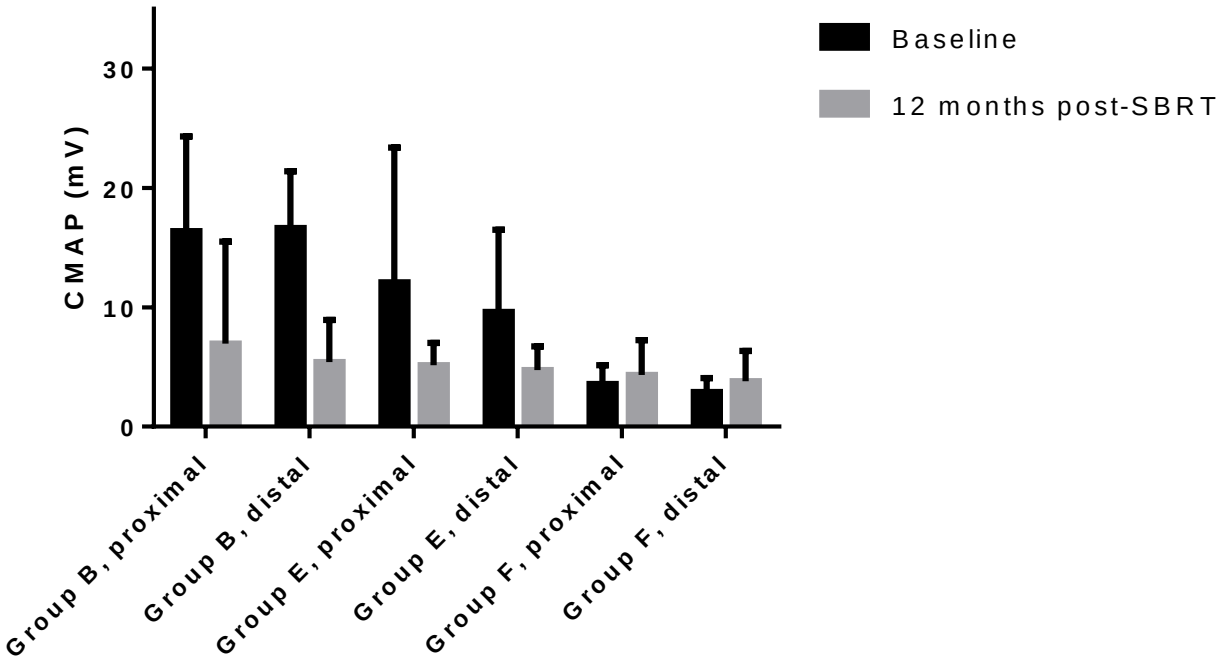

Figure 3.6. Dose-response study: Compound muscle action potentials (CMAP) before and after SBRT at proximal and distal recording sites

Post-Mortem Examination

Grossly, the prostate gland from dogs in groups E and F was small and firm; the neurovascular bundle was normal to slightly thickened, and the colon and penis were grossly unremarkable. Histologically, the prostate from dogs in group E displayed severe gland atrophy (more extensive centrally than peripherally) and replacement fibrosis, with mild to moderate ectasia of remaining glands. There was moderate, multifocal lymphocytic inflammation, with moderate perineural and perivascular lymphocytic cuffing. There was severe adventitial thickening, and intimal hypertrophy with subendothelial hemorrhage and occasional medial necrosis in small and medium-sized arteries. A large number of these vessels were also thrombosed, often with remodeling around the thrombi. The peripheral nerve bundles had increased amounts of

interstitial collagen. The neurovascular bundles from dogs in group E were characterized by moderate interstitial fibrosis of the fibrofatty connective tissue, moderate increases in interstitial collagen within peripheral nerves and ganglia, and moderate vascular changes, including severe intimal proliferation and mild to moderate perivascular fibrosis of medium-sized arteries, multifocal lymphocytic cuffing of arteries and arterioles, and thrombosis and reorganization of several medium to large arteries. No histologic abnormalities were noted in the penis in group E. The prostate from dogs in group F had moderate glandular atrophy and replacement fibrosis, with mild ectasia of remaining glands. There was mild, multifocal lymphocytic inflammation of the prostatic interstitium, occurring in aggregates. Nerves and vessels appeared normal. The neurovascular bundles and penis from dogs in this group were histologically unremarkable.

A summary of outcomes and statistics from semiquantitative pathologic evaluations is presented in Tables 3.26 and 3.27.

Table 3.26. Dose-response study: Summary statistics for semiquantitative pathology data

	Median Values				Statistics	
	50 Gy (B)	**40 Gy (E)**	**30 Gy (F)**	**0 Gy Control**	**Comparisons**	**Corrected P-value**
MVD (vessel count)	6.00	7.07	17.60	23.00	0 Gy vs. 30 Gy 0 Gy vs. 40 Gy 0 Gy vs. 50 Gy 30 Gy vs. 40 Gy 30 Gy vs. 50 Gy 40 Gy vs. 50 Gy	> 0.9999 0.0645 0.0093 > 0.9999 0.6445 > 0.9999
MVD (pixel count)	0.085%	0.506%	2.029%	1.863%	0 Gy vs. 30 Gy 0 Gy vs. 40 Gy 0 Gy vs. 50 Gy 30 Gy vs. 40 Gy 30 Gy vs. 50 Gy 40 Gy vs. 50 Gy	> 0.9999 0.5517 0.0161 0.7903 0.0503 > 0.9999
Collagen content, prostate	17.80%	49.90%	66.70%	10.41%	0 Gy vs. 30 Gy 0 Gy vs. 40 Gy 0 Gy vs. 50 Gy 30 Gy vs. 40 Gy 30 Gy vs. 50 Gy 40 Gy vs. 50 Gy	0.0507 0.0686 > 0.9999 > 0.9999 0.3847 0.4837
Nerve density, prostatic capsule	4.537%	4.094%	5.906%	3.524%	0 Gy vs. 30 Gy 0 Gy vs. 40 Gy 0 Gy vs. 50 Gy 30 Gy vs. 40 Gy 30 Gy vs. 50 Gy 40 Gy vs. 50 Gy	0.0037 > 0.9999 0.7710 0.1126 0.3163 > 0.9999
Neurofilament content in prostatic nerves	64.01%	68.36%	68.20%	76.75%	0 Gy vs. 30 Gy 0 Gy vs. 40 Gy 0 Gy vs. 50 Gy 30 Gy vs. 40 Gy 30 Gy vs. 50 Gy 40 Gy vs. 50 Gy	> 0.9999 > 0.9999 0.0747 > 0.9999 0.9427 0.7826
Collagen content in prostatic nerves	24.74%	49.06%	52.40%	48.16%	0 Gy vs. 30 Gy 0 Gy vs. 40 Gy 0 Gy vs. 50 Gy 30 Gy vs. 40 Gy 30 Gy vs. 50 Gy 40 Gy vs. 50 Gy	> 0.9999 > 0.9999 0.5166 > 0.9999 0.0471 0.4498
Neurofilament content in penile nerves	43.78%	71.87%	60.98%	75.51%	0 Gy vs. 30 Gy 0 Gy vs. 40 Gy 0 Gy vs. 50 Gy 30 Gy vs. 40 Gy 30 Gy vs. 50 Gy 40 Gy vs. 50 Gy	0.8537 > 0.9999 0.0961 > 0.9999 > 0.9999 0.3870
Collagen content in penile nerves	27.09%	72.20%	74.27%	67.70%	0 Gy vs. 30 Gy 0 Gy vs. 40 Gy 0 Gy vs. 50 Gy 30 Gy vs. 40 Gy 30 Gy vs. 50 Gy 40 Gy vs. 50 Gy	> 0.9999 > 0.9999 0.9680 > 0.9999 0.0364 0.0961
Arterial patency, NVB	21.00%	23.00%	27.30%	32.40%	Kruskal-Wallis test	0.3175

Table 3.27. Dose-response study: Summary statistics for prostatic microvascular density data

	Median Values				Statistics	
	50 Gy (B)	**40 Gy (E)**	**30 Gy (F)**	**0 Gy Control**	**Comparisons**	**Corrected P-value**
MVD (vessel count), Periurethral	5.5 vessels/field	7.0 vessels/field	10.8 vessels/field	14.5 vessels/field	0 Gy vs. 30 Gy 0 Gy vs. 40 Gy 0 Gy vs. 50 Gy 30 Gy vs. 40 Gy 30 Gy vs. 50 Gy 40 Gy vs. 50 Gy	> 0.9999 0.0855 0.0080 > 0.9999 0.6587 > 0.9999
MVD (pixel count), Periurethral	5.5%	7.0%	2.5%	17.2%	0 Gy vs. 30 Gy 0 Gy vs. 40 Gy 0 Gy vs. 50 Gy 30 Gy vs. 40 Gy 30 Gy vs. 50 Gy 40 Gy vs. 50 Gy	0.0005 0.0025 0.0008 0.7885 0.8850 0.9926
MVD (vessel count), Capsular	4.2 vessels/field	5.0 vessels/field	11.6 vessels/field	9.2 vessels/field	0 Gy vs. 30 Gy 0 Gy vs. 40 Gy 0 Gy vs. 50 Gy 30 Gy vs. 40 Gy 30 Gy vs. 50 Gy 40 Gy vs. 50 Gy	> 0.9999 0.4533 0.0338 0.5462 0.0668 > 0.9999
MVD (pixel count), Capsular	0.1%	0.3%	1.6%	1.1%	0 Gy vs. 30 Gy 0 Gy vs. 40 Gy 0 Gy vs. 50 Gy 30 Gy vs. 40 Gy 30 Gy vs. 50 Gy 40 Gy vs. 50 Gy	> 0.9999 0.7995 0.0305 0.4492 0.0204 > 0.9999
MVD (vessel count), Parenchymal	7.3 vessels/field	8.4 vessels/field	28.2 vessels/field	37.0 vessels/field	0 Gy vs. 30 Gy 0 Gy vs. 40 Gy 0 Gy vs. 50 Gy 30 Gy vs. 40 Gy 30 Gy vs. 50 Gy 40 Gy vs. 50 Gy	> 0.9999 0.0831 0.0129 > 0.9999 0.4727 > 0.9999
MVD (pixel count), Parenchymal	0.046%	0.324%	1.590%	1.429%	0 Gy vs. 30 Gy 0 Gy vs. 40 Gy 0 Gy vs. 50 Gy 30 Gy vs. 40 Gy 30 Gy vs. 50 Gy 40 Gy vs. 50 Gy	> 0.9999 0.6503 0.0212 0.9400 0.0543 > 0.9999

Table 3.28. Multivariable linear regression analysis of percent collagen in prostatic nerves

		95% Confidence Limits		p-value
Intercept		12.65	20.95	
Treatment Group	Control	Reference		
	A	-17.62	0.74	0.07
	B	-16.21	-1.84	0.01
	C	-4.63	11.93	0.39
	D	-9.58	3.98	0.42
	E	-4.24	9.31	0.46
	F	-0.24	13.31	0.06
Survival Group	1*	Reference		
	2	-11.89	2.69	0.22
	3	-8.07	9.08	0.91
	4	0	0	

*Survival was grouped into 4 categories: 0 to 3, 3 to 6, 6 to 9 and 9 to 12 months.

Table 3.29. Multivariable linear regression analysis of percent collagen in penile nerves

		95% Confidence Limits		p-value
Intercept		11.69	17.65	
Treatment Group	Control	Reference		
	A	-12.83	-1.33	0.016
	B	-15.02	-6.16	< 0.0001
	C	-4.83	5.19	0.94
	D	-7.55	0.88	0.12
	E	-0.22	8.22	0.06
	F	1.78	10.22	0.005
Survival Group	1*	Reference		
	2	-6.58	1.65	0.24
	3	-6.92	3.26	0.48
	4	0	0	

Further statistical analysis of the percent collagen within nerves was performed for all treatment groups, to correct for differences in the time after SBRT at which dogs were euthanized. A multivariable linear regression model of ranks for mean values was used to evaluate the effects of treatment group, and survival time. Results are presented in Tables 28 and 29.

Discussion

In this manuscript, we describe the feasibility of a canine model for studying the etiology of RI-ED. SBRT was chosen rather than more conventional fractionated irradiation techniques due to the convenience of a severely hypofractionated protocol; SBRT has been shown to result in a similar incidence of RI-ED, as compared with conventional protocols.[3] The initial prescription was based on results of a recent phase I clinical trial, which demonstrated the short-term safety and efficacy of protocols delivering 50 Gy to the prostate in 5 fractions via linear accelerator-based SBRT for low to intermediate risk prostate cancer in men.[28]

ED was observed in 5 of 22 (22.7%) irradiated dogs in this study. Several investigators have suggested that pelvic irradiation may alter endocrine status, and adversely affect erectile function. In fact, most men treated for prostatic cancer are elderly; with age, testosterone and luteinizing hormone (which is secreted by the pituitary gland and stimulates testicular and adrenal production of testosterone) levels decrease. The prostate contributes to the production of these hormones (testosterone is converted to dihydrotestosterone in the prostate by 5-alpha-reductase), so radiation may exacerbate an already tenuous situation. Some patients are on hormonal therapy to purposefully decrease testosterone levels, and this significantly contributes to decreased sexual function, likely due to shrinkage of the pudendal nerve's motor pool, and subsequent atrophy of perianal muscles, as these nerves and muscles require testosterone for normal health and maintenance (personal communication, Rick Johnson). However, recent clinical speculation has been largely dismissive of the notion that modulation of testosterone levels by prostatic irradiation contributes to RI-ED.[32-35] Zagars and Pollack (1997) observed a 9% fall in serum testosterone concentrations 3 months following external beam radiotherapy for

treatment of prostate cancer; overall, testosterone levels dropped in 71% of (85) men and rose in 29%. Compared with pre- and post-radiotherapy testosterone levels, which had a coefficient of variation of 33%, the 9% fall was quite small, and likely of no clinical or pathophysiological significance. It is unlikely that the observed drop in testosterone was related to simultaneous dramatic drops in PSA concentrations. The authors dismissed the likelihood of scattered radiation dose deposited in the testicles contributing to changes in testosterone concentrations, given that TLD measurements in ten patients demonstrated cumulative testicular doses no greater than 2.50 Gy. Although spermatogenesis can be depressed by as little as 0.30 Gy, Leydig cell function is more radioresistant. Furthermore, similar drops in testosterone have been noted in patients post-prostatectomy, suggesting that serum concentrations levels may fall after radiotherapy or surgery due to stress, rather than the localized therapy.[33] Nichols et al (2012) observed no significant change in serum testosterone levels within 24 months of proton irradiation of the prostate.[34] Kupelian et al (2006) found no association between testosterone and erectile dysfunction in aging men. They did note that testosterone levels are associated with a decrease in risk of ED in men with elevated serum concentrations of luteinizing hormone.[32,35] Though no *in vivo* dosimetry was performed, the maximum calculated testicular dose delivered to subjects in the present study was 11 Gy. This is likely high enough to alter Leydig cell function and decrease testicular production of testosterone. However, there were no significant changes in circulating serum concentrations of either testosterone or luteinizing hormone in these dogs.

All 5 dogs with ED were treated in groups A, B or C, and the rate of ED among those groups alone was 5 of 13 (38.5%). The median time to onset of RI-ED was 192 days (95% confidence

interval: 119 to 265; range: 105 to 325); 4 of those 5 dogs developed ED at least 5 months after irradiation. Conversely, the median survival time of dogs in groups A, B and C that did not develop ED was 118 days (95% confidence interval: 100 to 136 days; range: 99 to 398 days). Only 2 of those 7 dogs survived greater than 5 months; the remainder were euthanized early due to severe colorectal toxicity (further discussion of this toxicity is beyond the scope of this manuscript, but is the subject of Chapter 4). Dogs in which only the PB was irradiated, and dogs that received a lower total dose (and dose per fraction) of radiation developed neither clinically appreciable colorectal toxicity, nor measurable ED. This does not however, imply that dogs in groups D, E and F had no evidence of subclinical ED; in fact, neurophysiologic and perfusion studies evidenced neurogenic and/or vascular injuries in these dogs, which could contribute to RI-ED.

Observed electromyographic changes in the bulbospongiosus muscles of all irradiated dogs in this study indicate hypersensitive, denervated myofibers, which can be observed with either primary muscle or nerve disease. To further investigate potential nerve damage, nerve conduction studies were performed. Motor nerve conduction studies of the pudendal nerve were performed prior to radiation treatment and repeated at the 4 month and 1 year post treatment examinations. Since there are no established normal values for MNCV of the pudendal nerve in dogs, it was intended that the pre-treatment values were to be used as comparison for the post-treatment values in each dog. However, CMAPs were not obtained at all timepoints in all of the dogs. It is likely that the reason for inadequate data collection was due to inappropriate technique, stemming from (1) the stimulating electrode not being in close enough proximity to the pudendal nerve, as it travels between the coccygeus and superficial gluteal muscles, and (2)

placement of the recording electrode too far distal to the bulbospongiosus muscle. Similarly sensory nerve conduction studies were attempted prior to radiation treatment, as well as 4 months and 1 year post-treatment. Sensory nerve action potentials were not elicited in any of the dogs. The goal was to stimulate the dorsal nerve of the penis distally and record off the pudendal nerve as it travels between the coccygeus muscle and the superficial gluteal muscle. However, we believe that sensory nerve action potentials were not obtained due to incorrect placement of the electrodes. As the canine pudendal nerve anatomy was further reviewed, changes in the placement of the electrodes were made, allowing compound muscle and sensory nerve action potentials to be recorded in later studies. This revised technique should prove extremely useful in future electrophysiological studies. Cord dorsum potentials were also attempted in order to study the afferent information arising in the spinal cord segments as they received input from the dorsal nerve of the penis. The stimulating electrode was placed over the dorsal nerve of the penis and the recording electrode was placed in the interarcuate ligament at L4-L5. No cord dorsum potentials were successfully recorded in this set of dogs. Since the pudendal nerve enters the sacral spinal cord segments, which are located at the level of the L5-L6 vertebral bodies in most medium sized dogs, we decided to record further caudally in subsequent studies (from the interarcuate ligament at L5-L6). Again, this new technique proved effective, but neither sensory nerve conduction data nor cord dorsum potential data were successfully obtained from enough dogs, or at enough serial timepoints, in this study to make meaningful inferences about radiation-induced alterations in nerve function.

Therefore, from this study, we can effectively conclude that abnormal EMG activity was observed in all dogs in which post radiation treatment data was collected. This spontaneous

activity was consistent with nerve and/or muscle disease, likely secondary to radiation therapy. Further studies to evaluate motor and sensory nerve function (motor and sensory nerve conduction velocities and cord dorsum potentials) would be helpful in identifying and characterizing the underlying cause of the EMG changes.

In dogs for which pre- and post-SBRT CMAPs were recorded, the MNCV was slowed by SBRT in groups A, B, D, E and F. This slowing could be due to either axonal drop-out, or demyelination. Post-SBRT CMAP amplitudes were lower than baseline in dogs from groups A and B; this is evidence for axonal neuropathy, more so than demyelination.[36] Axonal loss is further supported by the histopathologic observation that the percent of neurofilament in penile nerves was lower than controls in irradiated subjects. The percent of neurofilament per nerve in the penis reflects the amount of viable axonal tissue, as neurofilament is the predominant intermediate filament in neurons and provides structural support for axons, ultimately controlling axonal diameter. Though the duration of the interfraction interval had no detectable impact on neurofilament levels, the percent of a nerve occupied by neurofilament was directly proportional to radiation dose. Furthermore, while there was no statistically significant difference in percent neurofilament when comparing control dogs with those in groups C and D, dogs in those treatment groups had absolute values of percent neurofilament which were intermediate between those in group B and the unirradiated controls, suggesting that irradiation of the prostate, NVB and PB are required for maximal axonal degradation. Further histologic evidence of radiation-induced penile nerve damage arises from analysis of the percent of each nerve occupied by collagen. Here, it was demonstrated that dogs in receiving 30 and 40 Gy had a higher percentage of each peripheral penile nerve occupied by collagen than the unirradiated control population;

this is consistent with the fact that neuronal fibrosis is a classic late effect. Interestingly, even when corrected for survival time, the percentage of collagen in penile nerves from dogs treated with 50 Gy was lower than controls. This may be explained not by a decrease in the absolute amount of collagen per nerve bundle, but instead, by nerve degeneration. The nerves were characterized by vacuolization, which appeared to be occurring within axons; this observation is supported by the fact that degeneration of non-myelinated axons can occur in the absence of Schwann cells or macrophages containing debris; such vacuolated appearance can be due to accumulation of axoplasmic organelles, particularly smooth endoplasmic reticulum and/or mitochondria, which can interfere with axoplasmic flow.[37] It should be noted though that based on light microscopic evaluation, Schwann cell degeneration and vacuolization, rather than axonal vacuolization, cannot be ruled-out. Schwann cell degeneration can lead to secondary axonal injury, and whether these degenerative changes are predominately occurring in axons or supportive Schwann cells, this study was not designed to determine whether neurogenic changes are primary radiation injury or secondary to vascular insults. Regardless of cause, vacuolization and swelling of either axons or Schwann cells would artificially decrease the percentage of collagen within each nerve bundle. Furthermore, this study was unable to characterize the origin of nerves for which there was histologically-evident damage; histochemistry could be performed in future studies to dissect out whether neuronal/axonal damage predominated in fibers originating from sympathetic, parasympathetic or somatic nerves.

In addition to observed neuropathic abnormalities in the pudendal and penile nerves, histopathologic evaluation of prostatic nerves also suggests that prostatic irradiation damages autonomic nerves that supply the urogenital tract. Parasympathetic control of penile erection is

supplied by the pelvic nerve; branches of this nerve travel through the NVB, which is divided into anterior and posterior nerves. The anterior nerves innervate the prostate, while the posterior nerves innervate the rectum and portions of the cavernosal nerve. And while not a predominant component of the NVB or a predominant contributor to the cavernosal nerve, there is also a prostatic subdivision of the posterior segment, which processes and relays erectogenic neural signals;[38,39] it is damage to this neural segment which could account for development of erectile dysfunction in patients treated with nerve-sparing prostatectomy. The cavernous nerves are responsible for release of nitric oxide and acetylcholine, which directly and indirectly causes calcium depletion in vascular smooth muscle (via activation of cyclic AMP and cyclic GMP), with subsequent smooth muscle relaxation. Intact parasympathetic nerve function is therefore essential to the vasodilatory processes which are responsible for the first phase of penile erection by allowing for increased arterial inflow into the penis and sinusoidal relaxation which enables blood trapping in the corpus cavernosa. The intraprostatic nerves were used in histologic evaluations of radiation-induced NVB damage for two reasons: (1) they represent a major branch of the NVB, and contribute to the neuronal component of erectile physiology, and (2) they were recovered at post-mortem examination in all subjects, whereas the predominant extraprostatic NVB was not recovered in several subjects due to the tissue being obscured and/or replaced by reactive peri-prostatic fibrosis. Post-irradiation changes in percent neurofilament in peripheral nerves of the prostate were similar to those observed in the penile nerves in that neurofilament was directly proportional to the dose of radiation. The percent of neurofilament per nerve was lower for dogs in groups B than C, D or the controls; this is not a surprising finding given that the prostate was not the primary target of irradiation in dogs from groups C or D, and upstream changes in nerve morphology are less likely than downstream effects (as was the case in the

penile nerves). Similar to the changes in percent collagen per nerve described for penile nerves, there was evidence of radiation-induced prostatic endoneurial fibrosis in dogs treated with 30 Gy; and dogs treated with 50 Gy had lower percent collagen per nerve than either control dogs, or those treated with 30 or 40 Gy, again attributed to axonal and/or Schwann cell degeneration and vacuolization.

Vasculopathies (due to alteration in NO production or due to primary radiation-induced vessel injury) were evidenced by DCE-MRI and ultrasound data.

Radiation-induced injuries in normal tissues are typically predictable with regard to type, severity and timing. DCE-MRI was hypothesized to be a good predictor of radiation-induced changes in tissue perfusion because the predominant late radiation-associated changes observed in most normal tissues relate to fibrotic and vascular changes. This study therefore attempted to characterize perfusion, vascular permeability and interstitial diffusibility in several pelvic organs (prostate, NVB and glans penis) of the dog, both before and after pelvic SBRT using serial DCE-MRI. Such use of DCE-MRI to study radiation-induced changes in normal tissues is logical, but unprecedented; the authors are aware of no previous studies which have validated DCE-MRI in this setting.

These DCE-MRI studies generated extensive and complex data. A great deal of variability in outcome measures was observed when comparing individual slices composing each VOI from a given dog, at a given point in time. To account for this variability when comparing averaged outcomes between different timepoints within a given treatment group, and when comparing

outcomes between treatment groups, data was analyzed using Friedman's test for non-parametric measures, which accounted for multiple measurements at each point in time, and repeated measurements on the same subject over time.

Despite using this robust statistical approach and having held many procedural and analytical variables constant (including systemic peripheral blood pressure, contrast dose and injection rate, scanning parameters and coil placement), one of the largest limitations to confident interpretation of the DCE-MRI data was a lack of consistent baseline values between subjects. The wide variation in these pre-irradiation values was unexpected, but there are several possible explanations for this variability.

One potential source of error is fluctuations in flow and blood velocity in smaller vessels, such as the internal pudendal arteries, which could have been related to fluid boluses and/or vasoactive drugs used to maintain relatively constant blood pressure. Another potential source of error is that the coil performance may have declined during the several years over which this study spanned. Yet another potential source of variability was the compartmental model that was used, which relies on an AIF. But those vessels used for the AIF are small, and detection of their signal and magnitude of that signal fluctuated between studies for the same dog, and between different dogs at the same time points. Also, variability may be attributed to perfusion heterogeneity in the organ. The large size of the prostatic volume of interest (VOI), which encompassed the entire prostate, means that not only was prostatic parenchyma analyzed, but so too was prostatic urethra and the indwelling urinary catheter. This may have "diluted" any changes in signal intensity unique to the prostate itself. Therefore, future studies should consider

use of a smaller ROI, encompassing only prostatic parenchyma. Alternatively, image inhomogeneity across different slices, due to factors such as magnetic field heterogeneity near the edges, or variations in coil sensitivity across the field could contribute to the observed variability. Further discussion of how the DCE-MRI protocol could have been optimized for this project is beyond the scope of this manuscript, but can be found in Chapter 5. One statistical approach to overcome this limitation would have been to pool baseline data; but although pooling would have brought the mean and median values at baseline closer to the population average, it may also have masked true differences between time points, and show differences that do not exist, hence making the analysis highly prone to both type I and II statistical errors. Another approach would have been evaluation of percent change over time, rather than absolute change over time; this approach was opted against, as it would have precluded consideration of intra-individual variability which is gained through use of multiple measurements at any given timepoint.

Nevertheless, the statistical analysis took into consideration individual temporal changes, and identified a number of interesting and significant changes between individuals, treatment groups and time points that seem to correspond well to histopathologic findings.

The only temporal change in DCE-MRI parameters of the prostate in group A was an increase in v_e. The increased volume of extravascular, extracellular space may be attributed to the marked glandular atrophy and concomitant replacement fibrosis (with mature collagen present, suggesting the fibrotic changes were chronic) noted on pathologic examination. These pathologic findings are expected radiation injuries, and increase the abnormal interstitial volume

through which contrast agents can diffuse in the prostate gland. The same trend towards increased leakage space was noted in group B, and in fact, the 12 month v_e was larger in group B than group A. Because glandular atrophy and fibrosis are typical late radiation effects, the duration of interfraction interval was not anticipated to have a strong impact on v_e when all other characteristics of the radiation protocols were equal. Therefore, despite a low p-value, type I error should be considered, and could be attributable to the fact that 12 month data for dogs in group A was only available for 2 subjects. Post-irradiation reduction in k_{ep} in group B appeared to be partially reversible; this change reflects impaired ability of contrast to be transported back into the vasculature once extravasated, and likely contributed to the transient decrease in v_p. These alterations in prostatic perfusion were also reflected by the noted changes in the model-free parameter, iAUGC.

The time-dependent decrease in penile K^{trans}, v_e and iAUGC noted in group A suggests decreased ability to transport contrast from the vascular compartment to the interstitium, and a decreased interstitial volume, and coincided with the onset of erectile dysfunction in the two dogs analyzed in this group. Temporal decreases in penile iAUGC and v_e in group B suggest similar pathophysiologic changes in this group, though the absence of detectable changes in K^{trans} for this group suggests that penile perfusion was impacted to a lesser extent in this group, which is further evidenced by the fact that the leakage space in group B was higher at 12 months than in group A. In the penis, maintenance of a large leakage space likely correlates with maintenance of healthy, distensible cavernosal tissue, which is requisite for normal penile erection. We hypothesize that the decrease in the aforementioned factors could relate functionally to decreases in penile distensibility as erectile dysfunction developed. As such, although vascular effects of

radiation are not thought to be dependent upon total treatment time, or duration of the interfraction interval, those parameters may affect male sexual health.

No perfusion changes were noted in the NVB for group A. The only changes that were consistent between the left and right NVB for group B was an increase in v_e during the first four months post-irradiation. This is likely due to reactive fibrosis (attributable to late radiation injury to the connective tissues of this neurovascular plexus), inflammation and edema (both of which are attributed to colorectal injury) which worsen with time, and increase in the leakage space in a tissue which is largely devoid of an interstitium (the NVB contains large nerves and vessels, held together in a thin layer of connective tissue, which is surrounded by and infiltrated with mature adipose tissue).

In the geographic irradiation study, dogs treated in group C showed changes in K^{trans}, k_{ep} and v_e of that prostate which were similar to what was seen in groups A and B. This is thought to be attributable, at least in part, to the fact that a portion of the prostate gland necessarily received primary irradiation as part of the irradiation protocol. Dogs treated in group D had no primary prostatic irradiation. This is reflected in the fact that v_e decreased with time after irradiation, which is thought to be consistent with maturation of the prostate gland, wherein the relative volume of parenchyma to interstitium increases due to glandular hyperplasia. The increase in k_{ep} is a reflection of how that parameter is derived ($k_{ep} = K^{trans} / v_e$), and likely does not reflect a true physiologic change. The transient rise in K^{trans} and iAUGC may reflect increased vascular resistance due to obstructed flow in vessels within the radiation field, distal to the prostate.

In comparing changes in DCE-MRI outcome variables between treatment groups for the geographic irradiation study, the higher prostatic v_e in group B as compared with group D at 4 and 12 months is attributable to the more profound glandular atrophy and prostatic fibrosis induced by irradiation in group B. All of the prostatic perfusion changes noted in comparing groups B and C are consistent with the fact that a larger percentage of the normal prostate gland was irradiated in group B than in group C, making more of the organ susceptible to glandular atrophy and fibrosis, which is evidenced by histopathologic findings. Interestingly, although the differences between prostatic perfusion in groups C and D are difficult to interpret due to lack of a clear pattern, the lower iAUGC measured in group D at one year may suggest that irradiation of the penile bulb adversely affects perfusion of pelvic parenchyma just as much, if not more so, than irradiation of the prostate or NVB. This interpretation must be tempered by the contradictory concept that normal age-related glandular hyperplasia should be associated with increases in overall prostatic perfusion.

Penile perfusion was affected in groups C and D. Dogs in group C had an elevated v_e at 12 months, and a decreased iAUGC. This suggests decreased tissue perfusion, and increased leakage space. The decrease in the global, model-free perfusion parameter suggests that NVB irradiation may decrease blood flow even in the flaccid state, which could contribute to tissue hypoxia and poor erectile function, as well as tissue fibrosis, reflected in the elevated v_e. Therefore, although maintenance of a high penile v_e may be necessary for penile health, in this scenario, rising v_e may also indicate tissue injury. And while irradiation of the NVB appears to adversely affect penile perfusion, changes were more profound in group B, suggesting that irradiation of the entire prostate and/or the penile bulb contributes to perturbations in penile

blood flow. This is further supported by the observation that dogs in group D also experienced decreases in iAUGC and K^{trans}, reflecting impaired perfusion of the penis after irradiation of the penile bulb. As with the prostate, comparison of penile perfusion after irradiation of just the NVB or just the PB is difficult due to inconsistent results.

Perfusion changes in the NVB of dogs from group C were similar to those from group B, and are attributed to primary radiation injury. Of interest are the changes in NVB perfusion noted in dogs from group D. Primary irradiation of the PB caused a transient increase, followed by a fall in K^{trans} in both NVB, as well as a time-dependent decrease in v_e and iAUGC. This suggests that irradiation of the PB adversely affects perfusion of not only the prostate, but also decreases bloodflow and normal transendothelial transport of fluid from the vascular compartment to the interstitium upstream of the radiation field.

For the dose-response study, serial DCE-MRI for the prostatic VOI of dogs in groups B, E and F showed a temporal decline in K^{trans} and iAUGC for all groups. There was also a temporal decline in k_{ep} in groups B and E. The v_e rose with time in group B, was relatively stable in group E and temporally decline in group F. These changes are thought to be consistent with progressive glandular atrophy and prostatic interstitial fibrosis, as well as decreased overall prostatic perfusion that are of greater magnitude with increasing radiation dose.

Again in the dose-response study, serial DCE-MRI of the glans penis in dogs from groups B, E and F showed a temporal decline in K^{trans} and iAUGC for all groups, which was unexpectedly of greater magnitude with decreasing total dose. There was no temporal change in K_{ep} in group B,

but the 12 month value was lower than baseline in groups E and F. v_e decreased with time in all treatment groups, but there was an unexpected difference between treatment groups, wherein, there was no difference between the 12 month v_e in groups B and E, but both were significantly higher than in group F. These changes suggest that overall penile perfusion worsens in the flaccid state after irradiation of the prostate, NVB and PB. They also suggest that there is an inverse dose-response relationship whereby lower total radiation doses (and lower doses per fraction) correlate with more dramatic declines in perfusion, and penile distensibility. This latter observation is not biologically plausible, and suggests that there was a type I statistical error, likely stemming from technical flaws in the DCE-MRI protocol that contributed to large amounts of intra- and inter-individual variability.

Serial DCE-MRI of the neurovascular bundles in dogs from groups B, E and F showed a temporal increase in K^{trans} for all groups, with direct dose-dependency at 12 months (highest in group B, lowest in group F). The v_e increased initially, then decreased in groups B and E, and temporally declined in group F; v_e was dose-dependent at 12 months, being highest in group B and lowest in group F. These changes in K^{trans} and v_e translated into a temporal decline in k_{ep} of the NVB, with k_{ep} higher in group B at 12 months, than either groups E or F. Finally, the iAUGC showed time-dependent decreases in all groups, and was highest in group B, and lowest in group F at 12 months. The temporal decline in perfusion was expected; however, it was not expected that perfusion would be inversely proportional to radiation dose. Histologic observations confirm that there is more NVB fibrosis in dogs treated with higher total doses of radiation, explaining the change in ve. However, the direct dose-dependency of Ktrans and iAUGC again calls into question the biological plausibility of this observation. Furthermore, the

value of studying perfusion changes in the NVB via DCE-MRI is questionable, as this is a tissue which has no meaningful parenchymal component, which is traversed by large vessels, and which difficult to localize on MRI. All DCE-MRI data pertaining to the NVB should therefore be interpreted with caution.

Additional statistically significant findings can be found in the Results section. However, they are not emphasized here due to a lack of clear biological significance. In many cases, their statistical significance can likely be attributed to type I statistical error.

Ultrasonographic evaluation of the urogenital tract revealed a temporal decline in pre-papaverine SRT that was evident in the first 4 months after 50 Gy was delivered to the prostate, NVB and PB via SBRT. Pre-papaverine SRT was shown to be higher at 12 months in group A than group B; the lack of biological rationale for why changing the interfraction interval would alter vascular response to otherwise identical irradiation protocols suggests the weak statistical relationship is likely attributable to type I error. Of particular interest is the fact that papaverine-induced hastening of the systolic rise time is not only ablated by irradiation with 50 Gy of radiation, but is in fact paradoxical; in the post-irradiation setting in dogs from groups A and B, SRT of the internal pudendal artery is actually slowed by intracavernosal administration of papaverine.

As with irradiation of all sites (group B), irradiation of the NVB or PB alone (groups C and D, respectively) resulted in a time-dependent hastening of the pre-papaverine SRT. There was no significant difference in the magnitude of slowing between these treatment groups. However,

unlike the slowing of SRT in response to papaverine after irradiation of all sites, irradiation of the NVB or PB alone did not significantly alter the vascular response to papaverine administration.

The hastening of pre-papaverine SRT was consistent between treatment groups B and E. However, the pre-papaverine SRT does not demonstrate temporal shortening (hastening) in group F, suggesting radiation dose-dependency of altered vascular tone in the internal pudendal artery. Also supporting this dose-dependent alteration in vascular tone is the fact that while dogs in groups B and E show time-dependent enhancement of the paradoxical vasoconstrictive effects of papaverine in the irradiated internal pudendal artery, the effect is more profound in the higher dose group (B). Furthermore, the vascular response to papaverine did not change in dogs from group F.

Papaverine is a potent vasodilator, which acts in an endothelial-independent fashion to increase cytosolic concentrations of cGMP and cAMP via phosphodiesterase inhibition, which leads to decreased intracellular calcium and dissociation of actin from myosin. A paradoxical response to papaverine treatment in the cerebral microvasculature has occasionally been reported in patients undergoing therapy for vasospasm.[40,41] The exact mechanism underlying this altered response is unknown. It is known, however, that microvessels can have an altered response to papaverine in the setting of vasospasm, and may constrict after exposure to low concentrations of the drug; in vitro studies suggest this is related to activation of protein kinase C (PKC).[42] Radiation is known to increase PKC activity in some cell types;[43-45] it is therefore plausible to consider that papaverine may have vasoconstrictive effects on pelvic vasculature in the post-irradiation setting,

which explains the altered vascular tone demonstrated herein. Changes in vascular tone correlated with the severity of morphologic injury to large vessels in the NVB as well. Although there was no statistically significant change in arterial patency, dogs in groups A, B and C showed severe changes in the vessel wall as well as arterial thrombosis. These changes are classic late radiation vasculopathies, and were much less severe in dogs from group E, and were very mild in dogs from group F. Furthermore, though not statistically significant, there was a trend towards lower luminal patency with higher total doses of radiation. This is potentially of great biological significance since small decreases in the degree of arterial patency can have large impacts on vascular resistance, given that Poiseuille's law concerning fluid dynamics states that resistance is inversely proportional to the fourth power of the radius. And because resistance is equal to blood pressure divided by the rate of flow, increased vascular resistance due to decreased luminal patency can cause slowing of the rate of blood flow if blood pressure is held constant. In this study, we did not measure pressures in the internal pudendal artery, therefore flow cannot be directly determined. However, the observed hastening of pre-papaverine systolic rise times can be explained by subtle decreases in arterial patency, if conservation of energy is applied to Bernoulli's principle, and laminar flow of blood, which is a relatively non-compressible fluid, is assumed (under these conditions, Bernoulli's equation states that flow equals the product of velocity and area). The only group for which internal pudendal arterial tone was affected, but for which there were no apparent histologic lesions in the NVB was group D. It is not surprising that vessels of the NVB were free of morphologic changes in this treatment group, since the NVB was outside the treatment field. But the fact that the response to papaverine was altered in group D suggests that injury to the internal pudendal artery can result

from irradiation of the PB, independent of irradiation of the prostate or NVB, altering penile arterial inflow, which may contribute to the onset of RI-ED.

Further studies are required to better validate this novel animal model for studying RI-ED. Particularly, it would helpful to have a more sensitive measure of erectile (dys)function. Penile diameter and subjective firmness scoring were used as the primary indicators of erection quality in this study, as these could be performed in unanesthetized dogs and were therefore considered more efficient quantifiers than measurement of intracavernosal pressure (ICP). However, measurement of intracavernosal pressure (ICP) within the corpora cavernosa is the most common method for quantification of erection quality in animal studies, and although this technique requires general anesthesia in dogs, all other evaluations (ultrasound, MRI, electrophysiology, etc) performed herein also required anesthesia. Therefore, investigators should consider use of ICP measurements in future studies. Furthermore, because the vascular response to SBRT is different than the response to conventionally fractionated RT, future studies should evaluate whether the same alterations in vascular tone result from finely fractionated RT protocols.[46,47]

Other limitations of this study include a flaw in study design, whereby formalin-fixed tissues were not embedded in paraffin within a standardized time. As such, while tissues from some dogs were fully processed for histopathology and immunohistochemistry within 24 to 48 hours of euthanasia, tissues from other subjects were maintained wet, in 10% neutral buffered formalin for more than a year before being further processed. This is problematic because methylene bridges from during fixation, which results in protein cross-linking and antigenic masking. Heat-induced epitope retrieval (in sodium citrate or Tris/EDTA buffer) and/or enzymatic methods

(trypsin, pepsin or other proteases) can be used to break the methylene bridges, which expose the antigenic site and overcome effects of fixation. But overfixation can make antigen retrieval difficult, and can ultimately alter immunohistochemical staining intensity due to incomplete retrieval. This was evident in several samples in this study, where staining intensity of tissue morphologically consistent with blood vessels (for CD31 staining) or peripheral nerves (for neurofilament staining) was incomplete or absent. Results of semi-quantitative pathologic image analysis omitted results from tissues where staining quality was poor. An alternative approach would have been to better optimize the antigen retrieval processes; this approach was precluded due to financial and time constraints.

A final consideration in interpretation of these data concerns the dose response assays. The reader is reminded that in order to study fractionation protocols similar to those in current clinical use for prostate cancer (each in 5 fractions, 30 Gy has been used for palliation, 37.5 Gy is perhaps the most commonly used clinical protocol, and the aforementioned RTOG trial delivered 50 Gy),[28,48,49] all SBRT in this study was delivered in five fractions. Inherent to this study design is the fact that total dose was incrementally changed not only by 20% per group (50 Gy vs. 40 Gy vs. 30 Gy), but so too was dose per fraction (10 Gy vs. 8 Gy vs. 6 Gy). This alters the biologically effective dose of the protocols more so than if only one of these parameters had been altered (total dose or dose per fraction), given the strong dependency of most late radiation tissue responses on dose per fraction (due to the low alpha to beta ratio for these late responding tissues, which speaks to their dependency on extensive repair of sublethal damage to maintain long-term tissue health).

Despite the limitations of this small, exploratory study, this canine model of RI-ED was successful in showing that prostatic irradiation impairs both phases of penile erection. Altered pelvic and penile perfusion, altered internal pudendal arterial tone and alteration of cavernous nerve branch morphology all point towards the fact that prostatic irradiation alters the first (full-erection) phase of erection, involving nitric oxide driven penile engorgement. Electrophysiologic studies of the pudendal nerve and bulbospongiosus muscles, with corresponding histologic alterations in penile nerve morphology support the fact that prostatic irradiation, and particularly, irradiation of the penile bulb, disrupts the second (rigid-erection) phase of erection, which involves a final increase in ICP subsequent to contraction of the ischiocavernosus, bulbospongiosus and ischiourethralis muscles, also innervated by branches of the pudendal nerve. Future studies should be aimed at further investigating the cause and character of alterations in vascular tone, as well as the role of pudendal nerve dysfunction in causing RI-ED.

REFERENCES

1. Dubbelman YD, Dohle GR, Schroder FH. Sexual function before and after radical retropubic prostatectomy: A systematic review of prognostic indicators for a successful outcome. *European Urology* 2006;50:711-720.
2. Walsh PC, Donker PJ. Impotence following radical prostatectomy - insight into etiology and prevention. *Journal of Urology* 1982;128:492-497.
3. Wiegner EA, King CR. Sexual function after stereotactic body radiotherapy for prostate cancer: results of a prospective clinical trial. *International Journal of Radiation Oncology Biology Physics* 2010;78:442-448.
4. Brown MW, Brooks JP, Albert PS, et al. An analysis of erectile function after intensity modulated radiation therapy for localized prostate carcinoma. *Prostate Cancer and Prostatic Diseases* 2007;10:189-193.
5. Dean RC, Lue TF. Physiology of penile erection and pathophysiology of erectile dysfunction. *Urologic Clinics of North America* 2005;32:379-+.
6. Incrocci L. Sexual function after external-beam radiotherapy for prostate cancer: What do we know? *Critical Reviews in Oncology Hematology* 2006;57:165-173.
7. Incrocci L, Slob AK, Levendag PC. Sexual (dys)function after radiotherapy for prostate cancer: A review. *International Journal of Radiation Oncology Biology Physics* 2002;52:681-693.
8. Mendenhall WM, Henderson RH, Indelicato DJ, et al. Erectile dysfunction after radiotherapy for prostate cancer. *American Journal of Clinical Oncology-Cancer Clinical Trials* 2009;32:443-447.
9. Goldstein I, Feldman MI, Deckers PJ, et al. Radiation-associated impotence - a clinical study of its mechanism. *Jama-Journal of the American Medical Association* 1984;251:903-910.
10. Solan AN, Cesaretti JA, Stone NN, et al. There is no correlation between erectile dysfunction and dose to penile bulb and neurovascular bundle following real-time low dose rate prostate brachytherapy. *International Journal of Radiation Oncology Biology Physics* 2009;73:1468-1474.
11. Merrick GS, Butler WM, Dorsey AT, et al. A comparison of radiation dose to the neurovascular bundles in men with and without prostate brachytherapy-induced erectile dysfunction. *International Journal of Radiation Oncology Biology Physics* 2000;48:1069-1074.
12. Merrick GS, Wallner K, Butler WM, et al. A comparison of radiation dose to the bulb of the penis in men with and without prostate brachytherapy-induced erectile dysfunction. *International Journal of Radiation Oncology Biology Physics* 2001;50:597-604.
13. van der Wielen GJ, Hoogeman MS, Dohle GR, et al. Dose-volume parameters of the corpora cavernosa do not correlate with erectile dysfunction after external beam radiotherapy for prostate cancer: Results from a dose-escalation trial. *International Journal of Radiation Oncology Biology Physics* 2008;71:795-800.
14. Carrier S, Hricak H, Lee SS, et al. Radiation-induced decrease in nitric oxide synthase containing nerves in the rat penis. *Radiology* 1995;195:95-99.
15. Merlin SL, Brock GB, Begin LR, et al. New insights into the role of endothelin-1 in radiation-associated impotence. *International Journal of Impotence Research* 2001;13:104-109.

16. van der Wielen GJ, Vermeij M, de Jong BWD, et al. Changes in the Penile Arteries of the Rat after Fractionated Irradiation of the Prostate: A Pilot Study. *Journal of Sexual Medicine* 2009;6:1908-1913.

17. Koontz BF, Yan H, Kimura M, et al. Feasibility Study of an Intensity-Modulated Radiation Model for the Study of Erectile Dysfunction. *Journal of Sexual Medicine* 2011;8:411-418.

18. Kimura M, Rabbani ZN, Zodda AR, et al. Role of Oxidative Stress in a Rat Model of Radiation-Induced Erectile Dysfunction. *Journal of Sexual Medicine* 2012;9:1535-1549.

19. Kimura M, Yan H, Rabbani Z, et al. Radiation-Induced Erectile Dysfunction Using Prostate-Confined Modern Radiotherapy in a Rat Model. *Journal of Sexual Medicine* 2011;8:2215-2226.

20. Heaton JPW, Varrin SJ, Morales A. The characterization of a bioassy of erectile functin in a rat model. *Journal of Urology* 1991;145:1099-1102.

21. Heaton JPW, Varrin SJ. Metoclopramide decreases apomorphine-induced yawning and penile erection. *Pharmacology Biochemistry and Behavior* 1991;38:917-920.

22. Probert JC. Animal experiments in radiotherapy II: large animals. *J Can Assoc Radiol* 1975;26:25-34.

23. Gianduzzo T, Colombo JR, Haber GP, et al. Laser robotically assisted nerve-sparing radical prostatectomy: a pilot study of technical feasibility in the canine model. *Bju International* 2008;102:598-602.

24. Gianduzzo TRJ, Colombo JR, El-Gabry E, et al. Anatomical and electrophysiological assessment of the canine periprostatic neurovascular anatomy: Perspectives as a nerve sparing radical prostatectomy model. *Journal of Urology* 2008;179:2025-2029.

25. Ong AM, Su LM, Varkarakis I, et al. Nerve sparing radical prostatectomy: Effects of hemostatic energy sources on the recovery of cavernous nerve function in a canine model. *Journal of Urology* 2004;172:1318-1322.

26. Shaaya AN, Kraus C, Bauman DH, et al. Pharmacokinetics and bioavailability of papaverine HCl after intravenous, intracorporeal and penis topical administeration in beagle dogs. *Methods and Findings in Experimental and Clinical Pharmacology* 1992;14:373-378.

27. Glina S, Buvat J, Casabe A, et al. Is Intracavernous Injection of Papaverine a Reliable Screening Test for Vascular Impotence?J. Buvat, M. Herbaut-Buvat, JL Dehaene, and A. Lemaire. *Journal of Sexual Medicine* 2009;6:2948-2953.

28. Boike TP, Lotan Y, Cho LC, et al. Phase I dose-escalation study of stereotactic body radiation therapy for low- and intermediate-risk prostate cancer. *Journal of Clinical Oncology* 2011;29:2020-2026.

29. Arbuck SG, Ivy P, Setser A, et al. Common toxicity criteria (CTC) version 2.0: Highlights and tools. *Annals of Oncology* 1998;9:12-12.

30. Tofts PS, Brix G, Buckley DL, et al. Estimating kinetic parameters from dynamic contrast-enhanced T(1)-weighted MRI of a diffusable tracer: Standardized quantities and symbols. *Journal of Magnetic Resonance Imaging* 1999;10:223-232.

31. Weidner N, Carroll PR, Flax J, et al. Tumor angiogenesis correlates with metastasis in invasive prostate carcinoma. *American Journal of Pathology* 1993;143:401-409.

32. Pickles T, Graham P, British Columbia Canc Agency P. What happens to testosterone after prostate radiation monotherapy and does it matter? *Journal of Urology* 2002;167:2448-2452.

33. Zagars GK, Pollack A. Serum testosterone levels after external beam radiation for clinically localized prostate cancer. *International Journal of Radiation Oncology Biology Physics* 1997;39:85-89.

34. Nichols RC, Morris CG, Hoppe BS, et al. Proton radiotherapy for prostate cancer is not associated with post-treatment testosterone suppression. *International Journal of Radiation Oncology Biology Physics* 2012;82:1222-1226.

35. Kupelian P, Katcher J, Levin H, et al. External beam radiotherapy versus radical prostatectomy for clinical stage T1-2 prostate cancer: Therapeutic implications of stratification by pretreatment PSA levels and biopsy gleason scores. *Cancer Journal from Scientific American* 1997;3:78-87.

36. Raynor EM, Ross MH, Shefner JM, et al. Differentiation between axonal and demyelinating neuropathies: identical segments recorded from proximal and distal muscles. *Muscle & Nerve* 1995;18:402-408.

37. Mitchell J, Caren CA. Degeneration of non-myelinated axons in the rat sciatic nerve following lysolecithin injection. *Acta Neuropathologica* 1982;56:187-193.

38. Costello AJ, Brooks M, Cole OJ. Anatomical studies of the neurovascular bundle and cavernosal nerves. *Bju International* 2004;94:1071-1076.

39. Tewari A, Takenaka A, Mtui E, et al. The proximal neurovascular plate and the tri-zonal neural architecture around the prostate gland: Importance in the athermal robotic technique of nerve-sparing prostatectomy. *Bju International* 2006;98:314-323.

40. Clyde BL, Firlik AD, Kaufmann AM, et al. Paradoxical aggravation of vasospasm with papaverine infusion following aneurysmal subarachnoid hemorrhage - Case report. *Journal of Neurosurgery* 1996;84:690-695.

41. Pennings FA, Albrecht KW, Muizelaar JP, et al. Abnormal Responses of the Human Cerebral Microcirculation to Papaverin During Aneurysm Surgery. *Stroke* 2009;40:317-320.

42. Jin YC, Sagher O, Thai QA, et al. The effects of papaverine on phorbon dibutyrate-induced vasoconstrction in brain slice microvessels. *Journal of Neurosurgery* 1994;81:574-578.

43. Kizub IV, Pavlova OO, Ivanova IV, et al. Protein kinase C-dependent inhibition of BKCa current in rat aorta smooth muscle cells following gamma-irradiation. *International Journal of Radiation Biology* 2010;86:291-299.

44. Soloviev AI, Tishkin SM, Zelensky SN, et al. Ionizing radiation alters myofilament calcium sensitivity in vascular smooth muscle: potential role of protein kinase C. *American Journal of Physiology-Regulatory Integrative and Comparative Physiology* 2005;289:R755-R762.

45. Alapati K, Gopinath S, Malla RR, et al. uPAR and cathepsin B knockdown inhibits radiation-induced PKC integrated integrin signaling to the cytoskeleton of glioma-initiating cells. *International Journal of Oncology* 2012;41:599-610.

46. Garcia-Barros M, Lacorazza D, Petrie H, et al. Host acid sphingomyelinase regulates microvascular function not tumor immunity. *Cancer Research* 2004;64:8285-8291.

47. Garcia-Barros M, Paris F, Cordon-Cardo C, et al. Tumor response to radiotherapy regulated by endothelial cell apoptosis. *Science* 2003;300:1155-1159.

48. King CR, Brooks JD, Gill H, et al. Stereotactic body radiotherapy for localized prostate cancer: interim results of a prospective phase II clinical trial. *International Journal of Radiation Oncology Biology Physics* 2009;73:1043-1048.

49. Jereczek-Fossa BA, Beltramo G, Fariselli L, et al. Robotic image-guided stereotactic radiotherapy, for isolated recurrent primary, lymph node or metastatic prostate cancer. *International Journal of Radiation Oncology Biology Physics* 2012;82:889-897.

CHAPTER 4: PATHOLOGIC RESPONSES OF THE COLON TO STEREOTACTIC BODY IRRADIATION

Brief Overview

Introduction: Stereotactic body radiotherapy (SBRT) is an emerging means for treating pelvic tumors in humans and various veterinary species. The objective of this prospective study was to describe the dose-response relationship and time-dependency of late radiation-induced colorectal complications following SBRT in the dog.

Methods: Nineteen one-year intact male mixed breed hounds were irradiated with one of four different dose/fractionation schemes (50 Gy over either 5 or 11 days, 40 Gy over 11 days, or 30 Gy over 11 days, all delivered in a total of 5 fractions). Treatment volumes included the prostate plus a margin of five millimeters. Subjects were monitored for signs of colorectal toxicosis for up to one year following irradiation. Follow-up examinations included regular physical examinations, periodic non-invasive imaging, as well as fecal examinations and bloodwork (performed on an as-needed basis). Gross necropsy and histopathology were performed upon euthanasia. All toxicoses were graded according to the RTOG criteria for gastrointestinal toxicity.

Results: The frequency and severity of colorectal ulceration was higher in dogs treated with 5 fractions of 10 Gy delivered on consecutive days, as compared with those treated on an every

other day schedule. Vascular injury and serosal thickening occurred in all treatment groups, in a dose-responsive fashion.

Discussion/Conclusions: Severe gastrointestinal complications occur less frequently when interfraction intervals are at least 48 hours. The mechanism for this time-dependency is unclear, but likely related to completeness of epithelial regeneration.

Introduction

Stereotactic body radiation therapy (SBRT) is an emerging treatment option for prostate cancer (PC).[1-7] Because apparently similar efficacy is paired with favorable patient convenience and a potential improvement in cost-effectiveness, SBRT is currently regarded as one of the most promising therapeutic modalities for localized, low-to-intermediate risk prostate cancer.[8] SBRT is also being investigated for use in a variety of other pelvico-abdominal malignancies.[9-11]

Gastrointestinal (GI) and genitourinary (GU) toxicity following prostatic irradiation with SBRT appears comparable, if not improved, as compared with conventionally fractionated conformal radiation therapy (CFRT). However, several limitations exist in comparing outcome data from prostatic SBRT with CFRT. First, while late radiation toxicity can manifest years, if not decades after irradiation, the longest reported follow-up for prostatic SBRT is less than 3 years, suggesting that current documentation may underestimate the true magnitude of the incidence and severity of late GI and GU toxicities.[1] Second, the metrics used to quantify post-SBRT quality of life (QOL) are limited compared with CFRT.[12] Third, comparison of SBRT outcomes

with historical CFRT data may not adequately reflect the volume of tissue irradiated in modern fractionated CFRT protocols because SBRT is typically limited in use to low- and intermediate-risk cases of PC, whereas CFRT is also used for high-risk patients, in whom treatment fields may include the seminal vesicles; furthermore, CFRT is now often administered with smaller fields than previously employed, by using intensity-modulation and image-guidance technologies.[12] For these reasons, SBRT cannot yet be considered an equivalent (or perhaps better stated, non-inferior) treatment as compared with CFRT.

Despite this lack of long-term clinical follow-up describing normal tissue tolerances following pelvic SBRT, the incidence of radiation-induced sexual toxicity appears similar to CFRT. Erectile dysfunction (ED) has been noted in 23-33% of previously-potent men after prostatic SBRT,[3,13] which is comparable to the prevalence of ED following CFRT (11-73%).[14-16] Given that the pathophysiologic events underlying development of radiation-induced ED are incompletely understood, our group has initiated a series of studies to investigate GU toxicity following SBRT in a canine model; results of those studies have been presented elsewhere (Chapter 3). This chapter's focus is on unexpected severe colorectal toxicity in these dogs, following irradiation with an SBRT protocol which has thus far been associated with tolerable GI toxicity in humans.[2] Herein, the timing of colorectal fistula formation following administration of 50 Gray (Gy) in 5 consecutive daily fractions will be described, along with a clear improvement in the incidence of severe GI toxicity associated with lengthening of the interfraction interval; finally, results of a dose-response assay will be presented.

Methods

Data from a study investigating changes in erectile function after SBRT in a dog model have been reviewed and analyzed with emphasis on the issue of colorectal toxicity following SBRT for prostate cancer.

Animals

Twenty-two healthy, approximately one year old, intact male mixed breed hound dogs, weighing 24.9 - 40.4 kg, were purchased from a commercial breeding facility,[31] and transported to the Colorado State University Veterinary Teaching Hospital, Fort Collins, Colorado, USA. Dogs were housed in individual enclosures, and fed a commercially-manufactured dry dog chow and water ad libitum. Two weeks were allotted for environmental acclimation. All studies were conducted in accordance with a protocol approved by the Colorado State University Institutional Animal Care and Use Committee (IACUC). Tissues from four additional 2 to 4 year old dogs of mixed breed were used as unirradiated controls; these dogs were not subject to IACUC oversight for this project, as they were euthanized as part of an unrelated study.

Radiation Therapy

Radiation simulation and dose fractions were delivered while the dogs were under general anesthesia. Dogs were fasted for 12 hours and received a warm, soapy enema prior to anesthesia. Dogs were given acepromazine[32] (0.01 mg/kg), atropine[33] (0.04 mg/kg) and

[31] Antech, Inc, Barnhart, MO
[32] PromAce® Injectable; Fort Dodge Animal Health, Fort Dodge, IA
[33] Atropine Sulfate (0.54 mg/mL); Vedco Inc, St. Joseph, MO

hydromorphone[34] (0.05 mg/kg) subcutaneously 15-20 minutes before anesthetic induction, which was achieved with intravenous midazolam[35] (0.2 mg/kg) and propofol[36] (4-6 mg/kg). The dogs were then intubated and anesthesia was maintained using isoflurane gas[37] (1-3% in 100% O_2). Dogs were monitored with electrocardiography, invasive blood pressure measurement, and pulse oximetry. The mean arterial blood pressure was maintained above 65 mmHg; intravenous crystalloid fluid therapy and inotropic support (constant rate infusion of dopamine, 5-10 μg/kg/min) were used in hypotensive subjects. A sterile 8-Fr Foley urinary catheter was placed, as was a rectal balloon[38] that was insufflated with 30 cubic centimeters (cc) of air. Dogs were placed in dorsal recumbency in a standard foam trough, with their feet into the gantry. Their stifles were immobilized with a foam wedge, which was attached to the trough.

Computed tomography (CT) and magnetic resonance imaging (MRI) were performed for radiation therapy planning. Pre- and post-contrast CT scans of the pelvis and caudal abdomen were obtained with 1 mm slice thickness, using a 512 x 512 mm matrix before and after intravenous administration of contrast material (159.1 mg/kg iohexol IV).[39] The MRI study consisted of transverse T2, T1 obtained before and after intravenous administration of contrast material (21.3 mg/kg gadopentetate dimeglumine IV),[40] as well as dorsal and sagittal T1 post-contrast weighted images of the pelvis and caudal abdomen. Images were manually fused using

[34] Hydromorphone HCl Injection USP (2 mg/mL); West-Ward, Eastontown, NJ
[35] Midazolam Injection USP (5 mg/mL); Hospira Inc, Lake Forest, IL
[36] NovaPlus® (propofol emulsion USP, 1%); AAP Pharmaceuticals LLC, Schaumburg, IL
[37] Isoflurane USP; Piramal HealthCare, Andhra Pradesh, India
[38] Immobilizer Treatment Device (REF RB-100F); RadiaDyne, Houston, TX
[39] Omnipaque 350™; GE Healthcare, Broomfield, CO
[40] Magnevist; Bayer HealthCare Pharmaceuticals Inc, Wayne, NJ

the image registration function on the radiation treatment planning software.[41] The prostate, bilateral prostatic neurovascular bundles (NVB) and penile bulb (PB) were delineated as the gross target volume (GTV). The planning target volume (PTV) was represented by a 0.5 cm expansion of the prostatic and neurovascular bundle volumes, and a 0.7 cm expansion of the penile bulb volume; the rectal wall was excluded from PTV's. Dogs whose prostate and/or NVB was included in the treatment field were considered to have received prostatic SBRT for the purpose of interpreting data related to radiation-induced colorectal injury; dogs in which only the PB were irradiated were considered negative controls since their peri-prostatic colorectal tissue (that which is within 2.5 cm of the prostate) was not a primary target of irradiation, and received a total dose no greater than 2.7 Gy. The total radiation dose prescribed to the peri-prostatic colorectal tissue varied, but always involved delivery of 95% of the prescribed dose to the PTV, in five equal fractions, administered over either 5 (daily fractions, q24h) or 11 days (with an interfraction interval of no less than 48 hours, q48h). Briefly, treatment group A (6 dogs) received 50 Gy in 5 days (with fractions delivered every 24 hours; QD); group B (7 dogs) received 50 Gy in 11 days (with fractions delivered every 48 hours; QOD), group C (3 dogs) received 40 Gy in 11 days, group D (3 dogs) received 30 Gy in 11 days and group E was comprised of aged-matched dogs (3 hounds and 4 dogs of mixed breed) whose colon had not been irradiated. Treatment plans involved 7-9 isocentrically-placed coplanar 6 and 10 MV X-ray beams which were shaped using dynamic multileaf collimation in a sliding-leaf fashion to achieve intensity-modulation. Plans were constructed using iterative inverse-planning with heterogeneity corrections to meet specified goals for both target volumes and organs at risk (Table 4.1). Individual treatment plan review was performed by an American College of

[41] Eclipse™ (v8.6); Varian Medical Systems Inc, Palo Alto, CA

Veterinary Radiology board-certified veterinary radiation oncologist and an American College of Radiology board-certified medical physicist. Beam output was verified for each plan using gamma analysis of data generated from an electronic portal dosimeter. For quality-assurance purposes, a minimum of 95% gamma for a 3-mm distance to agreement and a 3% absolute dose difference was defined as a passing score. Daily image-guided patient position verification was performed with on-board kilovoltage cone-beam CT. Following position verification, intensity-modulated SBRT was delivered using a Varian Trilogy™ linear accelerator.[42]

[42] Varian Trilogy™; Varian Medical Systems Inc, Palo Alto, CA

Table 4.1. Dose-volume limits for organs at risk

Organ	**Volume**	**Dose**
Femoral heads	Less than 1 cc	> 30 Gy
Peri-prostatic anterior rectal wall	Maximum point dose	105% of Rx
Peri-prostatic lateral rectal wall	Maximum point dose Less than 0.3 cc cumulative (both sides)	100% of Rx > 90% of Rx
Peri-prostatic posterior rectal wall	Maximum point dose	45% of Rx
Skin	Maximum point dose	20 Gy
Small intestine	Maximum point dose Less than 1 cc	29 Gy > 19.5 Gy
Spinal cord	Maximum point dose Less than 0.8 cc	22 Gy > 20 Gy
Urethra	Maximum point dose	105% of Rx
Urinary bladder	Maximum point dose Less than 1 cc	105% of Rx > 18.3 Gy

Follow-up Evaluations

Dogs were monitored daily for toxicity. Toxicity was scored according to the Radiation Therapy Oncology Group (RTOG) rectal toxicity scale.[17] Patients were humanely euthanized via intravenous injection of propofol (6 mg/kg) and pentobarbital[43] (18 mg/kg) within three weeks of reaching any of the following endpoints: (1) confirmation of erectile dysfunction, (2) development of clinically-evident grade 3 or higher enterocolonic or genitourinary toxicity that was not responsive to aggressive medical therapy, or (3) 1 year after commencing radiotherapy. Post-mortem examination was performed on all dogs.

Post-Mortem Examination

Peri-prostatic colorectal tissue was removed and preserved in 10% neutral buffered formalin and processed for histologic evaluation. All specimens were routinely processed and embedded in paraffin, then sectioned at 5 μm. Sections were stained with hematoxylin and eosin (H&E) for morphologic evaluation, and Masson's trichrome for evaluation of fibrosis.

A modified semi-quantitative grade system was established for late colorectal radiation effects.[18,19] Ulceration was evaluated within the PTV, whereas three qualitative histologic abnormalities were evaluated 1 cm lateral to the margin of the PTV. Degree of submucosal fibrosis was determined by averaging the thickness of the submucosa, measured at 4 sites where the muscularis mucosa was parallel to the underlying muscularis propria. Degree of serosal thickening was determined by averaging the measured thickness of the serosa at four locations. For both the submucosa and serosa, thickness was measured at 40 times magnification, using an

[43] Beuthanasia-D Special (pentobarbital 390 mg/mL, with phenytoin 50 mg/mL); Schering-Plough Animal Health Corp, Union, NJ

eyepiece reticle, and reported as a unitless measure. Vascular injuries were qualitatively scored. Evaluations were done without knowledge of the treatment given. Definitions for the assignment of grade for ulceration and vascular injury were as follows:

Ulceration

Grade 0: Normal.

Grade 1: Partial thickness ulceration.

Grade 2: Full-thickness, trans-serosal ulcer.

Vascular injury (applies to non-capillary vessels, both venous and arterial)

Grade 0: Normal.

Grade 1: Slight thickening and hyalinization of vessel walls, slight perivascular fibrosis.

Grade 2: Vessel walls approximately double normal thickness with marked hyalinization and some diminishment of lumen diameter, moderate perivascular fibrosis, mild to moderate intimal proliferation.

Grade 3: Extreme thickening and hyalinization of walls with marked reduction in lumen diameter; fibrinoid medial necrosis, mural thrombosis or subendothelial hemorrhage and fibrin, perivascular fibrosis, severe intimal proliferation.

Statistical Analysis

The study design enabled evaluation of late GI toxicity severity as a function of both duration of the interfraction interval (q24h vs. q48h treatments) and total dose (30 vs. 40 vs. 50 Gy in 5 fractions, delivered q48h). Because sample sizes were small, and data were not normally distributed, nonparametric tests were employed to compare toxicity scores between treatment groups. The Kruskal-Wallis test was used; Dunn's test was performed for multiple comparisons.

Kaplan-Meier survival analysis was performed to study differences in time to onset of colorectal toxicity. All statistical analyses were performed using commercial software packages; to avoid type I statistical errors associated with the small sample size, significance levels were 10% for all tests.[44,45]

Results

Duration of the Interfraction Interval

The median time to onset of clinical signs associated with GI toxicity was 95.5 days for dogs in treatment group A, and 222 days for dogs treatment group B (log-rank statistic, $p = 0.068$). Furthermore, the grade of clinical toxicity was lower with a longer interfraction interval (median grade of 4 for dogs in group A, and 3 for group B; Mann-Whitney U-test statistic, $p = 0.044$), and the risk of developing grade 3 or higher clinical toxicosis was higher when 50 Gy was delivered over 5 days rather than 11 days (odds ratio = 5.91, 95% confidence interval: 0.231 – 151.3). Scores for colonic ulceration and vascular injury were higher in dogs from groups A and B than group E, as were measurements of serosal thickness. The submucosa of irradiated dogs (groups A and B) trended towards being thicker than that of unirradiated dogs; however, this difference was not statistically significant. The median ulcer score trended towards being greater for dogs in group A than group B, there were no statistically significant differences in any of the evaluated pathologic parameters when dogs from groups A and B were compared. Summary statistics for pathological data from dogs in groups A, B and E are presented in Table 4.2.

[44] SigmaPlot v.12; Systat Software Inc., San Jose, CA
[45] Prism v.6; Graphpad Software Inc, La Jolla, CA

Table 4.2. Pathology data: QD vs. QOD

	Median Values			Statistics	
	Group A 50 Gy QD	**Group B 50 Gy QOD**	**Group E 0 Gy**	**Comparisons (Dunn's multiple comparisons)**	**Corrected P-value**
Ulcer score	2.0	1.5	0.0	0 Gy vs. 50 Gy QD 0 Gy vs. 50 Gy QOD 50 Gy QD vs. 50 Gy QOD	0.0009 0.0165 0.7019*
Submucosal thickness	30.00	31.50	17.00	Kruskal-Wallis test	0.3555
Vascular injury	1.0	1.0	0.0	0 Gy vs. 50 Gy QD 0 Gy vs. 50 Gy QOD 50 Gy QD vs. 50 Gy QOD	0.0147 0.0392 > 0.9999
Serosal thickness	46.00	45.00	2.00	0 Gy vs. 50 Gy QD 0 Gy vs. 50 Gy QOD 50 Gy QD vs. 50 Gy QOD	0.0090 0.0202 > 0.9999

* When ranks of ulcer scores for the two treated groups are compared directly using the Mann-Whitney U-test, a trend is identified, whereby $p = 0.0979$.

Dose-Response Assay

As compared with a median clinical toxicity score of 3 in dogs that received 50 Gy over 11 days, none of the dogs in either group C or D (40 or 30 Gy total, respectively) had clinical evidence of colorectal toxicity during the one-year post-irradiation follow-up period. Analysis of necropsy data revealed differences in severity of pathologic lesions between the three dose groups, and is summarized in Table 4.3.

The majority of dogs in group B developed colorectal fistulas, which precluded analysis of tissue within the treatment field. There were however qualitative and quantitative differences in the pathologic lesions observed within the treatment fields of dogs from groups C and D; summary statistics are provided in Table 4.4.

Table 4.3. Pathology data: Dose-response assay

	Median Values				**Statistics**	
	Group B 50 Gy	**Group C 40 Gy**	**Group D 30 Gy**	**Group E 0 Gy**	**Comparisons (Dunn's multiple comparisons)**	**Corrected P-value**
Ulcer score	1.5	0.0	0.0	0.0	0 Gy vs. 30 Gy 0 Gy vs. 40 Gy 0 Gy vs. 50 Gy 30 Gy vs. 40 Gy 30 Gy vs. 50 Gy 40 Gy vs. 50 Gy	> 0.9999 > 0.9999 0.0036 > 0.9999 0.0525 0.0525
Submucosal thickness	31.50	22.00	15.30	17.00	Kruskal-Wallis test	0.1812
Vascular injury	1.0	1.0	0.0	0.0	0 Gy vs. 30 Gy 0 Gy vs. 40 Gy 0 Gy vs. 50 Gy 30 Gy vs. 40 Gy 30 Gy vs. 50 Gy 40 Gy vs. 50 Gy	> 0.9999 0.0215 0.0399 0.0829 0.2278 > 0.9999
Serosal thickness	45.00	23.00	2.00	2.00	0 Gy vs. 30 Gy 0 Gy vs. 40 Gy 0 Gy vs. 50 Gy 30 Gy vs. 40 Gy 30 Gy vs. 50 Gy 40 Gy vs. 50 Gy	> 0.9999 0.3109 0.0256 0.2667 0.0487 > 0.9999

Table 4.4. Pathology data: 30 vs. 40 Gy

	Median Values		Mann-Whitney U-Test, P-value
	Group C 40 Gy	Group D 30 Gy	
Submucosal thickness	22.00	15.00	0.0058
Vascular injury	3.0	0.0	0.0500
Serosal thickness	69.00	17.00	0.0040

Discussion

Severe gastrointestinal complications occurred less frequently when the interfraction interval was 48 hours, as compared to 24 hours. This provides further supports a similar observation made in prostate cancer patients treated with SBRT.[20] And yet, the mechanism for this time-dependency is unclear. The timeframe in which these complications developed (more than three months after completion of SBRT) suggests they would be appropriately classified as late radiation-associated side effects. This is consistent with the fact that classic late radiation injuries in the lower GI tract include chronic inflammation, ulceration and fibrosis, which manifest clinically as diarrhea, rectal bleeding, rectal pain, perforation and/or obstruction.[21]

Such late radiation injuries in the large intestine are characterized by an alpha to beta ratio of 3-5 Gy, meaning that repair of sublethal DNA damage (SLD) is critical to long-term tissue health.[22] Given that radiation causes a dose-dependent delay in repair of such damage, prolonging the interfraction interval could improve overall tissue health by allowing for more complete SLD repair.[23-25] The normal repair halftime for most epithelial tissues is approximately 1.5 to 2.5 hours, and at least one study suggests it may be as short as 0.2 to 0.4 hours.[26,27] The repair halftime is extended to approximately 3-4 hours for larger doses per fraction.[28] As such, the incidence and severity of classic late effects in the lower GI tract, even at high fractional doses,

should not be affected by changes in duration of the interfraction interval or total treatment time, because changes in completeness of SLD repair are inconsequential after 6 hours.[29]

The dependency of long-term tissue health on duration of the interfraction interval therefore implies that at high doses per fraction, the alpha to beta ratio for late toxicity is much higher than predicted, and is similar to that observed in acutely responding tissues. The occurrence of late radiation toxicity in a tissue with repair properties similar to those of acute radiation injuries suggests the adverse effects observed in this study should be classified as consequential late effects.[30] Consequential late effects are defined as those late effects which are directly influenced by the frequency and/or severity of acute changes in the same tissue.[31,32] They are particularly common in tissues for which mechanical barrier protection plays a role in tissue function, such as the GI tract. It has been clearly documented that disruption of the mucosal barrier in the intestines can lead to profibrogenic chronic inflammation of submucosal tissues.[33] By extension, it can be concluded that the decreased incidence of colorectal fistulas that occurred with elongation of the interfraction interval was directly related to completeness of epithelial regeneration between fractions.[34] This hypothesis is supported by the kinetics of colonic crypt repopulation and regeneration. In murine studies, the onset of regeneration occurs at about 3.5 days post-irradiation. This is not to say that crypt epithelia do not start repopulating before that, but instead speaks to the fact that repopulation is balanced by cell loss for the first few days, before cell loss temporarily slows. The initial 'steady-state' condition is characterized by loss of approximately 50% of newly produced cells to terminal differentiation, whereas each new cell produced probably retains its capacity for clonogenicity once maximal regeneration is reached.[35] Allowing more time between fractions increases the number of cells present at the next

treatment, thus making a given level of overall depopulation from a certain dose of radiation less probable. In fact, if the interfraction interval were elongated enough, regeneration would so effectively spare the mucosa, that colonic tolerance to irradiation following SBRT would be shifted towards reliance on more classically late-responding, and relatively non-proliferating tissues such as connective tissue and vasculature.[28,36]

Aside from increasing the interfraction interval, other strategies that may increase colorectal mucosal tolerance to severely hypofractionated irradiation protocols stem from the fact that disruption of the mucosal barrier promotes chronic inflammation. Although several anti-inflammatory drugs, including ibuprofen, acetylsalicylate and corticosteroids, have been studied in the setting of either preventing or treating radiation colitis/proctitis, to date, none have proven very useful.[37-41] This may be due in part to the fact that inhibition of prostaglandin synthesis by many anti-inflammatory drugs adversely affects the kinetics of colonic crypt turnover, thereby impeding mucosal regeneration during and after RT.[42-44] Since cyclooxygenase (COX) inhibitors are frequently administered to patients during RT, it is particularly important to resolve the issue of whether COX inhibition is beneficial or detrimental to the GI health in the weeks and months surrounding pelvic RT.

In addition to the observation that increasing the interfraction interval decreases the risk of severe consequential colorectal late effects, this study also demonstrated a clear dose response relationship, wherein dogs treated with 50 Gy via 5-fraction SBRT had high risk of severe ulceration between 3 and 6 months post-irradiation, and dogs treated at 40 Gy or less had no gross colorectal abnormalities one year after irradiation. Furthermore, there were significant

differences in degree of vascular injury and serosal thickening between dogs treated with 30 and 40 Gy. These histologic abnormalities in the dogs treated with 40 Gy could be viewed as precursors to the ulcers seen at 50 Gy, or could indicate that 50 Gy delivered in 10 Gy fractions results in consequential late toxicity arising from mucosal injury, while 40 Gy delivered in 8 Gy fractions results in more classic late radiation injuries arising from radiation-induced fibrosis, and vascular injury.

Fibrosis can occur as a consequential effect, wherein mucosal disruption exposes the lamina propria and submucosa to bacteria and proteolytic enzymes.[36] However, since serosal thickening was observed in the absence of detectable submucosal thickening, it is likely that fibrosis occurred as a 'true', or classic late effect in groups C and D. The long (48 hour) interfraction intervals used in these treatment groups positively influences the repopulation response, as does the lower fractional dose used in those groups. Given the fractional dose-dependency of mitotic block, which determines how soon after irradiation repopulation starts, it makes sense that fibrosis in these groups wasn't a consequential late effect.[45,46] The lack of a consequential mechanism in these dose groups is further evidenced by the observed vascular changes, including adventitial fibrosis, thrombosis and intimal proliferation, which are also classic late effects of radiation, with no known consequential mechanism.[47,48]

In summary, the incidence and severity of colorectal ulceration was inversely proportional to duration of the interfraction interval. This likely reflects the consequential mechanism underlying late colorectal toxicity when 50 Gy is delivered in 5 fractions via SBRT. Furthermore, there was a clear relationship between total dose and risk and severity of vascular

and fibrotic colorectal injuries one year after delivery 30 and 40 Gy via 5 fraction SBRT; these changes are thought to have been classic late radiation effects, and were mild or absent at 30 Gy, and severe at 40 Gy.

REFERENCES

1. King CR, Brooks JD, Gill H, et al. Long-term outcomes from a prospective trial of stereotactic body radiotherapy for low-risk prostate cancer. *International Journal of Radiation Oncology Biology Physics* 2012;82:877-882.

2. Boike TP, Lotan Y, Cho LC, et al. Phase I Dose-Escalation Study of Stereotactic Body Radiation Therapy for Low- and Intermediate-Risk Prostate Cancer. *Journal of Clinical Oncology* 2011;29:2020-2026.

3. Madsen BL, Hsi RA, Pham HT, et al. Stereotactic hypofractionated accurate radiotherapy of the prostate (SHARP), 33.5 Gy in five fractions for localized disease: First clinical trial results. *International Journal of Radiation Oncology Biology Physics* 2007;67:1099-1105.

4. Tang CI, Loblaw DA, Cheung P, et al. Phase I/II Study of a Five-fraction Hypofractionated Accelerated Radiotherapy Treatment for Low-risk Localised Prostate Cancer: Early Results of pHART3. *Clinical Oncology* 2008;20:729-737.

5. Aluwini S, van Rooij P, Hoogeman M, et al. CyberKnife Stereotactic Radiotherapy as Monotherapy for Low- to Intermediate-Stage Prostate Cancer: Early Experience, Feasibility, and Tolerance. *Journal of Endourology* 2010;24:865-869.

6. Kang JK, Cho CK, Choi CW, et al. Image-guided stereotactic body radiation therapy for localized prostate cancer. *Tumori* 2011;97:43-48.

7. Jabbari S, Weinberg VK, Kaprealian T, et al. Stereotactic body radiotherapy as monotherapy or post-external beam radiotherapy boost for prostate cancer: technique, early toxicity and PSA response. *International Journal of Radiation Oncology Biology Physics* 2012;82:228-234.

8. Hodges JC, Lotan Y, Boike TP, et al. Cost-Effectiveness Analysis of SBRT Versus IMRT: An Emerging Initial Radiation Treatment Option for Organ-Confined Prostate Cancer. *American Journal of Managed Care* 2012;18:E186-E192.

9. DeFoe SG, Bernard ME, Rwigema JC, et al. Stereotactic body radiotherapy for the treatment of presacral recurrences from rectal cancers. *Journal of Cancer Research and Therapeutics* 2011;7:408-411.

10. Higginson DS, Morris DE, Jones EL, et al. Stereotactic body radiotherapy (SBRT): Technological innovation and application in gynecologic oncology. *Gynecologic Oncology* 2011;120:404-412.

11. Guckenberger M, Bachmann J, Wulf J, et al. Stereotactic body radiotherapy for local boost irradiation in unfavourable locally recurrent gynaecological cancer. *Radiotherapy and Oncology* 2010;94:53-59.

12. Zaorsky NG, Studenski MT, Dicker AP, et al. Stereotactic body radiation therapy for prostate cancer: is the technology ready to be the standard of care? *Cancer Treat Rev* 2013;39:212-218.

13. Wiegner EA, King CR. Sexual function after stereotactic body radiotherapy for prostate cancer: results of a prospective clinical trial. *International Journal of Radiation Oncology Biology Physics* 2010;78:442-448.

14. Brown MW, Brooks JP, Albert PS, et al. An analysis of erectile function after intensity modulated radiation therapy for localized prostate carcinoma. *Prostate Cancer and Prostatic Diseases* 2007;10:189-193.

15. van der Wielen GJ, van Putten WLJ, Incrocci L. Sexual function after three-dimensional conformal radiotherapy for prostate cancer: Results from a dose-escalation trial. *International Journal of Radiation Oncology Biology Physics* 2007;68:479-484.

16. Incrocci L. Sexual function after external-beam radiotherapy for prostate cancer: What do we know? *Critical Reviews in Oncology Hematology* 2006;57:165-173.

17. Arbuck SG, Ivy P, Setser A, et al. Common toxicity criteria (CTC) version 2.0: Highlights and tools. *Annals of Oncology* 1998;9:12-12.

18. Black WC, Gomez LS, Yuhas JM, et al. Quantitation of the late effects of x-radiation on the large-intestine. *Cancer* 1980;45:444-451.

19. Halberg FE, Larue SM, Rayner AA, et al. Intraoperative radiotherapy with localized radioprotection - diminished duodenal toxicity with intraluminal WR2721. *International Journal of Radiation Oncology Biology Physics* 1991;21:1241-1246.

20. King CR, Brooks JD, Gill H, et al. Stereotactic body radiotherapy for localized prostate cancer: interim results of a prospective phase II clinical trial. *International Journal of Radiation Oncology Biology Physics* 2009;73:1043-1048.

21. O'Brien PC. Radiation injury of the rectum. *Radiotherapy and Oncology* 2001;60:1-14.

22. Tucker SL, Thames HD, Michalski JM, et al. Estimation of alpha/beta for late rectal toxicity based on RTOG 94-06. *International Journal of Radiation Oncology Biology Physics* 2011;81:600-605.

23. Thames HD. Repair kinetics in tissues - alternative models. *Radiotherapy and Oncology* 1989;14:321-327.

24. Rojas A, Joiner MC. The influence of dose per fraction on repair kinetics. *Radiotherapy and Oncology* 1989;14:329-336.

25. Rojas A, Joiner MC, Johns H. Recovery kinetics of X-ray damage in mouse skin - the influence of dose per fraction. *International Journal of Radiation Biology* 1991;59:517-536.

26. Guerrero M, Li XA. Halftime for repair of sublethal damage in normal bladder and rectum: an analysis of clinical data from cervix brachytherapy. *Physics in Medicine and Biology* 2006;51:4063-4071.

27. Terry NHA, Denekamp J. RBE values and repair characteristics for colorectal injury after cesium 137 gamma ray and neutron irradiation. 2. Fractionation up to 10 doses. *British Journal of Radiology* 1984;57:617-629.

28. Withers HR, Mason KA. Kinetics of recovery in irradiated colonic mucosa of mouse. *Cancer* 1974;34:896-903.

29. Bentzen SM, Ruifrok ACC, Thames HD. Repair capacity and kinetics for human mucosa and epithelial tumors in the head and neck: Clinical data on the effect of changing the time interval between multiple fractions per day in radiotherapy. *Radiotherapy and Oncology* 1996;38:89-101.

30. Peck JW, Gibbs FA. Mechanical assay of consequential and primary late radiation effects in murine small intestine: alpha/beta analysis. *Radiation Research* 1994;138:272-281.

31. Dorr W, Hendry JH. Consequential late effects in normal tissues. *Radiotherapy and Oncology* 2001;61:223-231.

32. Peters LJ, Ang KK, Thames HD. Accelerated fractionation in the radiation treatment of head and neck cancer: a critical comparison of different strategies. *Acta Oncologica* 1988;27:185-194.

33. Langberg CW, Sauer T, Reitan JB, et al. Relationship between intestinal fibrosis and histopathologic and morphometric changes in consequential and late radiation enteropathy. *Acta Oncologica* 1996;35:81-87.

34. Dorr W, Kummermehr J. Increased radiation tolerance of mouse tongue epithelium after local conditioning. *International Journal of Radiation Biology* 1992;61:369-379.

35. Withers HR. Regeneration of intestinal mucosa after irradiation. *Cancer* 1971;28:75-&.

36. Langberg CW, Waldron JA, Baker ML, et al. Significance of overall treatment time for the development of radiation-induced intestinal complications - an experimental study in the rat. *Cancer* 1994;73:2663-2668.

37. Mennie AT, Dalley VM, Dinneen LC, et al. Treatment of radiation-induced gastrointestinal distress with acetylsalicylate. *Lancet* 1975;2:942-943.

38. Stryker JA, Demers LM, Mortel R. Prophylactic ibuprofen administration during pelvic irradiation. *International Journal of Radiation Oncology Biology Physics* 1979;5:2049-2052.

39. Goldstein F, Khoury J, Thornton JJ. Treatment of chronic radiation enteritis and colitis with salicylazosulfapyridine and systemic corticosteroids - Pilot study. *American Journal of Gastroenterology* 1976;65:201-208.

40. Kochhar R, Patel F, Dhar A, et al. Radiation-induced proctosigmoiditis - prospective, randomized, double-blind controlled trial of oral sulfasalazine plus rectal steroids versus rectal sucralfate. *Digestive Diseases and Sciences* 1991;36:103-107.

41. Sanguineti G, Franzone P, Marcenaro M, et al. Sucralfate versus mesalazine versus hydrocortisone in the prevention of acute radiation proctitis during conformal radiotherapy for prostate carcinoma - A randomized study. *Strahlentherapie Und Onkologie* 2003;179:464-470.

42. Cohn SM, Schloemann S, Tessner T, et al. Crypt stem cell survival in the mouse intestinal epithelium is regulated by prostaglandins synthesized through cyclooxygenase-1. *Journal of Clinical Investigation* 1997;99:1367-1379.

43. Morteau O, Morham SG, Sellon R, et al. Impaired mucosal defense to acute colonic injury in mice lacking cyclooxygenase-1 or cyclooxygenase-2. *Journal of Clinical Investigation* 2000;105:469-478.

44. Houchen CW, Sturmoski MA, Anant S, et al. Prosurvival and antiapoptotic effects of PGE(2) in radiation injury are mediated by EP2 receptor in intestine. *American Journal of Physiology-Gastrointestinal and Liver Physiology* 2003;284:G490-G498.

45. Taylor JMG, Withers HR, Hu ZX. A comparison of mathematical models for regeneration in acutely responding tissues. *International Journal of Radiation Oncology Biology Physics* 1988;15:1389-1400.

46. Denham JW, Hauer-Jensen M, Kron T, et al. Treatment-time-dependence models of early and delayed radiation injury in rat small intestine. *International Journal of Radiation Oncology Biology Physics* 2000;48:871-887.

47. Powers BE, Thames HD, Gillette EL. Long-term adverse effects of radiation inhibition of restenosis: Radiation injury to the aorta and branch arteries in a canine model. *International Journal of Radiation Oncology Biology Physics* 1999;45:753-759.

48. Hoopes PJ, Gillette EL, Withrow SJ. Intraoperative irradiation of the canine abdominal aorta and vena cava. *International Journal of Radiation Oncology Biology Physics* 1987;13:715-722.

CHAPTER 5: CONCLUSIONS AND FUTURE DIRECTIONS

Though the three studies described in this dissertation each address different scientific questions and concerns through observation and by testing unique hypotheses, each part is linked by a common thread. The purpose of this body of research, shared by each individual study, was to better understand the effects of abdominopelvic irradiation in dogs. Specifically, Chapter 2 hypothesized that fractionated, full-course irradiation could be delivered safely to dogs with intensity-modulated and image-guided radiation therapy (IM/IGRT), and that such therapy would lead to improvements in event-free and overall survival times as compared with historical reports in the veterinary literature. Unlike the clinical research described in Chapter 2, the research described in Chapters 3 and 4 were prospective, laboratory-based pilot studies, testing a series of hypotheses aimed at modeling late pelvic radiation toxicoses which occur in humans after stereotactic body radiation therapy (SBRT), using a canine model. Chapter 3 was devised to develop a canine model of radiation-induced erectile dysfunction (RI-ED). It was hypothesized that SBRT could be used to induce ED in dogs. Furthermore, it was hypothesized that ante-mortem bioassays of perfusion (magnetic resonance imaging and ultrasound) and electrophysiological changes (electromyography, motor nerve conduction studies and sensory nerve conduction studies) would correlate with and be predictive of pathological post-mortem lesions evidencing vascular and neurologic injuries that may contribute to RI-ED. That model was then to be used to study the influence of specific anatomical irradiations on risk of developing RI-ED. We hypothesized that both vascular and neurologic injuries arising from irradiation of the neurovascular bundles would contribute to RI-ED, but that irradiation of only the penile bulb would not cause pathophysiologic alterations that would contribute to RI-ED.

Finally, we hypothesized that vascular and neurologic injury (as measured via functional bioassays, and as quantified in semiquantitative pathologic evaluations) would occur in a directly dose-responsive manner. Finally, Chapter 4 was designed to study pathologic changes in the colorectal tissue of dogs after irradiation with clinically-relevant SBRT protocols. Because colonic ulcers developed rapidly (about 3 months) after irradiation with 50 Gy of SBRT, delivered in 5 daily fractions, it was postulated that this was a consequential late effect, and hypothesized that 50 Gy would be better tolerated when delivered every other day. It was also anticipated that dogs treated with 50 Gy would have histologic changes in the colorectal tissue consistent with ongoing acute toxicity, rather than classic late toxicity (i.e., dogs would have evidence of mucosal injury, but not of vascular or fibrotic changes). We also expected that colorectal toxicity would be better tolerated and that associated pathologic changes would be of intermediate severity after irradiation with 40 Gy in 5 fractions, and that 30 Gy in 5 fractions would be well-tolerated, with mild pathologic changes when evaluated 1 year post-irradiation.

Chapter 2 described tumor control and tolerability of a novel approach to irradiation of genitourinary (GU) tumors in pet dogs. At face value, it seems the most important thing learned from this study is that IM/IGRT is active against canine urogenital carcinomas, and that application of full-course, fractionated radiotherapy (RT) yields survival times that compare favorably with previously reported outcomes after more conventionally accepted treatments (namely a combination of cytotoxic chemotherapy and non-steroidal anti-inflammatory drugs). But this interpretation of the data misses a bigger picture. While results of a relatively small retrospective case series can suggest activity of a novel therapeutic approach in a particular disease setting, it is important to remember two things: (1) based on historical reports, and on

radiobiological principles, these results should not be surprising, and (2) these results should not be over-interpreted by suggesting that this study confirms efficacy. Instead, the most important observation to be drawn from Chapter 2 is that the absence of moderate-to-severe early gastrointestinal (GI) tract toxicities after IM/IGRT made this treatment tolerable to pets and pet owners. The unarguable fact learned from this study is that high total doses (54 to 57 Gray [Gy] in 2.7 to 2.85 Gy fractions) of ionizing radiation can be delivered to focal, tumor-bearing sites within the caudal abdomen and pelvis with an acceptable acute toxicity profile. This is important because dogs could not be irradiated with such high doses using previously available external beam irradiation techniques (namely 2-dimensional RT or 3-dimensional conformal RT) without high risk of life-limiting acute GI toxicity. The study also illustrated that both locoregional tumor progression and late radiation toxicity in the genitourinary tract occur with a relatively high frequency (33% and 14%, respectively, in this study) after high-dose IM/IGRT. Therefore, results of Chapter 2 should be used to justify a prospective clinical trial aimed at improving the therapeutic ratio of multimodal management of canine GU carcinomas, via evaluation of tumor responses and normal tissue complications in a dose-escalation study.

Interestingly, although acute and late toxicities of the GI and urinary tracts were scored in Chapter 2, sexual function was not evaluated as a possible clinical toxicity. This is not surprising though, as clinically, we fail to recognize sexual dysfunction in most small animal veterinary patients. This is in large part due to the fact that the majority of pet owners in North America elect to have their pets sterilized at a young age. Without the ability to sexually reproduce, neither pet owners nor clinicians have reason to evaluate sexual function, or lack thereof. Furthermore, in veterinary clinical oncology, the cause of most malignancies is unknown. Given

the potential heritability of some cancers, and the impact that sex hormones have on other oncologic diseases, clinicians often encourage sterilization of sexually-intact small animal oncology patients. For example, to date only one sexually intact dog at Colorado State University has been treated with IM/IGRT for a TCC of the urinary bladder and proximal urethra. This dog also had ultrasonographic prostatomegaly and cytologic evidence of benign prostatic hypertrophy. Although there was no evidence of the carcinoma having grossly invaded the prostate, the prostate was included within the radiation field as part of the clinical target volume, and it was recommended that this patient be castrated about a month after completing therapy to avoid the possibility of androgen-driven progression of his prostatomegaly, which would likely have complicated his lower urinary tract health at some point in the future via partial or complete non-malignant urethral obstruction.

With the encouraging clinical results presented in Chapter 2 of this dissertation, the number of IM/IGRT procedures performed for TCC is rapidly increasing. Perhaps now is the time to investigate the feasibility of using dogs that are irradiated for TCC of the lower urinary tract as a model for studying the pathogenesis of normal tissue toxicoses associated with pelvic irradiation. Specifically, these dogs may be an excellent model for studying erectile dysfunction (ED). This may seem counterintuitive since the presence or absence of sexual dysfunction in a neutered pet dog is unlikely to impact its perceived quality of life, or overall health. But conceivably, the best opportunity to study a debilitating complication of cancer treatment in people is in a model for which that toxicity occurs without clinical consequence. Furthermore, studying RI-ED in a population of pets with cancer of the lower urinary tract enables us to account for potential impacts that the presence of a spontaneously occurring tumor may have on the local

microenvironment, and on normal tissue function. And although penile erection is thought to be androgen-dependent, the exact contribution of testosterone to erectile physiology is unclear. Available data suggests that testosterone concentrations, far below the normal range, are necessary for normal erection in men.[1,2] This is consistent with rat data which demonstrates dependency of erectile quality on circulating testosterone concentration, thought to be related to decreased activity of nitric oxide synthase (NOS) in the absence of testosterone.[3] The androgen-dependency of erectile function is further supported by a small study in dogs showing that the level of energy need to induce erection following electrical stimulation is higher, and peak intracavernosal pressures (ICP) are lower in castrates.[4] But, clinical observations clearly indicate that sexual sterilization does not preclude penile erection in dogs. It is hypothesized that central-mediated behavioral stimuli are sufficient to override the decreased NOS activity which results from testosterone deprivation. Another possible explanation for the ability of castrated male dogs to have and maintain penile erections is that phase I of erection (the engorgement phase) is an androgen-independent process, while phase II (the rigid erection phase) is dependent upon testosterone. In this scenario, castrated male dogs could have a penile erection, but chronic androgen deprivation would cause shrinkage of the pudendal nerve's motor pool, ultimately resulting in atrophy of the bulbospongiosus and ischiocavernosus muscles, and precluding terminal priming to maximal intracavernosal pressures in this population of dogs. Regardless, this is therefore an opportunity to study components of RI-ED in an androgen-independent setting, which is important given that many of the more aggressive human prostate cancers have (or develop) an androgen-independent/hormone-refractory phenotype. If it can be shown that IM/IGRT results in RI-ED in this spontaneous tumor model, the novel model would be a perfect complement to the normal, non-tumor-bearing and androgen dependent dog model described

herein. Of course, further characterization of erectile function and dysfunction in the chronic androgen-deprived state is required before such studies can be commenced.

Before jumping into investigation of another novel animal model for studying RI-ED, it is important to first reflect upon what has been learned thus far. Data was presented in Chapter 3 which described a novel animal model for studying RI-ED, using normal dogs that had received prostatic stereotactic body RT (SBRT). Vascular (MRI and ultrasound) and neurologic [5] outcome measures were described before and after RT to determine their utility as surrogate measures of ED by providing objective, supportive evidence for clinical endpoints. Although this study did not provide sufficient evidence to support use of any single or combination of these outcome measures as a fully validated surrogate, several considerations should be made. First and foremost, as described in Chapter 3, the electrophysiology studies did not work as well as anticipated. Electromyography of the bulbocavernosus muscle confirmed the presence of post-irradiation muscle and/or nerve disease. This damage was further interrogated by performing motor nerve conduction studies, sensory nerve conduction studies and cord dorsum potentials. Compound muscle action potentials were recorded in many dogs, but unfortunately, none of the motor, sensory or cord dorsum parameters were successfully recorded both pre- and post-irradiation in all of the dogs. Modified techniques, used in the last few electrophysiology studies in our experiment, were described in Chapter 3 that allowed for successful recording of these data. We have therefore demonstrated that it is possible to record reliable electrophysiologic parameters which may reflect neurological changes associated with pudendal nerve injury in the dog. Even though these techniques are possible, they are very difficult to record; the procedure is time consuming, requires a great deal of experience with the technical

aspects of performing clinical electrophysiological studies, and also requires intricate knowledge of perineal neuroanatomy due to the small size of the nerves which are being probed. The physical probing of the nerve could be facilitated by surgical dissection, but this would preclude sequential exams, as post-operative inflammatory and fibrotic changes would likely alter nerve function, and conduction velocities, independent of radiation associated changes. Therefore, an alternative methodology is presented for future neurological investigations of RI-ED. The proposed neurophysiological evaluation is simpler to execute because it does not require direct measurement of any single nerve's function. Instead, it is suggested that electroejaculation techniques be used to provide exogenous nervous erectogenic stimulation, followed by measurement of the physical penile erection. Specifically, the erectile response should be probed using two separate stimulations: intrapelvic and percutaneous perineal electrostimulation.[6-8] Although physical penile diameter measurements and subjective description of erection quality should be performed (as described in Chapter 3), it is also recommended that intracavernosal pressure (ICP) be quantified (and normalized to mean systemic arterial pressure [MAP]) before and after electroejaculation, as an objective measure of penile erection quality; the ICP/MAP ratio could be used as an outcome measure, reflective of erectile response to electrostimulation.[9] Normal erectile response to intrapelvic electrostimulation in an irradiated dog provides evidence that the local neurovascular pathway responsible for penile erection is intact. If the erectile response to intrapelvic stimulation is abnormal, percutaneous perineal stimulation should help dissect where the problem lies. For example, if there is abnormal erection after pelvic stimulation, but normal erection after perineal stimulation, this suggests that the intracavernous nervous tissue is capable of releasing normal concentrations of neurotransmitters, and that the penile vasculature is healthy enough to respond to erectogenic neuronal stimulation. Conversely,

if there is abnormal erection after pelvic and perineal stimulation, it is possible that the radiation injury precluding penile erection affects any of the tissues necessary for erection, nervous (small cavernous nerves or large nerves of the neurovascular bundle) or vascular (internal pudendal artery, penile arteries or veins). In this latter scenario, further interrogation of vascular health should aid in narrowing down the potential cause(s) of RI-ED. See Appendix 2.

Given the limitations of data analysis for DCE-MRI in Chapter 3, if this imaging modality is to be used in future studies using this novel animal model to study RI-ED, it is recommended that the protocol be revised to further improve image quality and validated in several normal (unirradiated dogs) prior to use. Several considerations must be made in revising the protocol. First, this study employed a gradient echo (GE) technique. Unlike spin echo (SE) pulse sequences, which use a 90 degree excitation pulse followed by a 180 degree radiofrequency pulse which serves to refocus some of the dephasing that occurs after the initial RF pulse, GE sequences use a smaller initial excitation pulse, and no refocusing. These differences allow GE sequences to be performed with faster echo times than are possible with SE sequences. And if the flip angle is small, the relaxation time (TR) can also be small. The shorter TE and TR enable faster scanning than is possible with SE sequences, making GE sequences preferable for DCE studies. One downside of not refocusing the dephased protons with a second (180 degree) RF pulse is that image contrast is dominated by T2* rather than T2, magnetic field inhomogeneities persist and the signal-to-noise ratio is comparatively low. Though it may slow image acquisition a bit, reduced signal could be mitigated by increasing the TR and potentially, TE; alternatively, use of a smaller flip angle could also improve the signal to noise ratio. Another potential problem with the DCE-MRI protocol is that the prostate was drawn as a single volume of interest

(VOI), encompassing the entire organ. Though the canine prostate lacks zonal organization, and the glandular anatomy is homogeneously well-differentiated, the VOI used in this study was relatively large. The large size of the VOI means that not only was prostatic parenchyma analyzed, but so too was prostatic urethra and the indwelling urinary catheter. This may have "diluted" any changes in signal intensity unique to the prostate itself. Therefore, future studies should consider use of a smaller VOI, encompassing only prostatic parenchyma. Finally, the DCE-MRI performed in this study was evaluated using model-based and model-free parameters. In general, pharmacokinetic modeling is felt to be more rigorous than model-free analysis, and has the benefit of direct correlation between model parameters and physiologic events. As described in Chapter 3, the Toft's model employed an arterial input function (AIF), which was intended to "clean up" the DCE-MRI data by essentially normalizing tissue enhancement patterns to systemic (large artery) enhancement. The study was thoughtfully designed to minimize changes in systemic blood pressure during DCE-MRI studies, as changes in pressure affect tissue perfusion (the rate of blood flow equals the quotient of pressure and resistance). However, the means for maintaining a relatively stable systemic blood pressure (fluid boluses, vasoactive drugs, etc.) likely affected peripheral vasculature to effect change in local tissue perfusion. Furthermore, even if the local flow patterns were completely stable, the chosen artery (branches of the internal pudendal artery) for the AIF was quite small, and it was not possible to standardize which branch was used. Finally, this study showed that prostatic SBRT caused internal pudendal arterial injury, calling into question the utility of that vessel in longitudinal studies. Future studies should consider using a model which doesn't rely on an AIF, or using normal muscle enhancement for normalization, rather than an AIF.

Aside from these recommendations for future studies, there are also several techniques that could be used to improve quality of the data from the present study, through manipulation of the DCE pharmacokinetic modeling used. Specifically, data could be reprocessed using the same Toft's modeling procedure, but eliminating the v_p component from the curve-fitting procedure, and normalizing K^{trans} and iAUGC for each VOI by the iAUGC for the pudendal vein. This approach would be undertaken to improve the AIF; though the shape of the AIF for most cases is appropriate, the magnitude of the signal intensity is highly variable, whereas the magnitude of intensity for the corresponding vein is seemingly repeatable between time points. Removal of the v_p component of the curve-fitting procedure would be justified, at least in the prostate, by the fact that the prostate is perfused largely by microvasculature, with minimal arterial flow of its own. Another option is to keep the v_p component in the model, but still normalize to iAUGC for a reference vein. A final means for re-analyzing this data is to process the curves using model-free techniques to determine parameters such as AUC, peak height, slope and time to enhancement.

Despite this problem using the internal pudendal artery for the AIF, one of the most exciting observations made in the studies comprising Chapter 3 was the fact that the ultrasound studies were able to document internal pudendal arterial dysfunction after prostatic SBRT. This is exciting because pudendal arterial injury has been implicated as a potential contributor to RI-ED, but has been poorly studied (see Chapter 1). Unfortunately, the internal pudendal arteries were not harvested during necropsy of our study dogs, and are therefore not available for additional evaluation. However, it would be interesting to study the nature of the internal pudendal arterial dysfunction in more depth, using *in vivo* functional studies to determine whether the dysfunction

is endothelium dependent or not, and necropsy studies to describe and correlate histologic changes with degree of RI-ED,[10,11] to try and elucidate whether the radiation induced arterial changes were due to endothelial dysfunction or changes in the wall (subendothelial fibrosis, intimal/medial proliferation, muscular injury, etc.). It would also be prudent to study these changes using fractionated RT protocols rather than SBRT, as the vascular biology following large dose-per-fraction RT is thought to vary considerably from finely fractionated RT.[12,13] Elucidating mechanisms underlying vascular dysfunction following RT should aid in developing means for prevention and/or treatment of such changes.

There are countless ways in which these studies could have been done differently, and an equally large number of new research questions which have been generated. Many have been outlined above with varying levels of detail. Several more interesting questions are posed below:

- The dose-response curves for late toxicity in most normal tissues are quite steep compared with tumors (due to tumor heterogeneity), therefore, in order to maximize the therapeutic ratio, it is important to know precisely the shape of the dose-response curve for organs at risk. We have demonstrated in a dog model that there is significant difference in the colorectal tolerability of 30, 40 and 50 Gy as delivered via 5 fraction SBRT. What is the ED_5 (dose which causes unacceptable toxicity in 5% of treated subjects) at 1, 3 and 5 years for severe colorectal toxicity in this model? This question can be answered by performing a very slow dose escalation study, using small dose intervals for escalation.

- What is the effect of cyclooxygenase inhibition on the risk for developing consequential colorectal complication of radiotherapy?
- One of the overriding questions which led to the development of a canine model for studying RI-ED was whether or not highly conformal irradiation techniques could be used to limit risk of developing RI-ED by sparing certain structures in the pelvis, such as the NVB or PB. Our data suggests irradiation of the base of the penis may increase the risk of radiation-induced erectile dysfunction due to radiation injury to the internal pudendal artery, and/or the pudendal nerve (which may be damaged primarily, or secondary to vascular injury). One could test the hypothesis that radiation injury to these structures increases risk of RI-ED in a clinical trial if it is possible to conformally avoid the internal pudendal artery and nerve (as it branches into the dorsal nerve of the penis, near the base of the penis) without sacrificing dose to the tumor. But if such avoidance would risk underdosing any portion of the prostate tumor, then further preclinical investigation in warranted before taking this hypothesis to the clinic floor. Data presented herein also supports the notion that irradiation of the neurovascular bundle may play a role in RI-ED, though it seems it may not be as critical as the structures near the base of the penis. Avoidance of the NVB would be difficult, but introduction of a spacer between the prostate and colon could limit the volume of the bilateral NVB's that receive high doses in a modulated plan. Since irradiated volume is strongly linked to risk for late toxicity, and because spacers appear to be well tolerated and limit risk for colorectal toxicity, you could easily test the hypothesis that use of a spacer limits how much of the NVB receives high doses of RT, and thereby decreases the incidence of RI-ED.

Before answering these questions, perhaps the most judicious use of resources would be to answer the following questions which arise from our studies, and which can be answered using tissues and/or data which have already been collected:

- Does urethral radiosensitivity vary depending upon site irradiated? Our study involved irradiation of the pre-prostatic, prostatic and membranous urethra and/or bulbar urethra with varying doses of SBRT. Does the severity of histologically-evident radiation injury differ between segments of urethra for the same administered dose?
- Similarly, what is the radiosensitivity (based upon type and severity of histologic lesions) of the trigone of the urinary bladder after SBRT?
- Neuronal NOS activity has been shown to decrease in the post-irradiation setting in the cavernosal tissue of rats. It is not possible to study changes in NOS activity in our set of tissues (because NO is quite labile, and cannot be reliably measured in formalin-fixed tissues), but commercially available antibodies have been validated for detection of expression levels of inducible, neuronal and endothelial NOS in formalin-fixed, paraffin embedded tissues of dogs via immunohistochemistry. A question that would be simple and important to answer is: does the expression of any of these isoforms of NOS change in tissues of the neurovascular bundle, prostate or penis in irradiated dogs?
- Would the DCE-MRI data be more predictive of changes in prostatic perfusion if the DCE-MRI data were to be re-analyzed with the urethra excluded from the prostatic region of interest? Are there any other DCE-MRI models (such as the aforementioned AIF-free models) which better correlate with the concentration time curves collected in our studies?

In closing, these studies have been a great first step in developing a normal dog model for studying RI-ED, and have brought to light the potential utility in studying sexual toxicity in tumor-bearing dogs. This model provides a platform for studying radiation-induced internal pudendal arterial dysfunction, which may play an important role in development of RI-ED. And with further development, this model is expected to be an important large animal model that is complementary to existing small animal platforms. Furthermore, our normal dog work has provided human and veterinary clinicians important data regarding SBRT-associated colorectal complications, and a useful model for studying such complications.

REFERENCES

1. Mikhail N. Does testosterone have a role in erectile function? *American Journal of Medicine* 2006;119:373-382.
2. Buvat J, Maggi M, Guay A, et al. Testosterone deficiency in men: systematic review and standard operating procedures for diagnosis and treatment. *Journal of Sexual Medicine* 2013;10:245-284.
3. Penson DF, Ng C, Rajfer J, et al. Adrenal control of erectile function and nitric oxide synthase in the rat penis. *Endocrinology* 1997;138:3925-3932.
4. Muller SC, Hsieh JT, Lue TF, et al. Castration and erection - an animal study. *European Urology* 1988;15:118-124.
5. Gianduzzo TRJ, Colombo JR, El-Gabry E, et al. Anatomical and electrophysiological assessment of the canine periprostatic neurovascular anatomy: Perspectives as a nerve sparing radical prostatectomy model. *Journal of Urology* 2008;179:2025-2029.
6. Shafik A, Shafik AA, Shafik IA, et al. Percutaneous perineal electrostimulation induces erection: Clinical significance in patients with spinal cord injury and erectile dysfunction. *Journal of Spinal Cord Medicine* 2008;31:40-43.
7. Brindley GS. Electroejaculation - Its technique, neurological implications and uses. *Journal of Neurology Neurosurgery and Psychiatry* 1981;44:9-18.
8. Santos IP, Ramos C, Ramos JLG, et al. Efficient association between PGF2 alpha and Methyl 4-hydroxybenzoate sex pheromone prior to electroejaculation in dogs. *Reproduction in Domestic Animals* 2013;48:160-164.
9. Kimura M, Yan H, Rabbani Z, et al. Radiation-induced erectile dysfunction using prostate-confined modern radiotherapy in a rat model. *Journal of Sexual Medicine* 2011;8:2215-2226.
10. Soloviev AI, Tishkin SM, Parshikov AV, et al. Mechanisms of endothelial dysfunction after ionized radiation: selective impairment of the nitric oxide component of endothelium-dependent vasodilation. *British Journal of Pharmacology* 2003;138:837-844.
11. Orton EC, Reeves JT, Stenmark KR. Pulmonary vasodilation with structurally altered pulmonary vessels and pulmonary hypertension. *Journal of Applied Physiology* 1988;65:2459-2467.
12. Garcia-Barros M, Lacorazza D, Petrie H, et al. Host acid sphingomyelinase regulates microvascular function not tumor immunity. *Cancer Research* 2004;64:8285-8291.
13. Garcia-Barros M, Paris F, Cordon-Cardo C, et al. Tumor response to radiotherapy regulated by endothelial cell apoptosis. *Science* 2003;300:1155-1159.

APPENDIX 1

Brief overview of Toft's[1] model as pertains to Chapter 3:

The factors determining behavior of gadolinium in a tissue after injection are perfusion, permeability and interstitial diffusibility. The arterial input function (AIF) is combined with compartmental models to account for differences in the rate of contrast medium injection, and subject-to-subject variation in baseline blood flow rates. In this study, contrast (0.1 mmol/kg gadolinium DTPA) was administered intravenously via controlled injector, at 3 mL/second; the internal iliac artery was used for the AIF. Toft's model applies pharmacokinetic principles to interpretation of dynamic contrast enhanced MRI, and is summarized in Table A1.1.

Table A1.1. Summary of parameters from Tofts's model

	Parameter	**Unit**	**Explanation**
Volume transfer constant	K^{trans}	min^{-1}	Transendothelial transport of contrast media from vascular compartment to tumor interstitium
Area under the gadolinium curve	*AUGC*	mM gadolinium per minute	Model-free, mixed parameter of K^{trans} and k_{ep}; iAUGC = 1st 120s (initial AUGC)
Rate constant	k_{ep}	min^{-1}	Reflects reverse transport of contrast back into the vascular space; $k_{ep}= K^{trans}/v_e$, derived from shape of gadolinium concentration vs. time curve
Fractional plasma volume	v_p	Unitless	Plasma volume
EES fractional volume	v_e	Unitless	Volume of extravascular extracellular space per unit volume of tissue

- Whereas K^{trans} and v_e relate directly to physiologic processes, the k_{ep} is a derived value; k_{ep} should always be greater than K^{trans}.
- When permeability is high, flux across the endothelium is flow limited; therefore K^{trans} is equal to the blood plasma flow per unit volume of tissue.

- If permeability is low, tracer flux is permeability limited, and K^{trans} is equal to the permeability surface area product between blood plasma tissue and the EES, per unit volume of tissue; this is seen in areas of fibrosis and tissue atrophy.[2]
- Model-free parameters (e.g., time to onset of enhancement, maximum signal intensity, maximum slope of increase, time to peak concentration, washout gradient, and initial area under the curve) are simpler to measure, but the physiologic meaning of these parameters, and relationship to quantitative markers are poorly defined. These semiquantitative markers can be measured quantitatively, but do not account for normal tissue perfusion (AIF).[3]
- Quantitative parameters seem to have inherently high variability due to temporal changes in perfusion.
- Figures A1.1 and A1.2, respectively, summarize principles of model-free parameters and parameters used in the Tofts model.

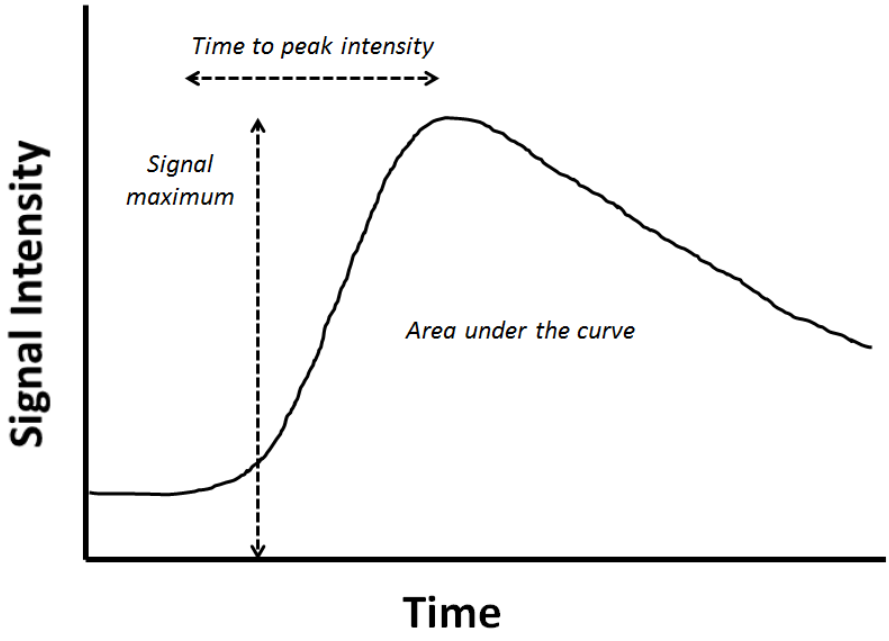

Figure A1.1. Signal intensity versus time plot

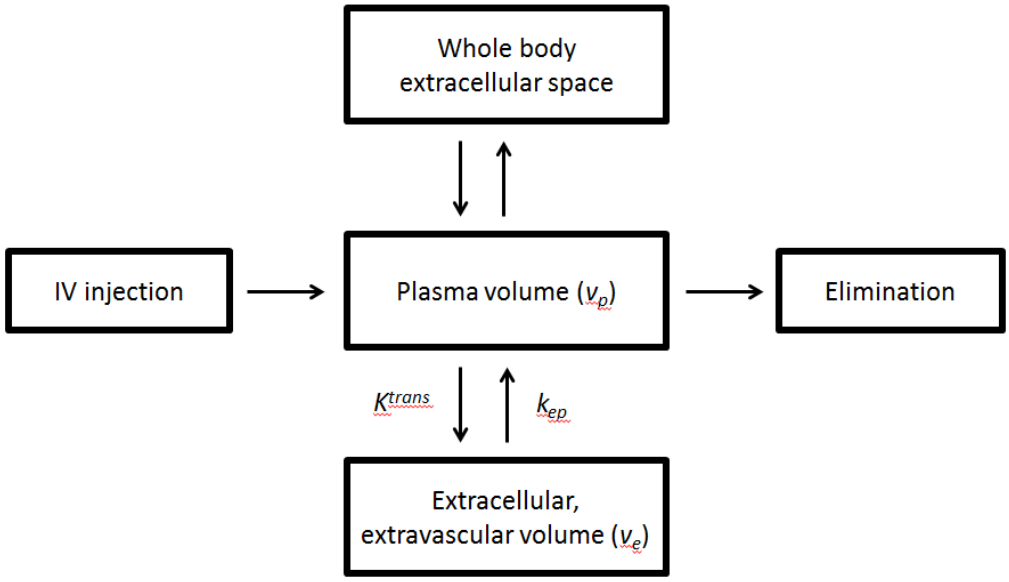

Figure A1.2. Compartments of Toft's model

REFERENCES

1. Tofts PS, Brix G, Buckley DL, et al. Estimating kinetic parameters from dynamic contrast-enhanced T(1)-weighted MRI of a diffusable tracer: Standardized quantities and symbols. *Journal of Magnetic Resonance Imaging* 1999;10:223-232.

2. Alonzi R, Padhani AR, Allen C. Dynamic contrast enhanced MRI in prostate cancer. *European Journal of Radiology* 2007;63:335-350.

3. Walker-Samuel S, Leach MO, Collins DJ. Evaluation of response to treatment using DCE-MRI: the relationship between initial area under the gadolinium curve (IAUGC) and quantitative pharmacokinetic analysis. *Physics in Medicine and Biology* 2006;51:3593-3602.

APPENDIX 2

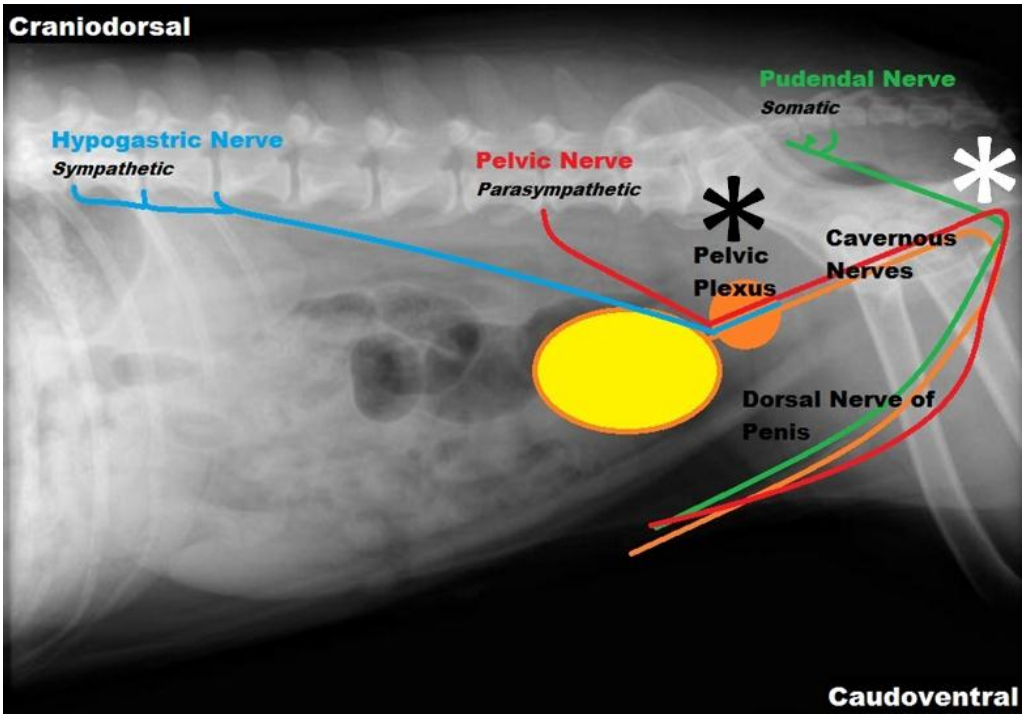

Figure A2.1. Diagrammatic representation of electrostimulation studies proposed in Chapter 5.

Black asterisk = Intrapelvic electrostimulation site
White asterisk = Percutaneous perineal electrostimulation site

1. ***Normal erectile response to intrapelvic electrostimulation:*** local neurovascular pathways are intact.
2. ***Abnormal erectile response to intrapelvic electrostimulation, but normal erectile response after percutaneous perineal electrostimulation:*** intracavernous nerves are capable of releasing normal concentrations of NO, and penile vasculature is healthy enough to respond to erectrogenic neuronal stimulation, but the parasympathetic impulses through the neurovascular bundles are disturbed.
3. ***Abnormal erectile response to intrapelvic and percutaneous perineal electrostimulation:*** erectile dysfunction may arise from nervous (small cavernous nerves, large parasympathetic nerves of the neurovascular bundle, or the pudendal nerve) or vascular (internal pudendal artery, penile arteries or veins) injury.
    a. Ultrasonographic evaluation of the internal pudendal artery and penis should aid in determining whether abnormal arterial inflow and/or cavernosal blood flow contribute to erectile dysfunction.
    b. Normal erectile response to intracavernosal papaverine suggests that vascular smooth muscle is responds normally to endothelium-independent vasodilatory stimuli.
    c. Normal erectile response to acetylcholine suggests that vascular smooth muscle is normally responsive to endothelium-dependent vasodilatory stimuli.
    d. If all of the above (a through c) are normal, primary nerve damage is most likely.